Report Number: 7930 November 2009

Project #153H Corrosion Assessment Guidance for High Strength Steels

(Phase 2)

GL Industrial Services Restricted

Restricted to: BP Exploration,US DOT PHSMA, Electicore & GL Industrial Services

Prepared for:

R Espiner

BP Exploration

Chertsey Rd
Sunbury-on-Thames
Middlesex
TW16 7LN
UK

Prepared by:

J Liu, L Mortimer and A Wood

GL Industrial Services UK Ltd

Holywell Park
Ashby Road
Loughborough Leicestershire
LE11 3GR
United Kingdom

Tel: +44 (0)1509 28 2011
Fax: +44 (0)1509 28 3119

E-mail: Jianhui.Liu@gl-group.com

Website: www.gl-group.com

Customer Reference: BP Contract No: P000014601
US DOT DTPH56-05-T0003 Project #153H

Report Issue / Amendment Record

Report Title: Project #153H Corrosion Assessment Guidance for High Strength Steels (Phase 2)	
Report Number: 7930	Project Title: Project #153H Corrosion Assessment Guidance for High Strength Steels (Phase 2) Project SAP Code: 1/12435

Amendment details

Issue	Description of Amendment	Originator/Author
1.0	Draft Report for Customer Comment	J Liu, L Mortimer and A Wood
2.0	Re-issue of report incorporating BP comments	J Liu, L Mortimer and A Wood
3.0	Re-issue of report incorporating PRCI comments	J Liu
3.1	Tables modified to include US customary units	J Liu

Report approval

Issue	Checked by	Approved by	Date
1.0	V Chauhan	P Ingham	28 Nov 2008
2.0	V Chauhan	P Ingham	12 Feb 2009
3.0	V Chauhan	P Ingham	09 Jun 2009
3.1	V Chauhan	P Ingham	27 Nov 2009

Previous issues of this document shall be destroyed or marked SUPERSEDED

Project Code: 1/12435

Distribution

Name	Company
R Espiner	BP Exploration Chertsey Rd Sunbury-on-Thames Middlesex TW16 7LN UK
R Smith S Nanney J Merritt	US DOT PHMSA
M Piazza R Owen D Johnson R Owen	PRCI
I Wood	Electricore, Inc.

DISCLAIMER

Executive Summary

Extensive research has been carried out for many years by Pipeline Research Council International, Inc. (PRCI) and others to develop methods for assessing the remaining strength of corroded pipelines. This has led to the development of assessment methods such as ASME B31G and RSTRENG. Research by Germanischer Lloyd (hereafter GL[1], formerly Advantica) has developed new criteria such as the LPC method and extended the range of assessment methods to include numerical analysis. While there has been substantial progress, there remain areas where existing criteria require improvements. The needed improvements identified include limitations on the interaction of closely spaced defects; the effects of external loading, and cyclic pressure loading. Furthermore, as operators start to use higher strength materials there will be an increasing need to assess the integrity of corroded high strength pipelines and to further validate the application of existing criteria and models to these materials. Phase 1 of the work was conducted to investigate the application of existing assessment methods to high strength pipelines and is described in GL Report R9017. PRCI, the Pipeline and Hazardous Materials Safety Administration (PHMSA) and BP Exploration have funded research to address these issues in recent years. A method for extending the assessment of corroded pipelines of strength grade up to X65, subject to combined internal pressure and external loading, to assess corrosion damage in pipelines subject to cyclic pressure loading, is described in GL Report R9068.

In GL Reports R9107, R7702 and, work was undertaken to investigate the performance of methods such as ASME B31G, RSTRENG and LPC when applied to the assessment of higher strength pipeline materials (API 5L/ISO 3183 grade L555/X80 and L690M/X100M). In addition to this work, GL has been commissioned by BP Exploration to conduct an operational trial using 48-inch diameter grade X100 pipe. The operational trial will generate substantial data on long term performance by testing sections of X100 pipeline in near real world conditions. An accelerated operational period will be simulated by two years of pressure cycling, equivalent to forty years operation. This large scale trial will be complemented by a range of laboratory scale tests. During the course of the trial a substantial amount of data related to the assessment of corrosion defects in X100 grade pipe will be gathered. This report presents the results of a program of work that builds on the development work being conducted for PHMSA/PRCI Project #153 and for the corrosion defect assessment section of the BP X100 operational trial.

Conclusions

1. Miniature flat tensile (MFT) testing was able to provide the relative change in tensile properties through the pipe wall thickness. Stress versus strain curves from the MFT tests have to be calibrated using results obtained from standard ST tests.
2. From the standard tensile (ST) test results, it was concluded that tensile properties in the longitudinal direction tended to be lower than those in the transverse direction.
3. Scatter in tensile properties was observed from X100 grade linepipe material obtained from three different manufacturers. No identifiable trends in tensile properties through the pipe wall thickness could be determined from the three different manufacturers. It was, however, concluded that in general lower tensile strengths were obtained towards the inner surface of the pipe.
4. Two full scale vessel burst tests were successfully conducted with relatively long axially orientated groove defects that were machined onto the external surface of the pipe. Both defects were targeted to have a depth of 50% of the pipe wall with lengths of 29.3 inch (745mm) and 78.7 inch

[1] Germanischer Lloyd acquired Advantica in 2007

(2000mm). Failure pressures predicted using ASME B31G and SHELL92 methods were lower than the actual burst pressures recorded from tests. The RSTRENG and LPC-1 methods predicted failure pressure very close (within 3%) to the recorded burst pressures. However, the predicted failure pressures were marginally higher the recorded burst pressures. For both burst tests, the Modified ASME B31G method predicted failure pressures higher than the recorded burst pressures.

5. Normalized failure locus diagrams have been derived for assessing corrosion damage in pipelines of strength grade up to X100 subject to combined internal pressure and external loading.

Recommendations

1. Validation of the assessment methods described in this report should be undertaken on completion of the BP X100 Operational Trial.
2. The normalized failure locus diagrams derived in this report should be incorporated into the PRCI Guidance Document for assessing corrosion damage in pipelines.

Nomenclature

D	Diameter	in (m)
E	Young's Modulus	psi (MPa)
F	Axial compressive Fforce	lbf (N)
F_0	Critical axial compressive force under unique loading	lbf (N)
F_{crit}	Critical compressive force	lbf (N)
I	Second moment of area	in^4 (m^4)
K	Spring constant	lbf/ft (N/m)
M	Moment	ft·lbf (Nm)
M_0	Critical moment under unique loading	ft·lbf (Nm)
M_{crit}	Critical bending moment	ft·lbf (Nm)
M_e	Moment at yield	ft·lbf (Nm)
P	Internal pressure	psi (MPa)
P_0	Critical pressure under unique loading	psi (MPa)
P_A	Burst pressure	psi (MPa)
P_{crit}	Axial compressive load	psi (MPa)
P_f	Failure pressure	psi (MPa)
R_i	Inner radius	in (m)
R_m	Tensile strength	psi (MPa)
R_o	Outer radius	in (m)
$R_{p0.2}$	Yield strength	psi (MPa)
t	Thickness	in (m)
y	Length	in (m)
α	Outer radius/thickness ratio	-
ε	Strain	-
ε_m	Tensile strain	-
$\varepsilon_{p0.2}$	Yield strain	-
π	pi	-
σ_{by}	Bending yield stress	psi (MPa)
σ_{hp}	Hoop stress (under pressure)	psi (MPa)
σ_{SMYS}	Specified minimum yield strength	psi (MPa)
σ_{vm}	von Mises equivalent stress	psi (MPa)
σ_{xb}	Axial stress (under bending)	psi (MPa)
σ_{xf}	Axial stress (under compressive force)	psi (MPa)
σ_{xp}	Axial stress (under pressure)	psi (MPa)

Contents

1 Introduction

Extensive research has been carried out for many years by Pipeline Research Council International, Inc. (PRCI) and others to develop methods for assessing the remaining strength of corroded pipelines. This has led to the development of assessment methods such as ASME B31G [1] and RSTRENG [2], [3]. Research by Germanischer Lloyd (hereafter GL[2], formerly Advantica) has developed new criteria such as the LPC [4] method and extended the range of assessment methods to include numerical analysis. While there has been substantial progress, there remain areas where existing criteria require improvements. The needed improvements identified include limitations on the interaction of closely spaced defects; the effects of external loading, and cyclic pressure loading. Furthermore, as operators start to use higher strength materials there will be an increasing need to assess the integrity of corroded high strength pipelines and to further validate the application of existing criteria and models to these materials. Phase 1 of the work was conducted to investigate the application of existing assessment methods to high strength pipelines and is described in [5]. PRCI, the Pipeline and Hazardous Materials Safety Administration (PHMSA) and BP Exploration have funded research to address these issues in recent years [6] [3], [7]. In Reference [8] a method for extending the assessment of corroded pipelines of strength grade up to X65, subject to combined internal pressure and external loading is described; and in Reference [9], work is described to assess corrosion damage in pipelines subject to cyclic pressure loading.

In the aforementioned references, work was undertaken to investigate the performance of methods such as ASME B31G, RSTRENG and LPC when applied to the assessment of higher strength pipeline materials (API 5L/ISO 3183 grade L555/X80 and L690M/X100M)[4] [10]. In addition to this work, GL has been commissioned by BP Exploration to conduct an operational trial using 48-inch diameter grade X100 [11], [12]. The operational trial will generate substantial data on long term performance by testing sections of X100 pipeline in near real world conditions. An accelerated operational period will be simulated by two years of pressure cycling, equivalent to forty years operation. This large scale trial will be complemented by a range of laboratory scale tests. During the course of the trial a substantial amount of data related to the assessment of corrosion defects in X100 grade pipe will be gathered. This report presents the results of a program of work that builds on the development work being conducted for PHMSA/PRCI Project #153 and for the corrosion defect assessment section of the BP X100 operational trial.

2 Background to Project #153

A description of the work conducted in Phase 1 of Project #153H is given in Reference [5]. In Project #153J, methods for assessing the remaining strength of corroded pipelines subjected to combined internal pressure and external loading were developed [8] for material strengths up to grade X65. As part of Project #153, PHMSA also requested GL to investigate the performance of methods such as ASME B31G and RSTRENG against an integrated test database of burst test results which included grade X80 and X100 materials [7]. Work is also progressing in Project #153K to develop a method for assessing the integrity of corroded pipe under cyclic pressure loading [9].

---

[2] Germanischer Lloyd acquired Advantica in 2007

[3] Reference [6] is a confidential Advantica report for BP Exploration. Basic details of the tests conducted on grade X100 pipe are given in References [9] and [10].

[4] For brevity, these materials will hereafter be referred to as grade X80 and X100 in this report.

3 Interface Between Project #153 and the BP X100 Operational Trial

A detailed technical description of the BP X100 Operational Trial is given in [9]. Briefly the trial comprises two sections of pipe of large diameter (48-inch nominal diameter); one of approximately 1968 ft (600 m) in length and the second of length 656 ft (200 m). Mainline construction methods have been used wherever possible. The longer section simulates a pipeline in normal service and incorporates cold bends, induction bends and crack arrestors. The shorter section includes damage types of various types, such as mechanical damage and simulated volumetric corrosion. Detailed design of the corrosion defects forms part of Project #153 and is described in Reference [12].

Figure 1 shows how the operational trial interfaces with Project #153. Briefly, data is obtained from a number of separate projects as follows:

- Tensile tests conducted on grade X100 material used for the BP Exploration operational trial (described in this report).
- Burst tests conducted by GL on grade X100 pipe with simulated volumetric corrosion defects for BP Exploration (Reference [6] and tests described in this report).
- Assessment of volumetric corrosion defects on the BP X100 Operational Trial under accelerated operating period (to be conducted when the trial has been completed).

Using these results, guidance for assessing the remaining strength of corroded pipe in strength grade up to X100 under internal pressure, external loading and cyclic internal pressure loading will be developed.

4 Work Scope

The work described in this report summarizes the results of tensile tests conducted on grade X100 material from three different manufacturers. Using these results, the work described in Project #153J [8] is extended to provide guidance for assessing the remaining strength of corroded pipe up to grade X100 both under static internal pressure loading and under combined internal pressure and external loading.

One of the recommendations given in [6] was to conduct two additional vessel burst tests using grade X100 pipe. Two tests were proposed; one with a relatively long groove defect and one with a relatively short groove defect. The results from these tests would augment the results already obtained and help to determine the suitability of methods such as ASME B31G and RSTRENG when assessing the remaining strength of corroded pipelines up to grade X100.

Section 5 of this report summarizes the results of the tensile tests; Section 6 describes the results of the two vessel burst tests and Section 7 describes the results of the finite element (FE) analysis undertaken to develop failure loci of corroded pipe under combined internal pressure and external loading.

5 Tensile Testing

The work reported in [6] recommended that the through wall tensile properties of grade X100 pipe are investigated. Variations in through wall tensile behavior are not unexpected for high strength steels due to the potential cooling rates during plate manufacture. Variations in strain during the U and O stages of the pipe forming process may also lead to these variations. There are no standard experimental methods available to quantify the tensile behavior of relatively thin walled pipe material. When conducting failure investigations on in-service structures and only a small amount of material is available, or when there has been a specific interest in to characterizing the local variation of tensile properties, then some researchers have developed a method using MFT specimens to determine tensile properties, see for example [13], [14]. This method was used to determine the through wall thickness tensile properties of grade X100 line pipe.

Grade X100 material was obtained from three different manufacturers, designated in this report as Manufacturer A, B and C. Details of the pipe from each manufacturer are given in Table 12-1. Tensile testing was conducted using MFT tests, round bar tests and ring expansion tests. The results from the round bar tests were used to calibrate the stress versus strain curves obtained from the MFT tests.

5.1 Round Bar and Miniature Flat Tensile Tests

Tensile testing was conducted on the samples listed in Table 12-1, using round bar and MFT specimens. The technique of using MFT specimens has been used to determine the tensile properties in a number of cases including:

- Determination of tensile properties when only small amounts of material are available;
- Determination of tensile properties for small weld geometry; and
- Determination of through thickness tensile properties; particularly through welds

MFT testing requires specialized test equipment. Only a few test houses can undertake this type of testing. GL contracted The Institute of Materials Research, GKSS[5], based in Germany, to conduct the test program. GKSS have been developing small scale tensile testing methods over the last 10 years.

A program of both ST and MFT testing was agreed with GKSS. The tests were conducted on six plates taken from the three different pipe manufacturers, A, B and C. The plates were machined from the pipe parent wall in both the longitudinal and transverse directions. With the longitudinal seam weld positioned at the 12 o'clock position, plates were machined at the 3 o'clock and 6 o'clock positions, as shown in Figure 2.

Ten MFT specimens were electro discharge machined (EDM) through the thickness of each of the six plates (Manufacturer A, B and C at the 3 o'clock and 6 o'clock positions in the longitudinal and transverse directions) to the dimensions given in Figure 3. A total of 120 test specimens were produced; these were numbered from one to ten, one being on the outer pipe surface and ten being on the inner surface. The identification numbers assigned to each of the samples is given in Table 12-1. Titanium oxide strips were sprayed onto each of the miniature specimens to allow strains to be measured using a laser system. Measurements of strains in this manner are preferred because they do not rely on contact with the specimen.

The results from the MFT specimens are capable of only providing the relative change in tensile properties through the pipe wall thickness. This is because the specimens are very thin and hence their fracture behavior can be affected by micro-structural constituents or cracking at structural discontinuities. To obtain a more representative material property variation through the wall thickness, GKSS recommended that the results obtained from the MFT specimens should be calibrated using standard round bar tensile specimens. For the ST test program, also conducted by GKSS, specimens were extracted from the middle of each plate in both the longitudinal and transverse directions, at the 3 o'clock and 6 o'clock positions. A total of 24 ST tests were conducted according to DIN 50125 [15], the results of which can be found in Table 12-7.

The calibration of MFT data was performed by calibrating the stress versus strain data from ST tests using a scaling approach. A calibration factor was determined from the difference between the MFT and standard tensile data, in strength ($R_{p0.2}$ and R_m) and strain ($\varepsilon_{p0.2}$ and ε_m). The MFT results were scaled by the factors calculated for each location and direction (see **Error! Reference source not found.** to Table 12-4); the results are shown in Figure 11 to Figure 22.

---

[5] http://www.gkss.de/institute/materials_research/index.html.en

When referring to the graphs and data tables, a system of numbering the samples has been applied such that each individual sample has a unique identifier. The first character in the MFT sample identifier refers to the manufacturer (A, B or C) the second refers to the circumferential location in relation to the seam weld (3 or 6 o'clock) the third character identifies whether the sample was taken in the longitudinal or transverse direction (L or T) and the final digits refer to the position through wall (1-10), where 1 is the outer pipe wall surface and 10 is the inner surface.

The calibration factors obtained from these tests vary with pipe manufacturer, specific material condition and test specimen orientation therefore they are not applicable to X100 grade steels in general. In order to determine a generalized calibration factor, an X100 sample with homogeneous microstructure and relieved residual stresses would have to be tested. Ideally a more sophisticated numerical approach to produce calibrated full stress-strain curves would have been used, but this would have proven more time consuming and costly.

5.1.1 Results

Figure 5 to Figure 10 show the stress versus strain results obtained from the ST tests for Manufacturers A, B and C. The calibrated stress-strain curves obtained from the MFT specimens are shown in Figure 11 to Figure 22 and the data is summarized in **Error! Reference source not found.** to Table 12-4. The trends in the results obtained from specimens for individual manufacturers are now discussed and consideration is given as to whether there are any particular patterns emerging from the full body of test data.

5.1.1.1 'Manufacturer A' Results

- The highest stresses for the 3 o'clock longitudinal samples [Figure 11] occurred at the outer wall and the lower stresses towards the inner wall. The variation between highest and lowest stress was 16%, suggesting that the properties do not vary to a large extent through the wall.
- This behavior appeared to be reversed in the 6 o'clock longitudinal samples [Figure 13], it should be noted that the through-wall stress behavior was difficult to establish as five of the ten MFT samples broke during testing, contributing to a large variation between highest and lowest stresses (24%). A low calibration factor of 0.964 was derived for the 6 o'clock longitudinal samples, which effectively reduced the calibrated MFT curves. However following correction all MFT samples still had a yield of 141,300 psi (974 MPa), which is above the specified minimum yield strength (SMYS) of 100,076 psi (690 MPa).
- The 3 o'clock transverse specimens [Figure 12] produced minimum yields which were in close agreement to the ring expansion test results (120,091 psi/828MPa and 121,831 psi/840MPa respectively) and the maximum yield values obtained were substantially above SMYS at 134,900 psi (930MPa). Two MFT samples broke during testing; hence it is difficult to establish the general behavior of the section. The highest yield stresses occurred towards the centre of the pipe wall and the variation between highest and lowest stress was 12%; suggesting that the properties do not vary to a large extent through the wall at the 3 o'clock location.
- As with the 3 o'clock transverse samples, the highest stress occurred at the centre of the pipe thickness and the lower stresses towards the outer wall [Figure 14]. The variation between highest and lowest stress was only 4%, suggesting that the properties do not vary to a large extent through the wall in the transverse direction.

5.1.1.2 'Manufacturer B' Results

- A large number of the MFT specimens failed with little elongation for this manufacturer; hence the plots of the experimental plots display incomplete stress-strain curves for a number of the samples.

- The 3 o'clock longitudinal plot [Figure 15] shows that the calibrated samples typically remained below the SMYS after scaling, mainly due to the fact that a small scaling factor was applied. A number of the samples broke during testing which resulted in a large variation in through-wall stress behavior (~40%) with the highest stress occurring at the inner wall and the lower stresses occurring at the outer wall. The unpredictable behavior of the samples may have been a result of the micro structural constituents of the samples.
- The through-wall stress behavior was again difficult to define in the 6 o'clock longitudinal tests [Figure 17] as three of the ten MFT samples broke, resulting in unpredictable through-wall characteristics. The variation between highest and lowest stress was 44%, which is similar to the variation seen at the 3 o'clock location in the longitudinal direction, as is the location of the highest yield stresses.
- The yield values of the 3 o'clock transverse specimens [Figure 16] were in good agreement with the values obtained from the ring expansion tests (121,700 psi/839 MPa and 123,100 psi/849 MPa). The variation between highest and lowest stress was only 11%, suggesting that the properties do not vary to a large extent through the wall at this direction and location. There was no particular trend as to the location of the highest and lowest yield stresses in these samples of material.
- There was a wide variation in the MFT results for the 6 o'clock transverse specimens [Figure 18]. The through-wall stress behavior was highly unpredictable with a large variation between the maximum and minimum yield stresses (~66%), with the highest and lowest stress occurring in the centre of the pipe wall, meaning that no common trends could be ascertained from this data set.

5.1.1.3 'Manufacturer C' Results

- The 3 o'clock longitudinal plot [Figure 19] shows that the scaled MFT samples, remained below SMYS due to a low calibration factor obtained from the ST tests. The through-wall stress behavior was fairly consistent with a minimal variation between highest and lowest stress of ~7% suggesting that the properties do not vary to a large extent through the wall for these samples.
- The 6 o'clock longitudinal plot [Figure 21] again showed MFT results with yields that were all below SMYS due to a low calibration factor obtained from the ST tests. The variation between highest and lowest stress was only 8%, suggesting that the properties do not vary to a large extent through the wall in the longitudinal direction. There was no particular trend as to the location of the highest and lowest yield stresses in these samples of material.
- The 3 o'clock transverse plot [Figure 20] showed good agreement between the MFT samples and the values obtained from the ring expansion tests [Table 12-6]. The variation between highest and lowest stress was only 13%, suggesting that the properties do not vary to a large extent through the wall. There was no particular trend as to the location of the highest and lowest yield stresses in these samples of material.
- The 6 o'clock transverse MFT specimens [Figure 22] were in good agreement with the values obtained from the ring expansion tests [Table 12-6]. The variation between highest and lowest stress was only 11%, suggesting that the properties do not vary to a large extent through the wall at the 6 o'clock location or in the transverse direction. There was no particular trend as to the location of the highest and lowest yield stresses in these samples of material.

5.1.1.4 Comparison of Results

There was generally greater variation in the yield strength of the MFT results in the longitudinal direction and lower yield strengths were achieved when compared to the transverse specimens. This reduction in longitudinal yield strengths was also identified in the manufacturer's data [Table 12-8] where the transverse yield strengths were typically 8-25% higher than those seen in the longitudinal direction.

No particular patterns emerged when considering the location from which the samples were taken (3 and 6 o'clock positions). The through wall stress distribution was reasonably consistent and typically varied by 10-25%, however when failures occurred in the samples much more variation in through-wall properties was seen (11-66%). No particular trends in terms of the location of maximum and minimum stress were observed across the samples and the variation in through wall stress does not appear to be linear.

It is difficult to establish the general behavior of the through-wall sections given that a large number of the MFT test specimens broke during testing, resulting in a large amount of scatter in the stress-strain curves. It is thought that the micro structure had a large influence on the results given the small sample sizes of the MFT specimens. Hence the scatter may be attributed to potential failure in the micro structural constituent, cracking at structural discontinuities or failure of the stripe due to straining. Given these results, it may have been useful to consider using less samples through the wall (e.g. five MFT specimens), therefore increasing the specimen sizes such that they were not as adversely influenced by the microstructural properties.

5.2 Hydraulic Ring Expansion Tests

Hydraulic ring expansion tests were carried out on GL's ring tension rig for each of the pipe samples given in Table 12-1. The objective was to compare the stress versus strain behavior of grade X100 material using ring expansion testing with that obtained from ST and miniature tensile tests.

The tests were carried out in accordance with ASTM A370 [16]. A full metrology of each ring was carried out prior to testing; the results are summarized in Table 12-5. Each ring specimen was instrumented using strain gauges as recommended in the testing standard. The test requirements were that the ring to be taken to a minimum of 0.5 % strain, which equates to a circumferential extension of $^{26}/_{32}$ inch (20.72 mm) for the 52 inch ring sample and ¾ inch (19.15 mm) for the 48 inch ring samples.

Additional strain gauges were also positioned directly opposite the seam weld, at 90° to the weld and adjacent to the weld cap. Two strain gauges were installed at each location spaced equally off centre to allow the circumferential tape to be positioned correctly, as is illustrated in Figure 23.

5.2.1 Results

The 48 inch diameter Manufacturer A and Manufacturer B ring samples showed a set of results that were not predictable. Two rings were tested for each manufacturer and in each case failure occurred unexpectedly at the seam weld heat affected zone at a strain level below 0.5 %. The failures occurred from the toe at the weld cap on the inner side of the ring; little necking was observed prior to failure. Examples of the failure are shown in Figure 24 and Figure 25. Figure 26 and Figure 27 plot the circumferential strain for these samples up to the point of failure.

In contrast, for the two ring expansion tests undertaken using 52 inch diameter Manufacturer C pipe, a strain level of 0.5 % was achieved. It was found that there was some plastic deformation at the seam weld but the deformation was uniform. Figure 28 shows the circumferential strain up to the point where the test was ended. A summary of the strains achieved for each sample and the yield stresses can be seen in Figure 29 and Figure 30.

6 Full Scale Burst Testing and Comparison of Failure Pressures with Assessment Methods

Reference [6] describes the results of ring expansion and vessel burst testing on grade X100 material with defects machined on the external surface of the pipe to simulate external corrosion damage. One of the recommendations given in [6] was to conduct two additional vessel burst tests using grade X100 pipe. Two tests were proposed; one with a relatively long groove defect and one with a relatively short groove defect such that the failure pressures would be targeted either side of the transition point on the ASME B31G assessment curve. It was considered that the results from these addition two burst tests would augment those already conducted to determine the suitability of methods such as ASME B31G and RSTRENG when assessing the remaining strength of corroded pipelines up to grade X100.

6.1 Vessel Preparation

52-inch (1320.8 mm) diameter grade X100 material was supplied by BP Exploration from Manufacturer C, see section 5 above. The nominal wall thickness of the pipe was $^{13}/_{16}$ inch (20.6 mm).

Two groove type defects were machined into the external surface of the pipe wall with a spherical radius, R that was equal to the target defect depth (50% of wall thickness). After machining, each pipe was subjected to a full metrology examination as shown in Appendix B. The defect depth and length for each test was chosen as follows:

1. Test 1

   Axial groove defect, length 79 inches (2000 mm) and with a target defect depth equal to 50% of the pipe wall thickness.

2. Test 2

   Axial groove defect, length 29 inches (745mm) and with a target defect depth equal to 50% of the pipe wall thickness.

Test ends were welded to each end of a pipe section to form a pressure vessel. The material used to construct the pup pieces for the test ends was 52 inches (1320.8 mm) diameter, 1 inch (26 mm) thick grade X80 linepipe. The dome ends were forged from $1^{18}/_{32}$ inch (40 mm) thick plate to grade P460NL1 to WPL6 specification. The end of each pup piece to be welded to a pipe test section was transitioned (1:4) to match the thickness of the pipe test section. A standard butt weld end preparation was machined onto the end of each pup piece, comprising a 30° flank angle and a $^{1}/_{32}$ inch (1mm) root face.

Each test end was fitted with a class 2500 long weld neck flange. The fittings were used for filling/draining, and pressurization.

The pup piece test ends were welded to the pipe test section using a SMAW procedure with low hydrogen electrodes for the fill and capping passes. The weld procedure used was the same procedure as that developed by GL for BP Exploration to conduct fracture propagation tests on grade X100 pipe. Figure 31 and Figure 32 show views of the fully fabricated and instrumented test vessels before the burst tests were conducted.

6.2 Test Method

Each test was carried out with the test vessel mounted on two heavy duty free standing ‘vee’ support frames. Once the vessel was positioned onto the supports, ratchet straps were used to restrain the vessel from moving. The ratchet straps were secured to anchoring points that were bolted to the ground.

Each vessel was instrumented with strain gauges to measure the nominal hoop and axial strain on the outer surface of the vessel. With the seam weld located at the 12 o’clock position, the defect located at the 9 o’clock position and hoop and axial strain gauges were located at the 3 o’clock and 6 o’clock positions.

The vessel was filled with water using twin Haskel DSF72 air driven positive displacement pumps. Once the vessel was full and all the air had been removed a Druck PTX1400 0-3625 psi (0-250bar) pressure transducer was connected to the vessel[6].

The tests were undertaken using a generic burst test risk assessment, which included the use of an exclusion zone and of 2204.6 lb (1 tonne) sand bags stacked adjacent to the dome ends that were used to contain any flying debris in the event that the vessel were to fail in a catastrophic manner.

During each test a data logger was used to continuously record test duration, ambient air temperature (from a K-type thermocouple), pressure and the strain gauges readings.

6.3 Results

The pressure versus time plot for Test 1 and 2 is shown in Figure 33 and Figure 34 respectively. Figure 35 and Figure 36 show photographs of each vessel after rupture. The failure pressures for Test 1 and 2 were 1755 psi (121 bar) and 1987 psi (137 bar) respectively.

6.4 Analysis and Assessment of Test Results

The predicted failure pressure (P_f) using ASME B31G, Modified ASME B31G, RSTRENG, LPC-1 and SHELL92[7] is compared to the recorded burst pressure P_A for each of the two tests. Values of the ratio (P_A/P_f) for each assessment method are summarized in Table 12-9. The predicted failure pressures were calculated using specified minimum material properties as required by standard assessment methods such as ASME B31G[8]. The results show that the ASME B31G and SHELL92 methods give predicted failure pressures lower than actual recorded burst pressures. The RSTRENG and LPC-1 methods predict failure pressure very close to the recorded failure pressure, however, the recorded failure pressures were marginally higher (3%) than the predicted failure pressure. The greatest discrepancy is obtained using the Modified ASME B31G method. For both cases the Modified ASME B31G method under predicts the failure pressure. This result is consistent with that already discussed in GL Reports 6781 [7] and R9017 [5]. In particular it is highlighted that use of the shape correction factor of 0.85 in the Modified ASME B31G method is considered inappropriate for relatively long defects, particularly when assessing machined defects.

It is to be noted that no other safety factors were included in the failure predictions. The recommendation has already been made in [7] (Section 8.3) that a focused program of full-scale burst tests are conducted on high strength pipe with simulated defects that represent real corrosion damage in the field.

7 Assessment of Corroded Pipelines under Combined Internal Pressure and Secondary Loading

Reference [8] summarizes the approach taken to develop a method for assessing the remaining strength of corroded pipelines under combined internal pressure and secondary loading. Results of a detailed non-

[6] The pressure transducer was calibrated against a dead-weight tester prior to connecting to the vessel.

[7] These methods are described in Advantica Report 6781 Issue 5.0

[8] The failure predictions were consistent with the Case 2 Assessments as described in Advantica Report 6781 Issue 5.0, i.e. the flow stress was calculated using specified minimum material properties.

linear finite element (FE) analysis study to develop a method for assessing the remaining strength of corroded pipelines subjected to combined internal pressure and external loading. The results described in [8] were obtained by investigating the following pipe geometries and materials:

- Pipe Diameter, D, 36 inch (914.4 mm) and wall thickness, t, ½ inch (12.7 mm)

  [D/t=72], API 5L Grade X65
- Pipe Diameter, D, 18 inch (457.2 mm) and wall thickness, t, $^{7}/_{32}$ inch (5.6 mm) [D/t=82], API 5L Grade B/X42
- Pipe Diameter, D, 8 inch(219.1 mm) and wall thickness, t, $^{5}/_{16}$ inch (8.2 mm)

  [D/t=27], API 5L Grade B/X42
- Pipe Diameter, D, 48 inch(1219.2 mm) and wall thickness, t, $^{15}/_{32}$ inch (11.73 mm) [D/t=104], API 5L Grade X65

For this project, the assessment method has been extended to cover higher strength grade X80 and X100 pipelines. The pipe geometry and material analyzed is summarized as follows:

- Pipe Diameter, D, 48 inch (1219.2 mm) and wall thickness, t, $^{25}/_{32}$ inch (19.8 mm) [D/t=61.6], API 5L Grade X80 and X100

This choice was made in agreement with the PRCI project team. For grade X80 material, the pipe geometry chosen is common for PRCI members; for grade 100 material, the pipe geometry chosen is consistent with that used for the BP X100 trial.

7.1 Non-Linear FE Analysis

Three dimensional FE models of the 48 inch (1219.2 mm) diameter pipe were constructed in an identical manner to that described in [8]. Models were constructed to simulate patch, axial/circumferential groove and pit volumetric corrosion defects on the external surface of the pipe wall. Defect depths of 20%, 50% and 80% of the pipe wall thickness were modeled. Typical examples of FE meshes generated are shown in Figure 37 to Figure 40. Young's modulus and Poisson's ratio used in the analyses were consistent with that used in [8]. Stress versus strain data for grade X80 pipe was obtained from [5]; the stress versus strain curve for grade X100 pipe was obtained following review of the material's test program described in Section 5. A comparison of the stress versus strain curves used in the FE analysis described in this report is shown in Figure 41. The true ultimate tensile strength of grade X80 and X100 material was taken to be 97,320 psi (671 MPa) and 119,729 psi (852.5 MPa) respectively.

7.2 Failure Criteria

The criteria used to assess failure of the pipe were again consistent with that described in [8] and was based on the following:

1. Local failure of the pipe at the remaining ligament.
2. Global yielding of the pipe cross section.

In each case, failure of the pipe is deemed to occur when the lowest combination of internal pressure/external loading from the above criteria is predicted.

7.2.1 Local Failure

Local failure occurs when the remaining ligament fails by local necking or buckling. Local necking is dominated by internal pressure loading with small negative bending moments for patch and axial groove defects or by positive bending moments for deeper circumferentially orientated groove defects. Very high compressive loads are required to cause local buckling failure. Figure 42 and Figure 43 show deformed FE plots of local necking and buckling failures in a pipe with a patch defect.

7.2.2 Global Yielding

Failure of the pipe by global yielding is deemed to occur when the von Mises equivalent stress in the pipe reaches the yield strength. The critical pressure, P_o, moment, M_o, and axial compressive force, F_o, are given by Equations 1 to 3.

$$P_0 = \frac{(2\alpha - 1)}{(\alpha - 1)\sqrt{3\alpha^2 - 3\alpha + 1}}\sigma_{SMYS} \quad (1)$$

$$M_0 = \frac{I\sigma_{SMYS}}{R_o} \quad (2)$$

$$F_0 = \pi\left(R_0^2 - R_i^2\right)\sigma_{SMYS} \quad (3)$$

When the pipe is subjected to combined internal pressure and in-plane bending, yielding will occur at either the 12 o'clock or 6 o'clock positions depending on whether a positive or a negative bending moment has been applied. The critical bending moment, M_{crit} and the critical internal pressure, P_{crit} is given by equations 4 below.

$$\frac{M_{crit}}{M_0} = \frac{1}{2}\sqrt{4 - 3\frac{(2\alpha - 1)^2}{3\alpha^2 - 3\alpha + 1}\left(\frac{P_{crit}}{P_0}\right)^2} - \frac{1}{2\sqrt{3\alpha^2 - 3\alpha + 1}}\left(\frac{P_{crit}}{P_0}\right) \quad (4)$$

For common transmission pipeline geometries, α tends to be relatively large and Equation (4) can be approximated by Equation (5).

$$\frac{M_{crit}}{M_0} \approx \sqrt{1 - \left(\frac{P_{crit}}{P_0}\right)^2} \quad (5)$$

For combined internal pressure and axial compressive loading, the relationship between the critical compressive force, F_{crit} and the critical internal pressure, P_{crit} to cause global yielding of the pipe can be expressed in non-dimensional form by Equation (6):

$$\frac{F_{crit}}{F_0} = \frac{1}{2}\sqrt{4 - 3\frac{(2\alpha - 1)^2}{3\alpha^2 - 3\alpha + 1}\left(\frac{P_{crit}}{P_0}\right)^2} - \frac{1}{2\sqrt{3\alpha^2 - 3\alpha + 1}}\left(\frac{P_{crit}}{P_0}\right) \quad (6)$$

As noted above, α tends to be relatively large for transmission pipelines and Equation (6) can be approximated by Equation (7).

$$\frac{F_{crit}}{F_0} \approx \sqrt{1-\left(\frac{P_{crit}}{P_0}\right)^2} \qquad (7)$$

Where; R_o and R_i are the pipe outer and inner radii; t is the pipe wall thickness; σ_{SMYS} is the specified minimum yield strength and $\alpha = \frac{R_0}{t}$. The derivation of these equations is presented in Appendix C; they were used as appropriate to determine global failure of the pipe.

7.3 Results

For corrosion defect depths up to 20% of the pipe wall thickness, t, failure is by global yielding rather than failure at the remaining ligament by local necking or buckling.

For the pit defects of depths up to 80% of the pipe wall thickness, t, failure is by global yielding rather than failure at the remaining ligament by local necking or buckling.

For combined internal pressure and bending loads, failure by local necking at the remaining ligament occurs for relatively high internal pressures and low bending moments which apply compressive loading. For circumferential groove defects, local necking at the remaining ligament occurs under a combination of relatively low internal pressure and high bending moments which apply tensile loading.

For combined internal pressure and compressive bending loads, failure by local necking occurs for relatively high internal pressures and low bending loads. Local bucking failure occurs under a combination of relatively low internal pressure and high bending moments which apply a tensile loading in the vicinity of the remaining ligament.

Failure locus diagrams similar to those described in [8] were derived for grade X80 and X100 material. Figure 44 to Figure 51 show non-dimensional failure locus diagrams for assessing patch, axial groove, circumferential groove and pit defects in pipelines of strength grades up to X100, using the equations given in section 7.2 as appropriate.

8 Summary and Discussion

A comprehensive tensile test program on grade X100 linepipe from three different manufacturers has been conducted. Tensile testing has been conducted using standard ST, ring expansion and MFT specimens.

The results from the MFT specimens were only able to provide the relative change in material properties through the pipe wall. Additional calibration of the results from MFT specimens was required using standard ST tests.

Using the ST and the MFT specimens, the following conclusions were drawn from the results:

- Scatter in tensile properties is observed for all three manufacturers. Yield strength and ultimate tensile strengths below specified minimum values were obtained from some of the MFT test results. A possible explanation of this may be due to the very thin size of the MFT specimens which may have affected the failure behavior. This is the reason why calibration of the MFT specimens using standard ST specimens was required. It would be possible to investigate this by extracting fewer, hence thicker, specimens through the pipe wall. It is suggested that no more than five through thickness MFT specimens should be used in any future test program to investigate the tensile properties of high strength pipe.

- There was no identifiable pattern of tensile property variation through the wall thickness.
- Stress versus strain behavior for Manufacturer A was the most consistent. Tensile strengths were greatest using material from Manufacturer B. However, the variation in tensile properties through the wall thickness was most pronounced for Manufacturer B.
- The tensile tests for Manufacturer C gave some inconsistent results. The 3 o'clock samples tended to give higher tensile strengths towards the outer pipe wall. Lower tensile strengths tended to be obtained at the inner pipe surface, with some variation through the pipe wall thickness.

Following a review of the calibrated test results from the three manufacturers, a lower bound stress versus strain curve for grade X100 material was derived; this curve was used for non-linear FE simulations to predict the failure behavior of corroded X100 pipe.

In Project #153J [8] the FE method was used to generate failure locus diagrams for assessing corrosion damage in pipelines subjected to both internal pressure loads and external loading. The approach described in [8] was developed for assessing damaged pipelines of strength grade up to X65. In this report, the method described in [8] has been extended to allow the assessment of pipelines up to grade X100. Using the results from [8] and those described in this report, failure locus diagrams have been normalized, allowing them to be used for the range of pipeline geometries and material grades up to X100.

A further two full scale vessel tests were conducted using 52 inch diameter grade X100 line pipe. The predicted failure pressure (P_f) using ASME B31G, Modified ASME B31G, RSTRENG, LPC-1 and SHELL92[9] was compared to the recorded burst pressure P_A for each of the two tests. The predicted failure pressures were calculated using specified minimum material properties as required by standard assessment methods such as ASME B31G[10]. The results show that the ASME B31G and SHELL92 methods give predicted failure pressures lower than recorded burst pressures. The RSTRENG and LPC-1 methods predict failure pressures very close to the recorded failure pressure, however, the recorded failure pressures were within 3% of the predicted failure pressure. The greatest discrepancy was obtained using the Modified ASME B31G method. For both cases the Modified ASME B31G method under predicts the failure pressure; this result is consistent with that already discussed previously [7], [5]. In particular it is highlighted that use of the shape correction factor of 0.85 in the Modified ASME B31G method is considered inappropriate for relatively long defects, particularly when assessing machined defects. It is to be noted that no other safety factors were included in the failure predictions. The recommendation has already been made in [7] (Section 8.3) that a focused program of full-scale burst tests are conducted on high strength line pipe with simulated defects that represent real corrosion damage in the field.

Once the BP X100 Operational Trial has been completed, pipe with machined defects to simulate volumetric corrosion will be available. BP Exploration may also have additional grade X100 pipe available for testing. It is recommended that this material is used to develop a focused program of tests to validate the methods described in this report and those described for Project #153K [9].

---

[9] These methods are described in GL Report 6781 Issue 5.0

[10] The failure predictions were consistent with the Case 2 Assessments as described in GL Report 6781 Issue 5.0, i.e. the flow stress was calculated using specified minimum material properties.

9 Conclusions

1. Miniature flat tensile (MFT) testing was able to provide the relative change in tensile properties through the pipe wall thickness. Stress versus strain curves from the MFT tests have to be calibrated using results obtained from standard ST tests.
2. From the standard tensile (ST) test results, it was concluded that tensile properties in the longitudinal direction tended to be lower than those in the transverse direction.
3. Scatter in tensile properties was observed from X100 grade line pipe material obtained from three different manufacturers. No identifiable trends in tensile properties through the pipe wall thickness could be determined from the three different manufacturers. It was, however, concluded that in general lower tensile strengths were obtained towards the inner surface of the pipe.
4. Two full scale vessel burst tests were successfully conducted with relatively long axially orientated groove defects that were machined onto the external surface of the pipe. Both defects were targeted to have a depth of 50% of the pipe wall with lengths of 29.3 inch (745mm) and 78.7 inch (2000mm). Failure pressures predicted using ASME B31G and SHELL92 methods were lower than the actual burst pressures recorded from tests. The RSTRENG and LPC-1 methods predicted failure pressure very close (within 3%) to the recorded burst pressures. However, the predicted failure pressures were marginally higher the recorded burst pressures. For both burst tests, the Modified ASME B31G method predicted failure pressures higher than the recorded burst pressures.
5. Normalized failure locus diagrams have been derived for assessing corrosion damage in pipelines of strength grade up to X100 subject to combined internal pressure and external loading.

10 Recommendations

1. Validation of the assessment methods described in this report should be undertaken on completion of the BP X100 Operational Trial.
2. The normalized failure locus diagrams derived in this report should be incorporated into the PRCI Guidance Document for assessing corrosion damage in pipelines.

11 References

1. Anon. ‘Manual for Determining the Remaining Strength of Corroded Pipelines. A Supplement to ASME B31 Code for Pressure Piping’, ASME B31G-1991. The American Society of Mechanical Engineers.
2. Kiefner, J. F. and Vieth, P.H. ‘A Modified Criterion for Evaluating the Remaining Strength of Corroded Pipe’, Final report on PR-3-805 to Pipeline Corrosion Supervisory Committee of the Pipeline Research Committee of the American Gas Association, Battelle, Ohio.
3. Vieth, P. H. and Kiefner, J. F. ‘RSTRENG2 User’s Manual’, Final report on PR-218-9205 to Corrosion Supervisory Committee, Pipeline Research Committee, American Gas Association, Kiefner & Associates, Inc., Ohio.
4. Fu, B. and Batte, A. D. ‘Advanced Methods for the Assessment of Corrosion in Linepipe’, Summary Report OTO 97065, UK Health and Safety Executive, London, 1998
5. Chauhan, V. and Crossley, J., ‘Project #153H Corrosion Assessment Guidance for High Strength Steels (Phase 1)’, GL Report Number R9017 Issue 3.0, October 2008
6. Wood, A., Morgan, G., and Swankie, T., ‘Ring Tension and Full Scale Burst Testing of Grade X100 Linepipe Material’, GL Report Number R7702, Issue 1.0, November 2005, Confidential Report Prepared for BP Exploration
7. Chauhan, V., Brister, J. and Dafea, M., ’A Review of Methods for Assessing the Remaining Strength of Corroded Pipelines’, GL Report 6781 Issue 5.0, October 2008 (to be revised)
8. Liu, J., Chauhan, V., Ng, P., Wheat, S., and Hughes, C.,’Project #153J Remaining Strength of Corroded Pipe Under Secondary (Biaxial) Loading’, GL Report Number R9068, Issue 2.0, June 2008
9. Swankie, T., Robinson, M., Liu, J., Crossley, J. and Morgan, G.,’Project #153K The Assessment of Corrosion Damage in Pipelines Subjected to Cyclic Pressure Loading’, GL Report R8928 Issue 2.0 (Draft), November 2008
10. Anon., ‘Specification for Linepipe’, ANSI/API Specification 5L, Fort-Fourth Edition/ISO 3183:2007 (Modified), Petroleum and Natural Gas Industries – Steel Pipe for Pipeline Transportation, American Petroleum Institute, October 2007
11. Andrews, R.M., ‘Operational Trial for X100 Pipelines – Technical Description for DOT OPS’, GL Technical Memorandum, Ref 1009323, December 2006
12. Andrews, R.M. and Crossley, J., ‘Corrosion Defect Design for the BP X100 Operational Trial’, GL Report R9245, Issue 2.0, December 2006
13. Dobi, D. and Junghans, E., ‘Determination of the Tensile Properties of Specimens with Small Dimensions’, Kovine, Zlitine, Technologije 33 (1999) 6
14. Ceyhan, U., Horstmann and Dogan, B., ‘High Temperature Cross-Weld Characterization of Steel Weldments’, Materials at High Temperature, Volume 23, Number 3/4 2006

15. Anon., ‘Testing of metallic materials - Tensile test pieces’, DIN 50125, January 2004.

16. Anon., ‘Standard Test Methods and Definitions for Mechanical Testing of Steel Products’ ASTM A370 - 08a, ASTM, 2008.

12 Tables

Diameter	Manufacturer	GL Identifier	Extraction Location	MFT Specimen Numbers		ST Specimen No.	
				Longitudinal (L)	Transverse (T)	Longitudinal (L)	Transverse (T)
48 inch	A	HLT	3 o'clock	A3L1-A3L10	A3T1-A3T10	A3L-ST1 A3L-ST2	A3T-ST1 A3T-ST2
			6 o'clock	A6L1-A6L10	A6T1-A6T10	A6L-ST1 A6L-ST2	A6T-ST1 A6T-ST2
48 inch	B	HLR	3 o'clock	B3L1-B3L10	B3T1-B3T10	B3L-ST1 B3L-ST2	B3T-ST1 B3T-ST2
			6 o'clock	B6L1-B6L10	B6T1-B6T10	B6L-ST1 B6L-ST2	B6T-ST1 B6T-ST2
52 inch	C	HKX	3 o'clock	C3L1-C3L10	C3T1-C3T10	C3L-ST1 C3L-ST2	C3T-ST1 C3T-ST2
			6 o'clock	C6L1-C6L10	C6T1-C6T10	C6L-ST1 C6L-ST2	C6T-ST1 C6T-ST2

Table 12-1 – Pipe Specimen Details

MFT Sample Number	3 o'clock Longitudinal Yield Stress (PSI)	3 o'clock Longitudinal Tensile Strength (PSI)	3 o'clock Transverse Yield Stress (PSI)	3 o'clock Transverse Tensile Strength (PSI)	6 o'clock Longitudinal Yield Stress (PSI)	6 o'clock Longitudinal Tensile Strength (PSI)	6 o'clock Transverse Yield Stress (PSI)	6 o'clock Transverse Tensile Strength (PSI)
1	113674.51 (783.8 MPa)	126944.76 (875.3 MPa)	130106.41 (897.1 MPa)	130802.56 (901.9 MPa)	122361.81 (843.7 MPa)	139359.33 (960.9 MPa)	102333.17 (705.6 MPa)	103174.34 (711.4 MPa)
2	108351.91 (747.1 MPa)	123377.02 (850.7 MPa)	120113.85 (828.2 MPa)	120984.03 (834.2 MPa)	113616.5 (783.4 MPa)	139605.88 (962.6 MPa)	104581.13 (721.1 MPa)	105132.25 (724.9 MPa)
3	103652.94 (714.7 MPa)	117561.32 (810.6 MPa)	135008.43 (930.9 MPa)	135008.43 (930.9 MPa)	-	-	102478.2 (706.6 MPa)	103594.93 (714.3 MPa)
4	107046.64 (738.1 MPa)	122419.82 (844.1 MPa)	-	-	-	-	105828.39 (729.7 MPa)	107655.77 (742.3 MPa)
5	103493.41 (713.6 MPa)	119011.62 (820.6 MPa)	-	-	137415.93 (947.5 MPa)	157081.99 (1083.1 MPa)	106248.98 (732.6 MPa)	107090.15 (738.4 MPa)
6	97344.136 (671.2 MPa)	114327.15 (788.3 MPa)	-	-	-	-	105001.72 (724 MPa)	107931.33 (744.2 MPa)
7	98156.304 (676.8 MPa)	114008.08 (786.1 MPa)	133427.6 (920 MPa)	134486.32 (927.3 MPa)	-	-	103594.93 (714.3 MPa)	106394.01 (733.6 MPa)
8	103014.81 (710.3 MPa)	118054.42 (814 MPa)	132035.31 (910.4 MPa)	133079.53 (917.6 MPa)	141302.73 (974.3 MPa)	159257.44 (1098.1 MPa)	105277.28 (725.9 MPa)	108496.94 (748.1 MPa)
9	98315.837 (677.9 MPa)	114167.62 (787.2 MPa)	130802.56 (901.9 MPa)	131861.28 (909.2 MPa)	-	-	106118.45 (731.7 MPa)	108772.5 (750 MPa)
10	101550.01 (700.2 MPa)	116589.62 (803.9 MPa)	122216.78 (842.7 MPa)	125189.9 (863.2 MPa)	123812.11 (853.7 MPa)	153441.74 (1058 MPa)	105973.42 (730.7 MPa)	108351.91 (747.1 MPa)

Table 12-2 – Manufacture A Yield & Tensile Strengths from MFT Tests

MFT Sample Number	3 o'clock Longitudinal Yield Stress (PSI)	3 o'clock Longitudinal Tensile Strength (PSI)	3 o'clock Transverse Yield Stress (PSI)	3 o'clock Transverse Tensile Strength (PSI)	6 o'clock Longitudinal Yield Stress (PSI)	6 o'clock Longitudinal Tensile Strength (PSI)	6 o'clock Transverse Yield Stress (PSI)	6 o'clock Transverse Tensile Strength (PSI)
1	109526.7 (755.2 MPa)	123203 (849.5 MPa)	96517.5 (665.5 MPa)	100505.8 (693 MPa)	97097.6 (669.5 MPa)	99751.6 (687.8 MPa)	84218.9 (580.7 MPa)	95284.7 (657 MPa)
2	104102.5 (717.8 MPa)	116270.6 (801.7 MPa)	102188.1 (704.6 MPa)	105103.2 (724.7 MPa)	-	-	94690.1 (652.9 MPa)	101027.9 (696.6 MPa)
3	111774.6 (770.7 MPa)	123768.6 (853.4 MPa)	107713.8 (742.7 MPa)	108946.5 (751.2 MPa)	93544.4 (645 MPa)	97532.7 (672.5 MPa)	87163 (601 MPa)	97054.1 (669.2 MPa)
4	105407.8 (726.8 MPa)	117401.8 (809.5 MPa)	102492.7 (706.7 MPa)	104030 (717.3 MPa)	95908.3 (661.3 MPa)	98867 (681.7 MPa)	99418 (685.5 MPa)	104726.1 (722.1 MPa)
5	-	-	98504.4 (679.2 MPa)	102043.1 (703.6 MPa)	-	-	94255 (649.9 MPa)	100882.9 (695.6 MPa)
6	-	-	101579 (700.4 MPa)	106176.5 (732.1 MPa)	-	-	85988.3 (592.9 MPa)	93950.4 (647.8 MPa)
7	105219.3 (725.5 MPa)	117952.9 (813.3 MPa)	140940.2 (971.8 MPa)	100505.8 (693 MPa)	-	-	139533.4 (962.1 MPa)	139968.5 (965.1 MPa)
8	145102.5 (1000.5 MPa)	145668.1 (1004.4 MPa)	-	-	97692.2 (673.6 MPa)	100795.9 (695 MPa)	116517.1 (803.4 MPa)	120795.5 (832.9 MPa)
9	122071.8 (841.7 MPa)	131629.2 (907.6 MPa)	103725.5 (715.2 MPa)	107104.7 (738.5 MPa)	118518.5 (817.2 MPa)	118968.1 (820.3 MPa)	-	-
10	107467.2 (741 MPa)	118895.6 (819.8 MPa)	98663.9 (680.3 MPa)	100505.8 (693 MPa)	134341.3 (926.3 MPa)	134631.3 (928.3 MPa)	104871.2 (723.1 MPa)	109439.6 (754.6 MPa)

Table 12-3 - Manufacturer B Yield & Tensile Strengths from MFT Tests

MFT Sample Number	3 o'clock Longitudinal Yield Stress (PSI)	3 o'clock Longitudinal Tensile Strength (PSI)	3 o'clock Transverse Yield Stress (PSI)	3 o'clock Transverse Tensile Strength (PSI)	6 o'clock Longitudinal Yield Stress (PSI)	6 o'clock Longitudinal Tensile Strength (PSI)	6 o'clock Transverse Yield Stress (PSI)	6 o'clock Transverse Tensile Strength (PSI)
1	87902.7 (606.1 MPa)	91557.4 (631.3 MPa)	99969.2 (689.3 MPa)	112166.2 (773.4 MPa)	90571.2 (624.5 MPa)	91020.8 (627.6 MPa)	103623.9 (714.5 MPa)	117938.4 (813.2 MPa)
2	90948.3 (627.1 MPa)	93399.3 (644 MPa)	103827 (715.9 MPa)	118866.6 (819.6 MPa)	95110.6 (655.8 MPa)	95719.8 (660 MPa)	105436.8 (727 MPa)	118533 (817.3 MPa)
3	90034.6 (620.8 MPa)	95386.2 (657.7 MPa)	109715.2 (756.5 MPa)	120897 (833.6 MPa)	94516 (651.7 MPa)	95415.2 (657.9 MPa)	104827.7 (722.8 MPa)	117735.4 (811.8 MPa)
4	93544.4 (645 MPa)	95386.2 (657.7 MPa)	112775.3 (777.6 MPa)	123130.5 (849 MPa)	93602.4 (645.4 MPa)	94211.5 (649.6 MPa)	104421.6 (720 MPa)	116720.1 (804.8 MPa)
5	88816.4 (612.4 MPa)	94922.1 (654.5 MPa)	107887.8 (743.9 MPa)	119881.8 (826.6 MPa)	91325.4 (629.7 MPa)	91470.4 (630.7 MPa)	110266.3 (760.3 MPa)	123783.1 (853.5 MPa)
6	92021.5 (634.5 MPa)	96604.5 (666.1 MPa)	105248.3 (725.7 MPa)	119272.7 (822.4 MPa)	92848.2 (640.2 MPa)	93906.9 (647.5 MPa)	102405.7 (706.1 MPa)	115719.4 (797.9 MPa)
7	90643.8 (625 MPa)	94313 (650.3 MPa)	111136.5 (766.3 MPa)	121709.2 (839.2 MPa)	93602.4 (645.4 MPa)	94052 (648.5 MPa)	99389 (685.3 MPa)	111484.6 (768.7 MPa)
8	92485.6 (637.7 MPa)	94617.6 (652.4 MPa)	110527.4 (762.1 MPa)	121303 (836.4 MPa)	87830.2 (605.6 MPa)	88598.8 (610.9 MPa)	104421.6 (720 MPa)	117126.2 (807.6 MPa)
9	93399.3 (644 MPa)	95850.3 (660.9 MPa)	102811.8 (708.9 MPa)	118054.4 (814 MPa)	94052 (648.5 MPa)	94516 (651.7 MPa)	105030.7 (724.2 MPa)	116720.1 (804.8 MPa)
10	94313 (650.3 MPa)	95850.3 (660.9 MPa)	113181.4 (780.4 MPa)	123333.5 (850.4 MPa)	92543.6 (638.1 MPa)	93906.9 (647.5 MPa)	105639.9 (728.4 MPa)	118736 (818.7 MPa)

Table 12-4 - Manufacturer C Yield & Tensile Strengths from MFT Tests

Pipe Manufacturer	Ring Sample Number	Ring Sample Wall Thickness (inches)								Ring Sample Outside Diameter (inches)			
		1	2	3	4	5	6	7	Average	1-5	2-6	3-7	Average
A	R1	0.79 (20.08mm)	0.80 (20.22mm)	0.79 (19.97mm)	0.79 (19.97mm)	0.79 (20.01mm)	0.79 (20.13mm)	0.79 (19.96mm)	0.79 (20.05mm)	47.99 (1219mm)	48.19 (1224mm)	47.83 (1215mm)	47.99 (1219mm)
	R2	0.79 (19.99mm)	0.80 (20.20mm)	0.79 (20.02mm)	0.79 (20.02mm)	0.79 (19.98mm)	0.80 (20.20mm)	0.80 (20.24mm)	0.79 (20.09mm)	47.87 (1216mm)	48.15 (1223mm)	47.99 (1219mm)	47.99 (1219mm)
B	R1	0.78 (19.80mm)	0.78 (19.90mm)	0.78 (19.78mm)	0.78 (19.84mm)	0.78 (19.74mm)	0.78 (19.79mm)	0.78 (19.87mm)	0.78 (19.82mm)	47.91 (1217mm)	47.99 (1219mm)	48.03 (1220mm)	47.99 (1219mm)
	R2	0.78 (19.89mm)	0.79 (19.96mm)	0.78 (19.80mm)	0.78 (19.91mm)	0.78 (19.80mm)	0.79 (19.94mm)	0.79 (19.94mm)	0.78 (19.89mm)	47.91 (1217mm)	48.03 (1220mm)	48.07 (1221mm)	47.99 (1219mm)
C	R1	0.80 (20.30mm)	0.81 (20.60mm)	0.80 (20.43mm)	0.80 (20.43mm)	0.80 (20.41mm)	0.81 (20.55mm)	0.81 (20.49mm)	0.81 (20.46mm)	51.89 (1318mm)	51.73 (1314mm)	51.85 (1317mm)	51.81 (1316mm)
	R2	0.80 (20.31mm)	0.81 (20.57mm)	0.80 (20.44mm)	0.81 (20.52mm)	0.80 (20.44mm)	0.81 (20.68mm)	0.81 (20.53mm)	0.81 (20.50mm)	51.89 (1318mm)	51.85 (1317mm)	51.97 (1320mm)	51.89 (1318mm)

Table 12-5 – Ring Sample Metrology Readings Prior to Testing

Pipe Manufacturer	Ring Sample Number	Max Stress (PSI)	% Strain
A	R1	122724 (846.2 MPa)	0.45
	R2	121651 (838.8 MPa)	0.44
B	R1	121666 (838.9 MPa)	0.47
	R2	123101 (848.8 MPa)	0.45
C	R1	106858 (736.8 MPa)	0.51
	R2	106031 (731.1 MPa)	0.51

Table 12-6 - Maximum Stresses Obtained in Ring Expansion Tests

		3 o'clock Longitudinal		3 o'clock Transverse		6 o'clock Longitudinal		6 o'clock Transverse	
		Yield Stress (PSI)	Tensile Strength (PSI)	Yield Stress (PSI)	Tensile Strength (PSI)	Yield Stress (PSI)	Tensile Strength (PSI)	Yield Stress (PSI)	Tensile Strength (PSI)
A	1	102826.3 (709 MPa)	126176.1 (870 MPa)	128061.5 (883 MPa)	129656.8 (894 MPa)	126321.1 (871 MPa)	127046.3 (876 MPa)	105436.8 (727 MPa)	124435.8 (858 MPa)
	2	104276.6 (719 MPa)	123710.6 (853 MPa)	130236.9 (898 MPa)	132412.4 (913 MPa)	129076.7 (890 MPa)	129801.9 (895 MPa)	104131.5 (718 MPa)	124725.8 (860 MPa)
B	1	114573.7 (790 MPa)	-	102971.3 (710 MPa)	-	117474.3 (810 MPa)	-	101521 (700 MPa)	-
	2	114573.7 (790 MPa)	-	100070.7 (690 MPa)	-	116024 (800 MPa)	-	101521 (700 MPa)	-
C	1	92094 (635 MPa)	106887.1 (737 MPa)	106597 (735 MPa)	112253.2 (774 MPa)	93544.4 (645 MPa)	107467.2 (741 MPa)	107177.2 (739 MPa)	111093 (766 MPa)
	2	90788.8 (626 MPa)	104856.7 (723 MPa)	108917.5 (751 MPa)	114718.7 (791 MPa)	91513.9 (631 MPa)	105001.7 (724 MPa)	101956 (703 MPa)	106016 (731 MPa)

Table 12-7 – Yield & Tensile Strength Values from ST Tests

	Longitudinal		Transverse	
	Yield Strength (PSI)	Tensile Strength (PSI)	Yield Strength (PSI)	Tensile Strength (PSI)
A	98765.4 (681 MPa)	124435.7 (858 MPa)	122550.4 (845 MPa)	132702.5 (915 MPa)
	96299.9 (664 MPa)	127771.4 (881 MPa)	120229.9 (829 MPa)	129221.7 (891 MPa)
	96445 (665 MPa)	126901.2 (875 MPa)	121680.2 (839 MPa)	129946.9 (896 MPa)
B	95429.7 (658 MPa)	119214.7 (822 MPa)	108047.4 (745 MPa)	120374.9 (830 MPa)
	92094 (635 MPa)	114283.6 (788 MPa)	108772.5 (750 MPa)	120229.9 (829 MPa)
C	93689.4 (646 MPa)	110802.9 (764 MPa)	106742.1 (736 MPa)	115008.8 (793 MPa)
	97460.2 (672 MPa)	111093 (766 MPa)	105581.8 (728 MPa)	113413.5 (782 MPa)
	98330.3 (678 MPa)	111528.1 (769 MPa)	106016.9 (731 MPa)	114283.6 (788 MPa)

Table 12-8 – Manufacturers' Yield & Tensile Data

Test Number	ASME B31G	Mod ASME B31G	RSTRENG	LPC-1	SHELL92
1	1.08	0.88	0.97	1.00	1.03
2	1.15	0.88	0.97	0.94	1.01

Table 12-9 – Comparison of Failure Predictions (P_A/P_f) for Tests 1 and 2

13 Figures

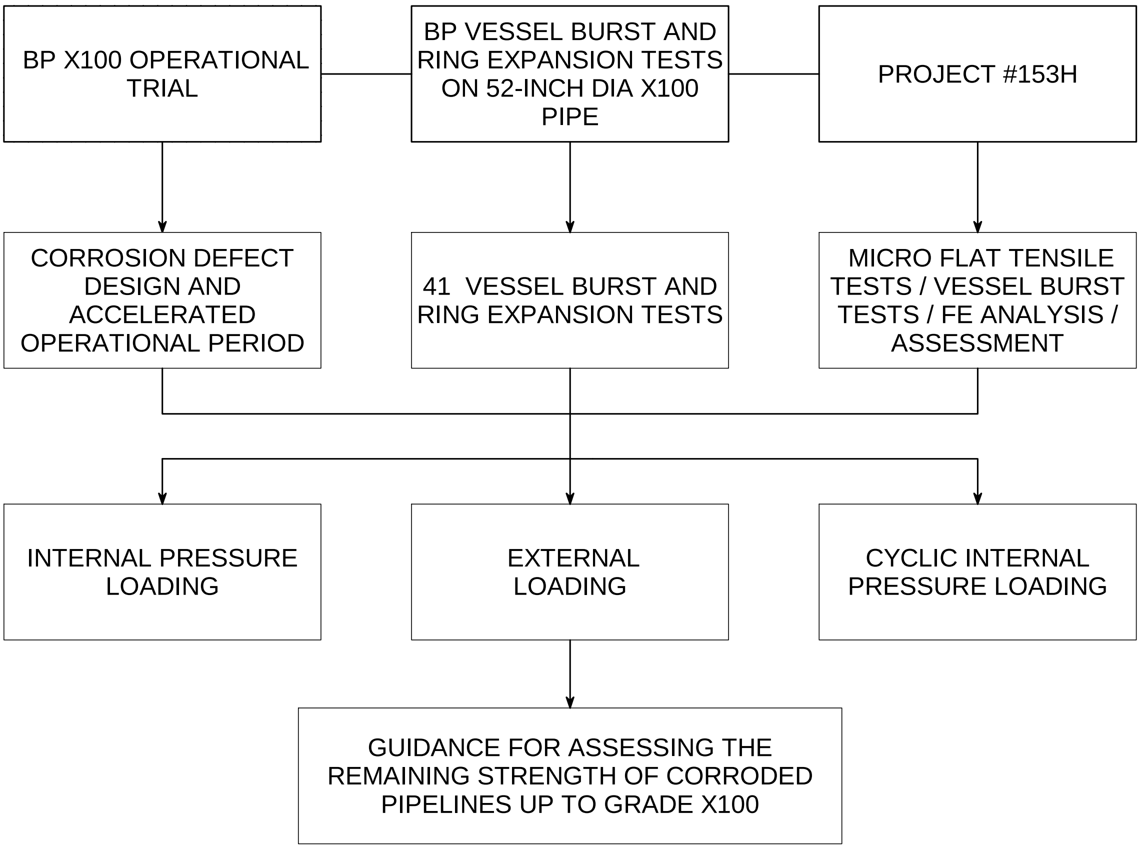

Figure 1 – Interface Between Project #153H and the BP X100 Operational Trial

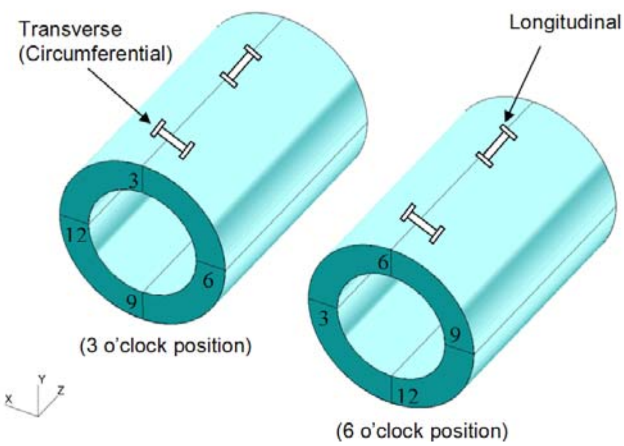

Figure 2 – Location of specimen extraction from 3 and 6 o'clock positions

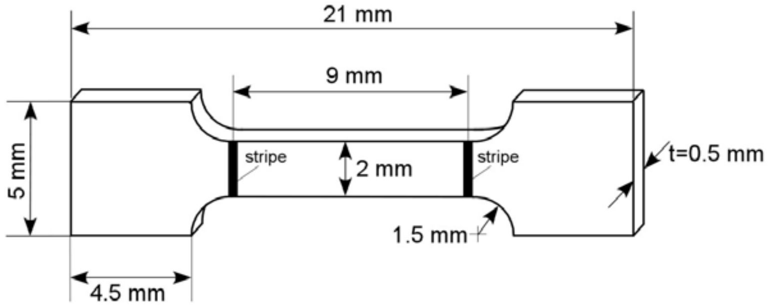

Figure 3 – MFT Specimen Dimensions

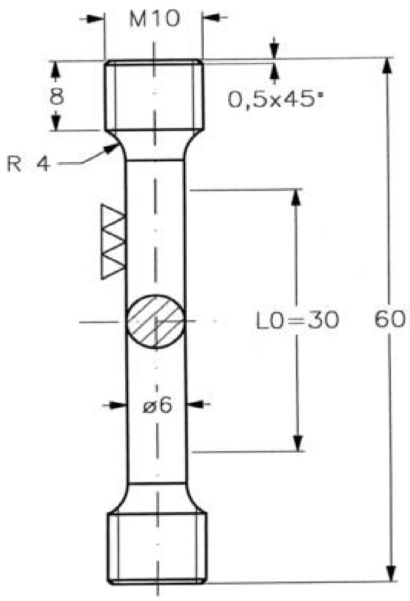

Figure 4 – ST specimen Dimensions to DIN50125-B 6x30, Ø6 mm and gauge length is 30 mm

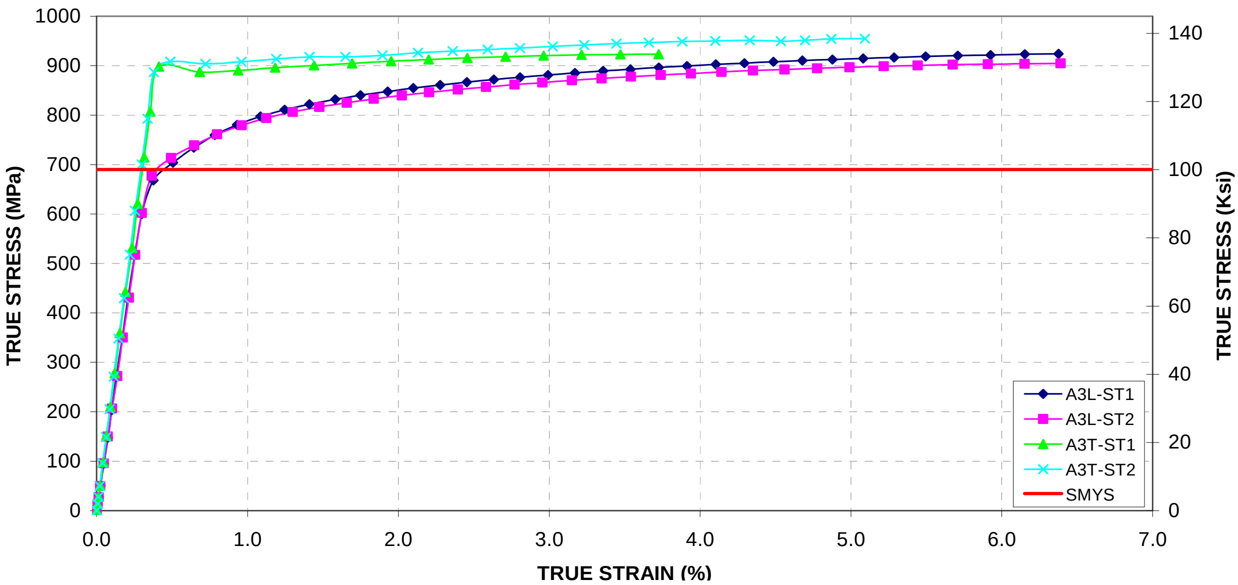

Figure 5 – ST Test Results for Manufacturer A 3 o'clock Samples

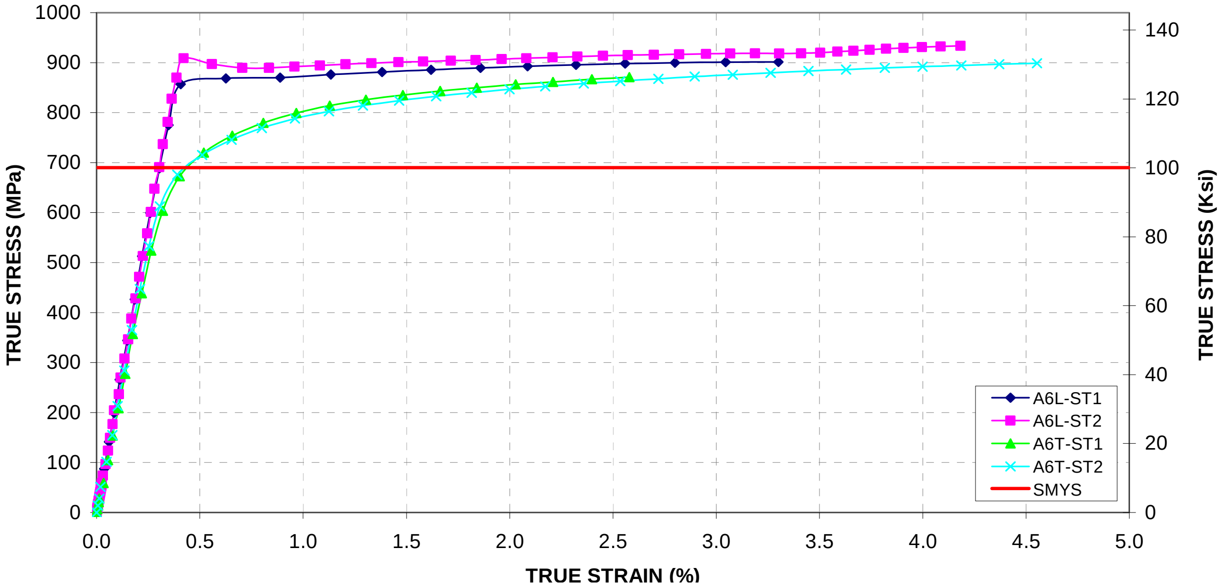

Figure 6 – ST Test Results for Manufacturer A 6 o'clock Samples

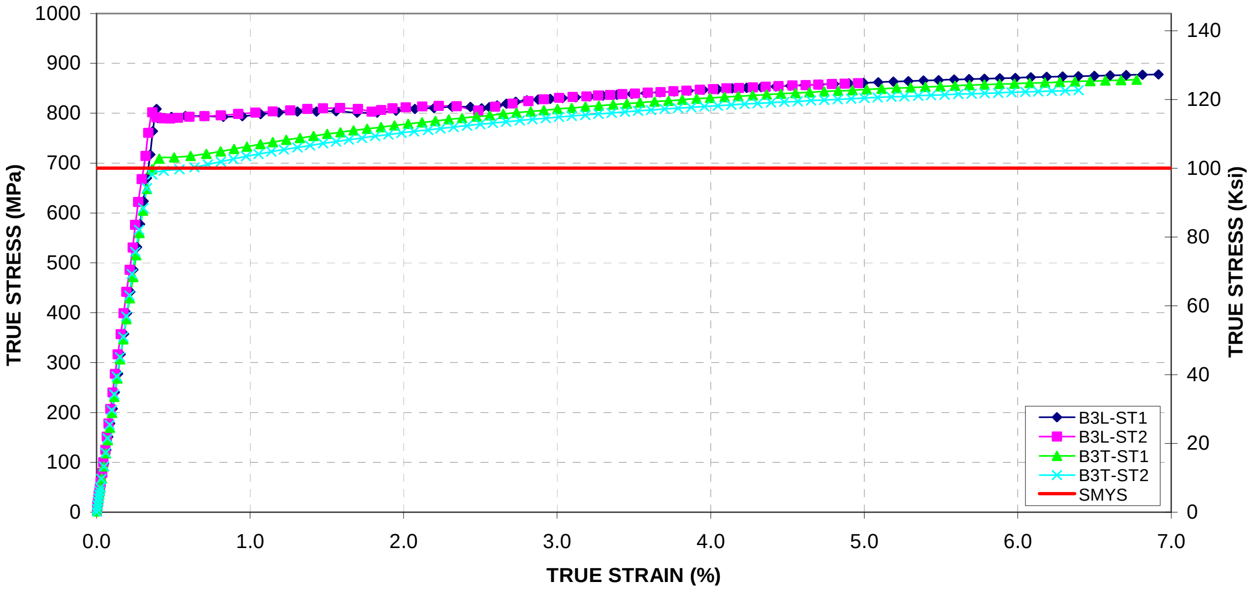

Figure 7 – ST Test Results for Manufacturer B 3 o'clock Samples

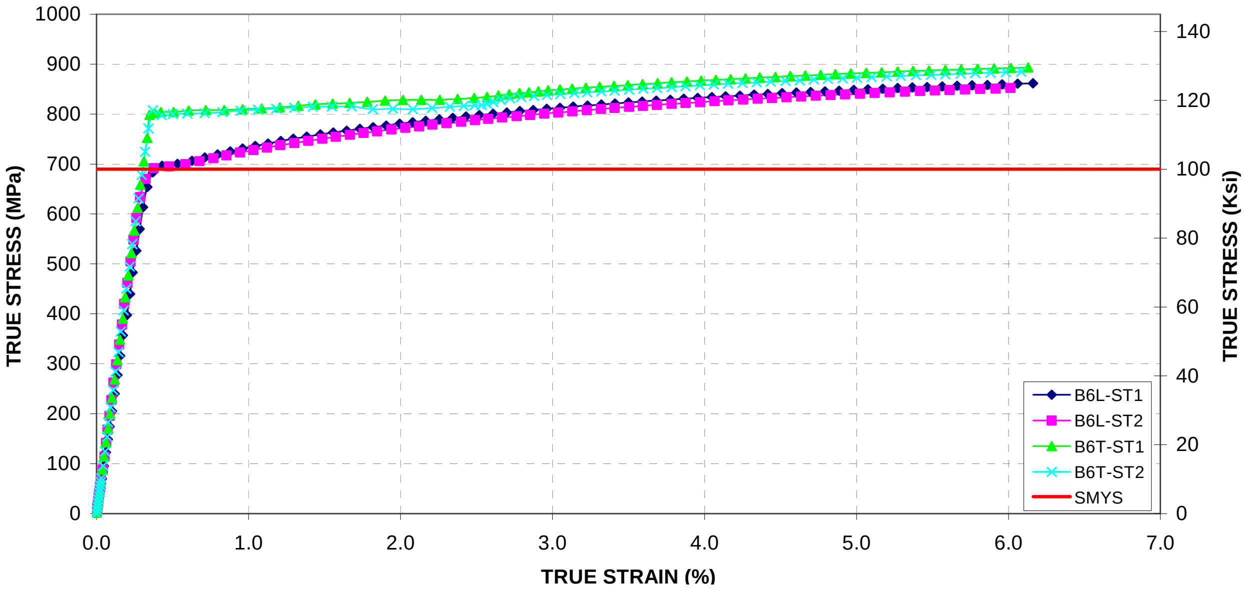

Figure 8 – ST Test Results for Manufacturer B 6 o'clock Samples

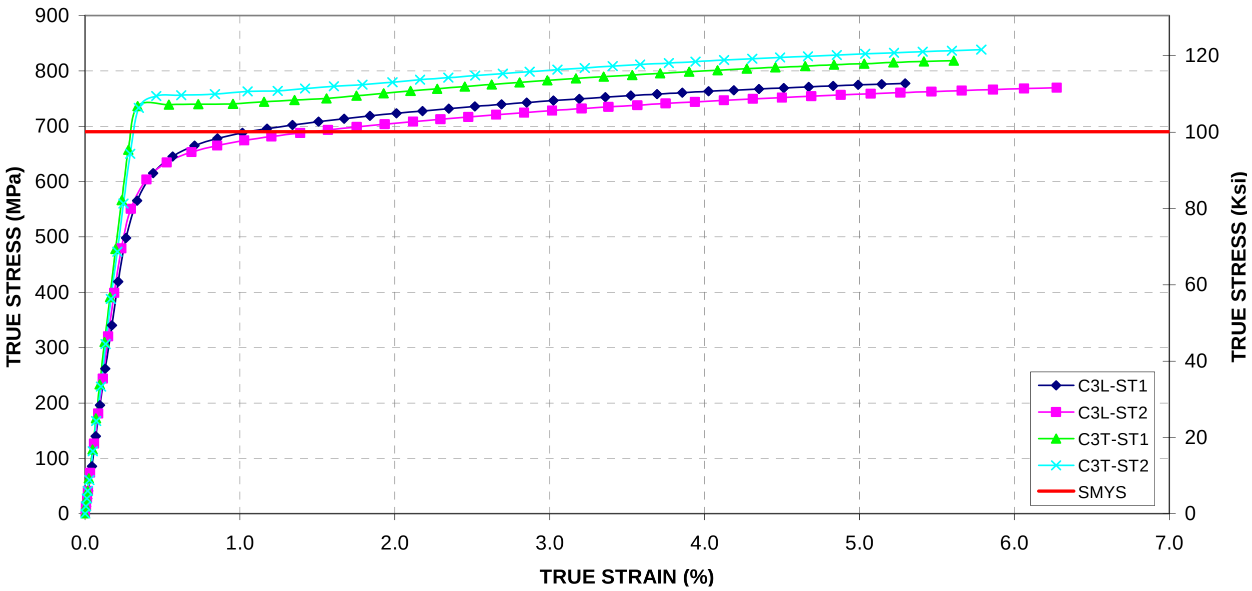

Figure 9 – ST Test Results for Manufacturer C 3 o'clock Samples

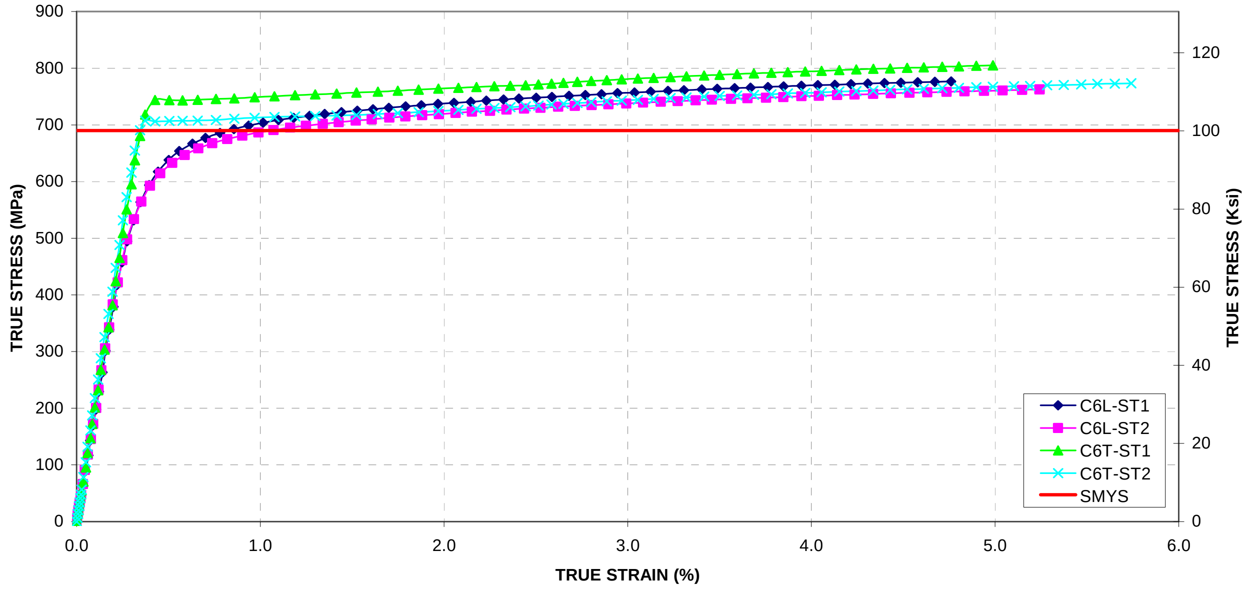

Figure 10 – ST Test Results for Manufacturer C 6 o'clock Samples

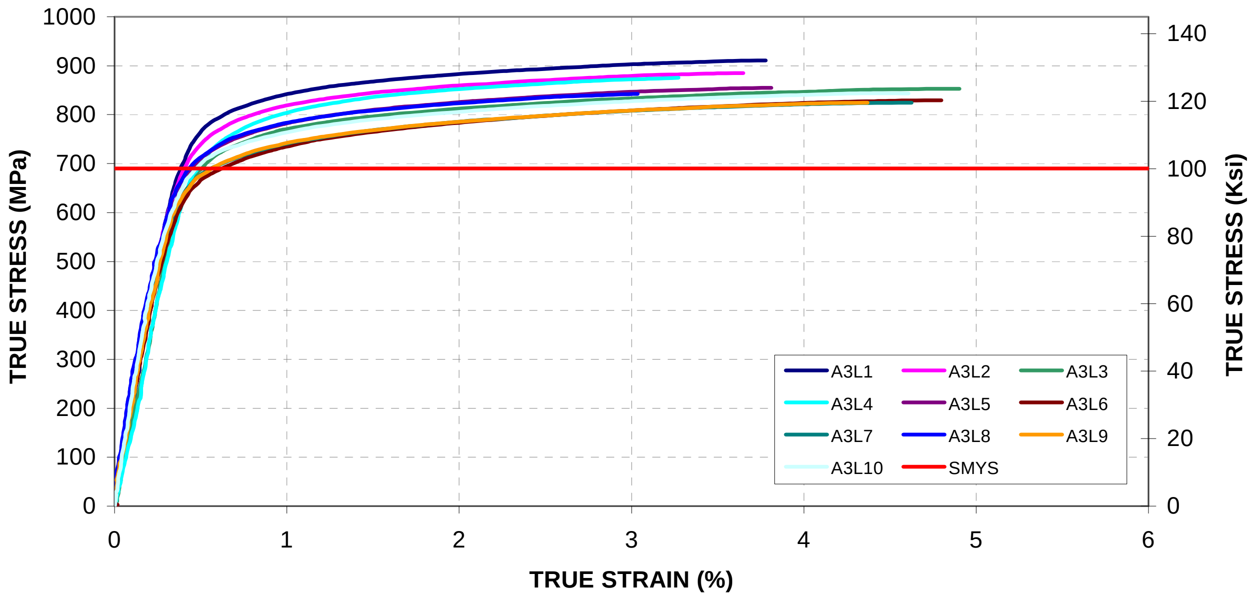

Figure 11 – MFT Results Plot for the Manufacturer A 3 o'clock Longitudinal Specimens

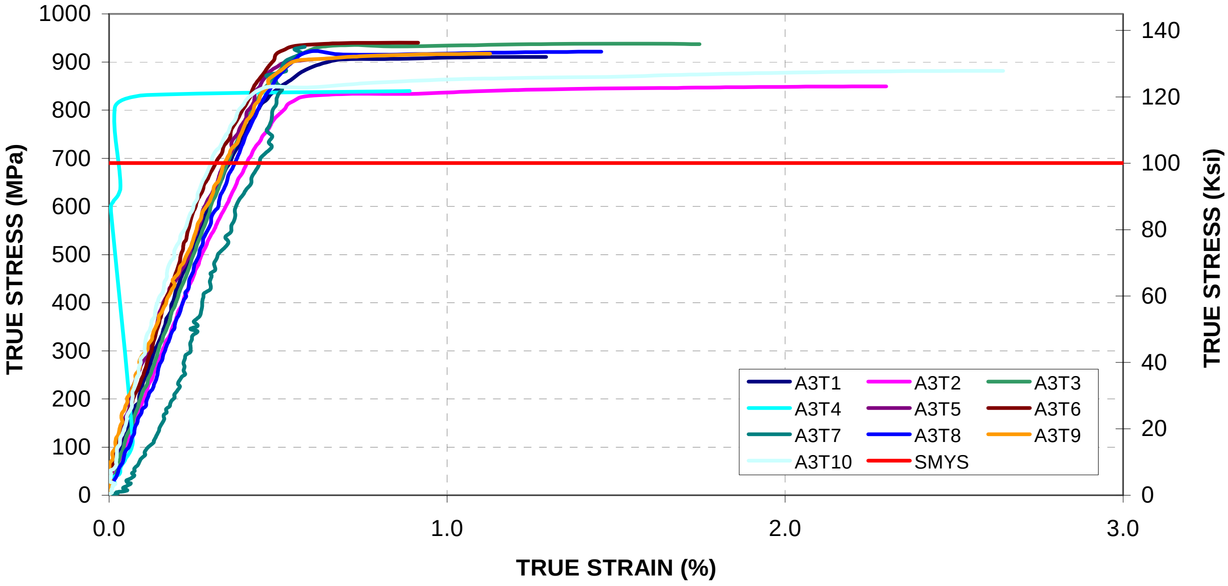

Figure 12 – MFT Results Plot for the Manufacturer A 3 o'clock Transverse Specimens

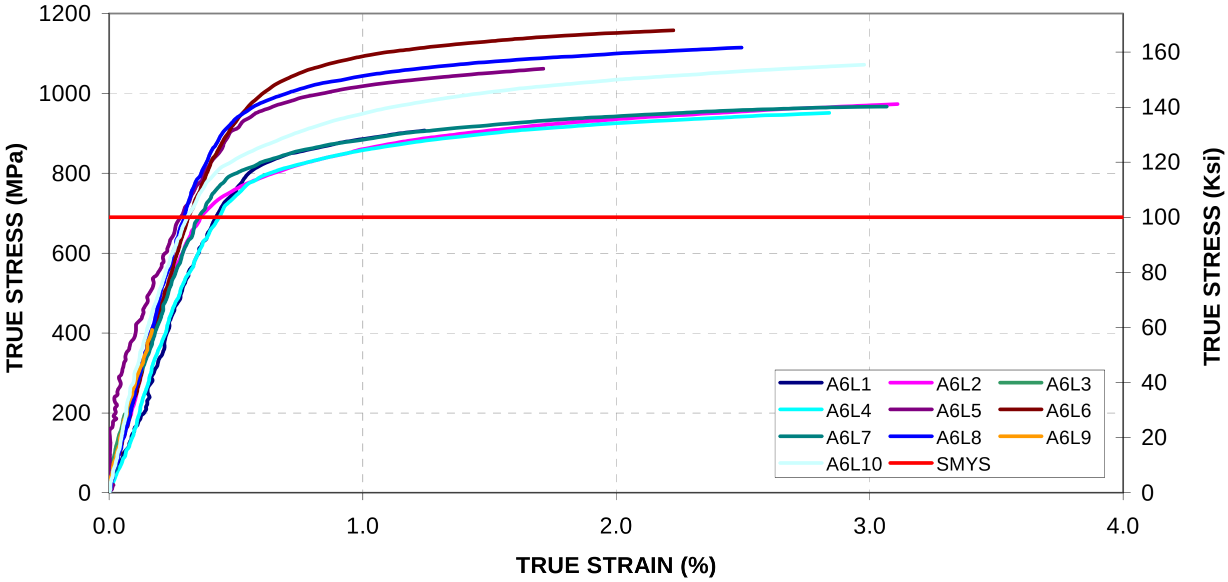

Figure 13 – MFT Results Plot for the Manufacturer A 6 o'clock Longitudinal Specimens

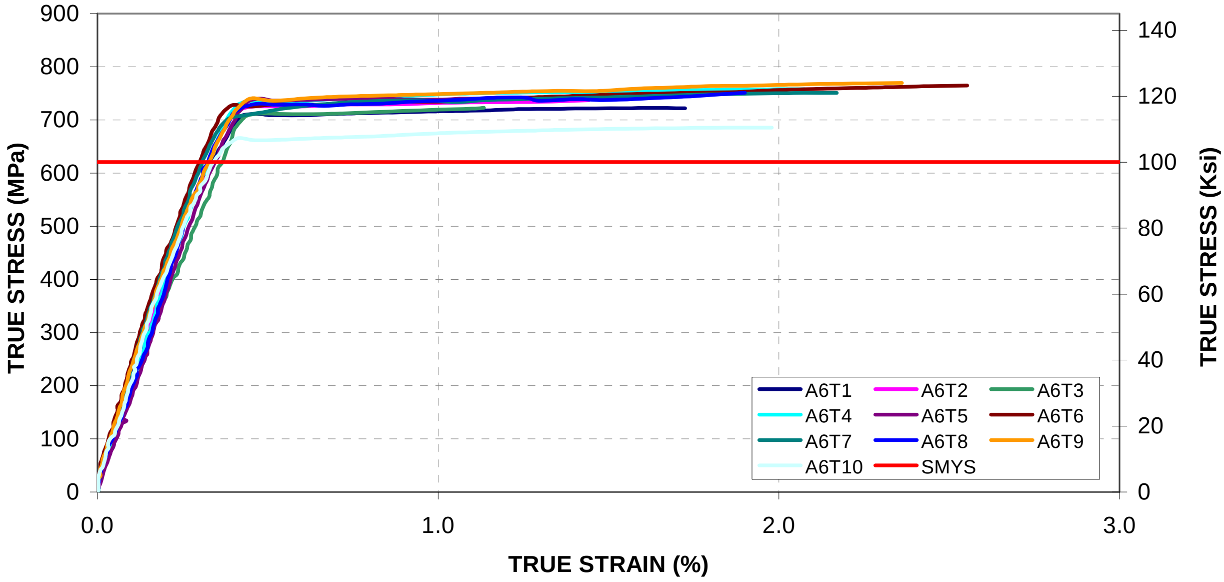

Figure 14 – MFT Results Plot for the Manufacturer A 6 o'clock Transverse Specimens

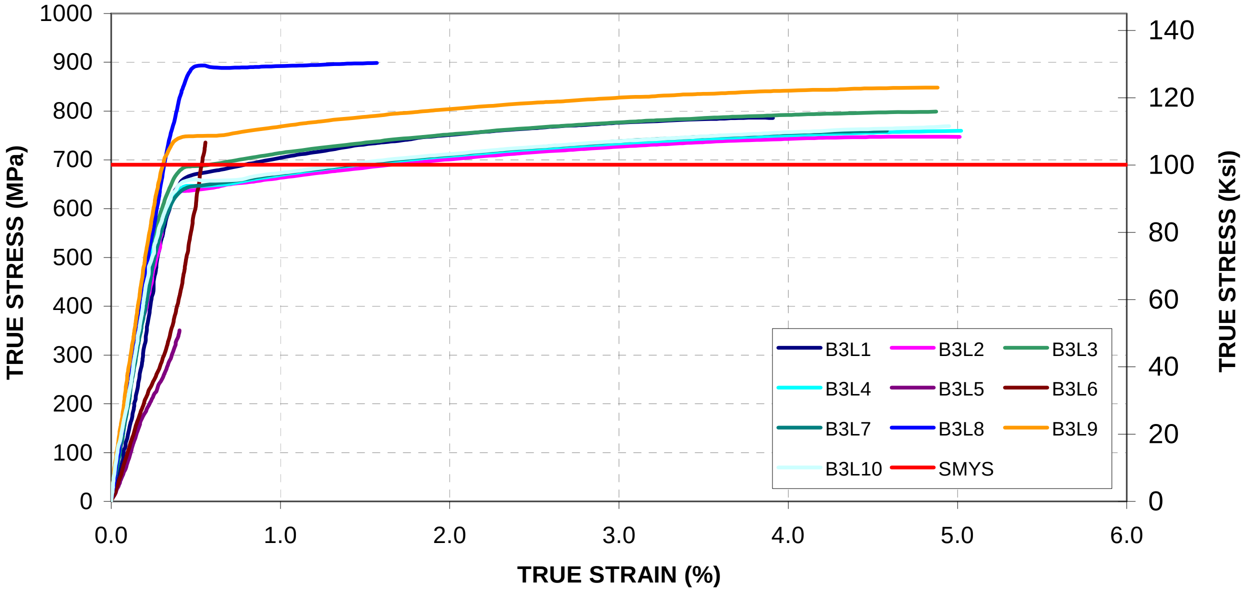

Figure 15 – MFT Results Plot for the Manufacturer B 3 o'clock Longitudinal Specimens

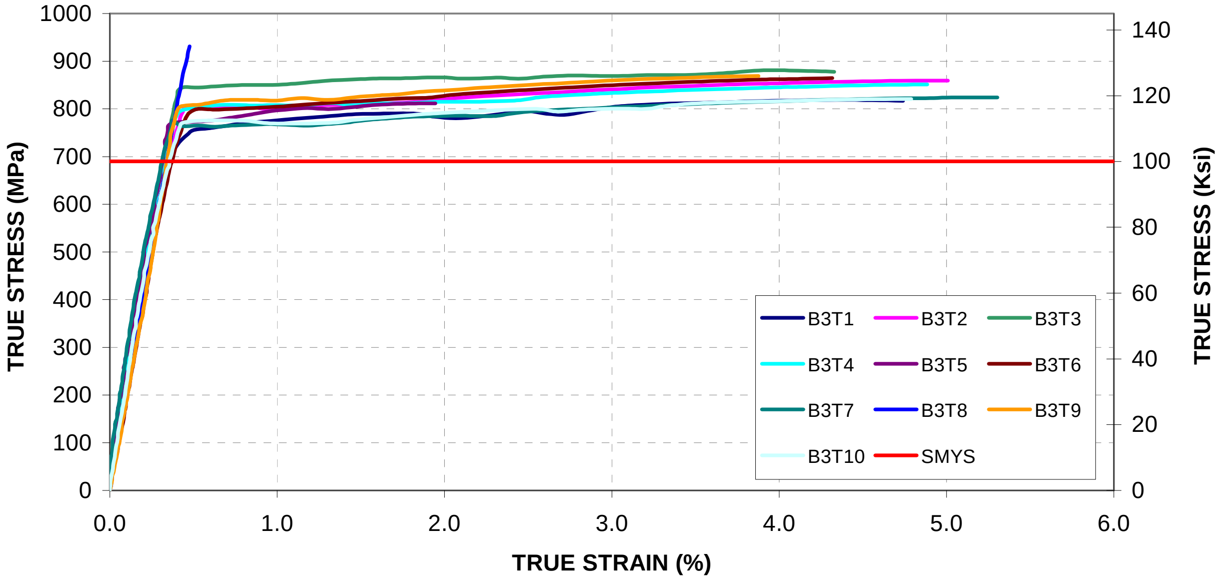

Figure 16 – MFT Results Plot for the Manufacturer B 3 o'clock Transverse Specimens

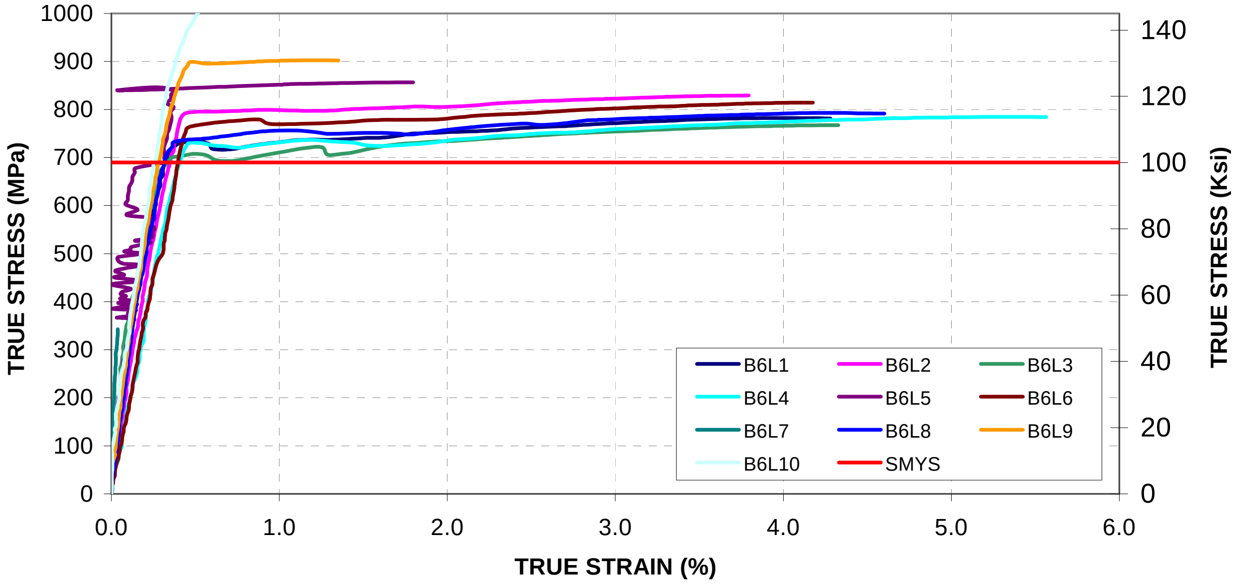

Figure 17 – MFT Results Plot for the Manufacturer B 6 o'clock Longitudinal Specimens

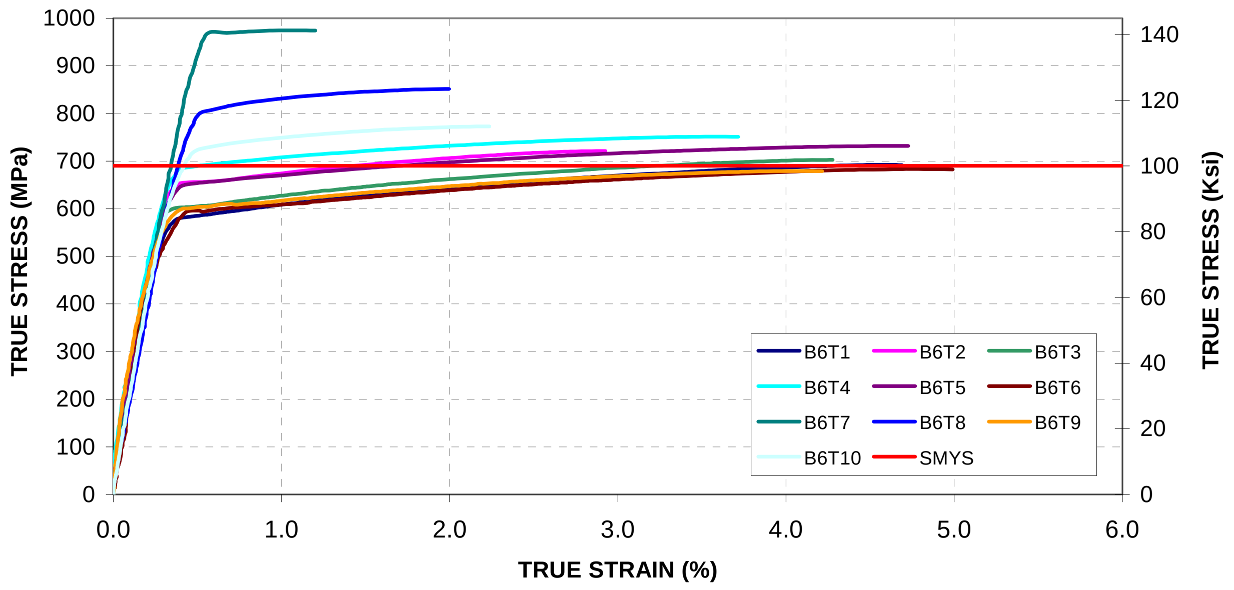

Figure 18 – MFT Results Plot for the Manufacturer B 6 o'clock Transverse Specimens

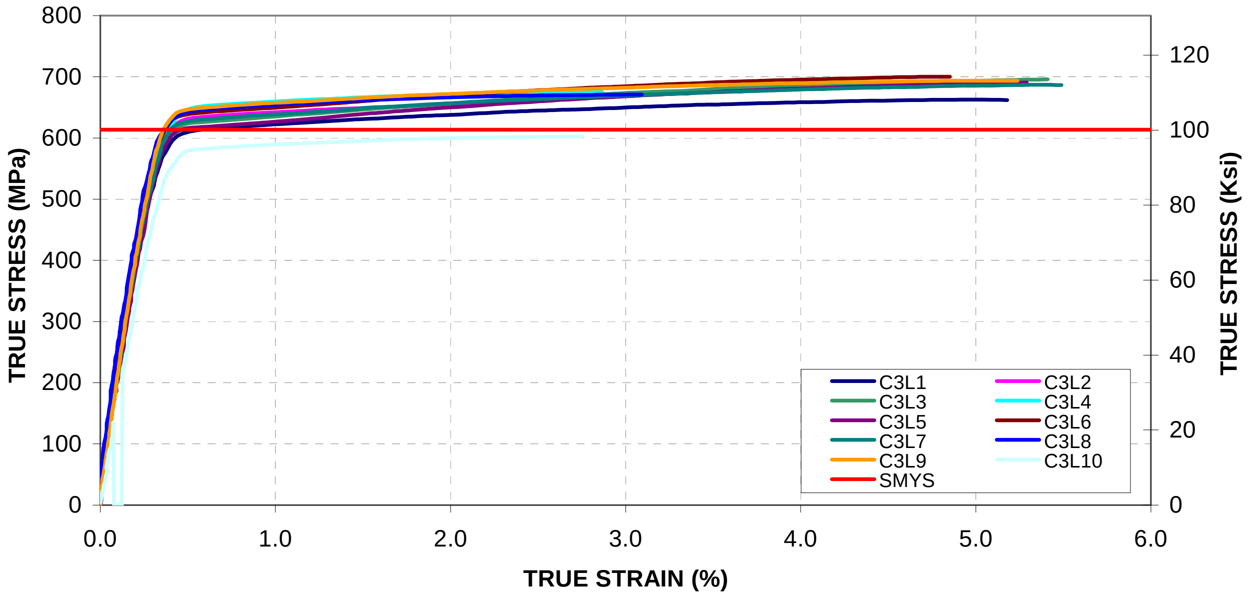

Figure 19 – MFT Results Plot for the Manufacturer C 3 o'clock Longitudinal Specimens

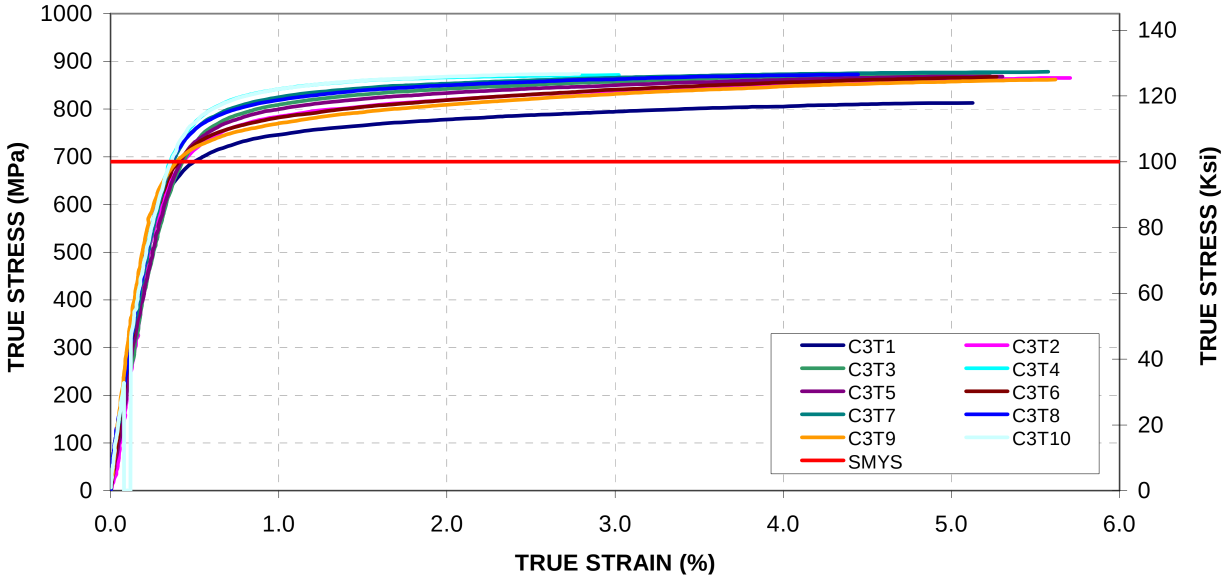

Figure 20 – MFT Results Plot for the Manufacturer C 3 o'clock Transverse Specimens

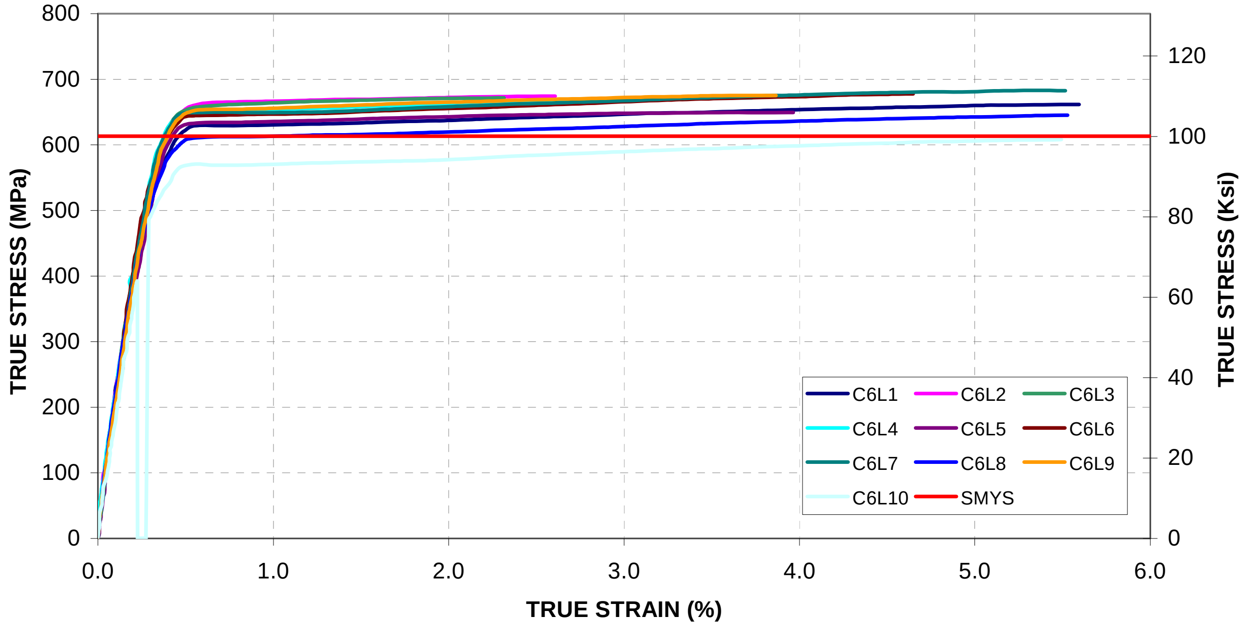

Figure 21 – MFT Results Plot for the Manufacturer C 6 o'clock Longitudinal Specimens

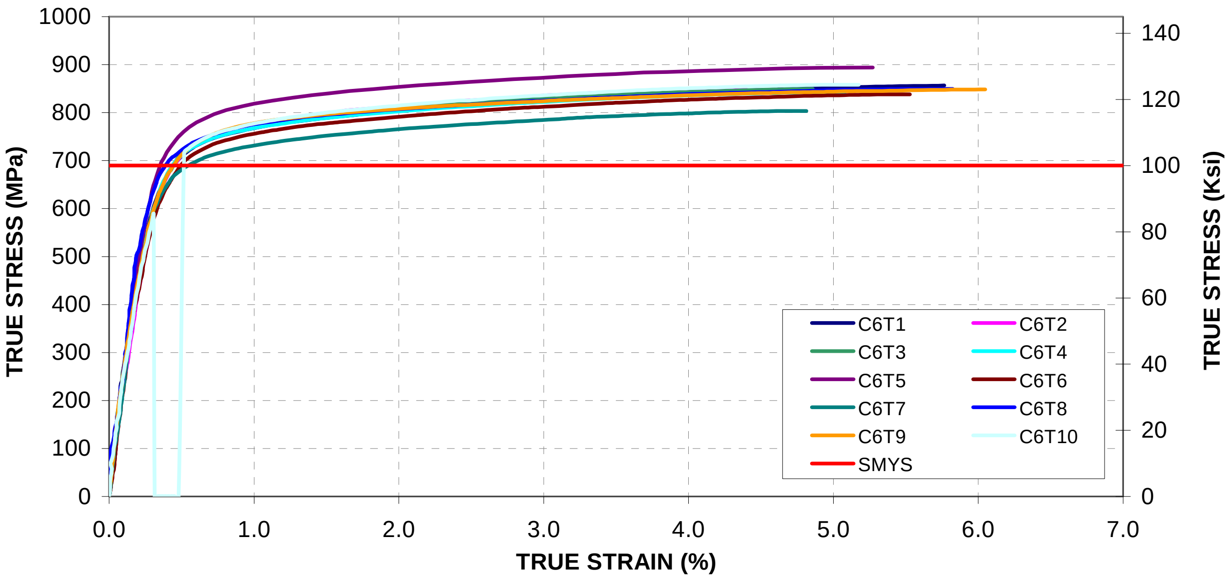

Figure 22 – MFT Results Plot for the Manufacturer C 6 o'clock Transverse Specimens

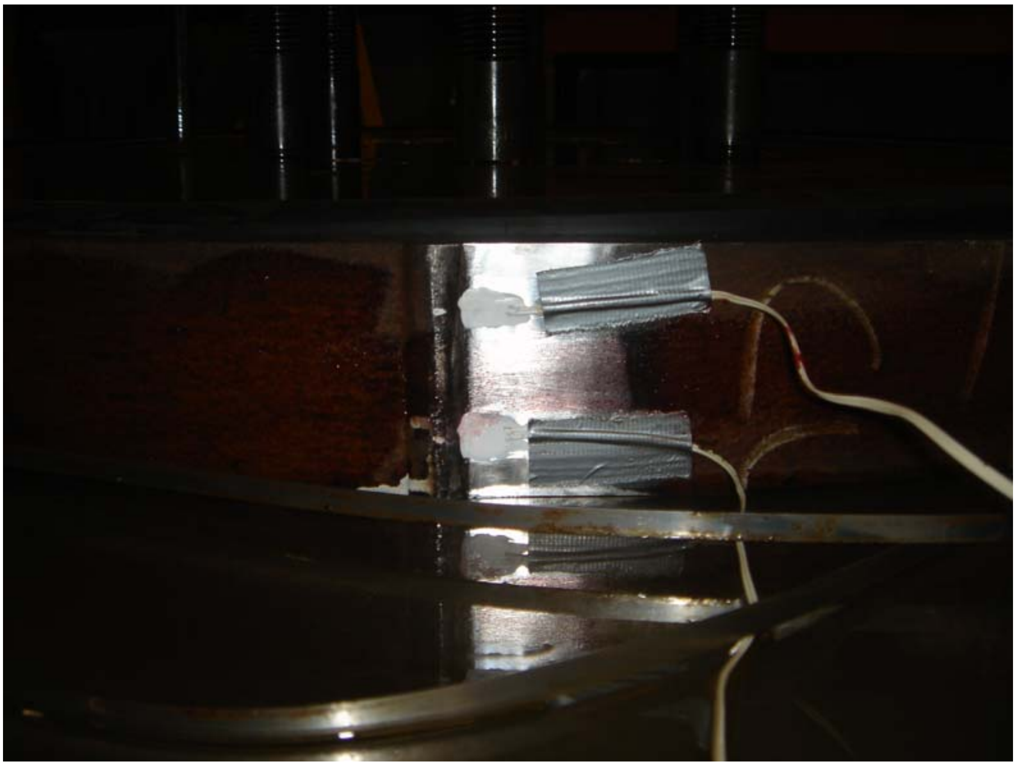

Figure 23 – Location of Strain Gauges

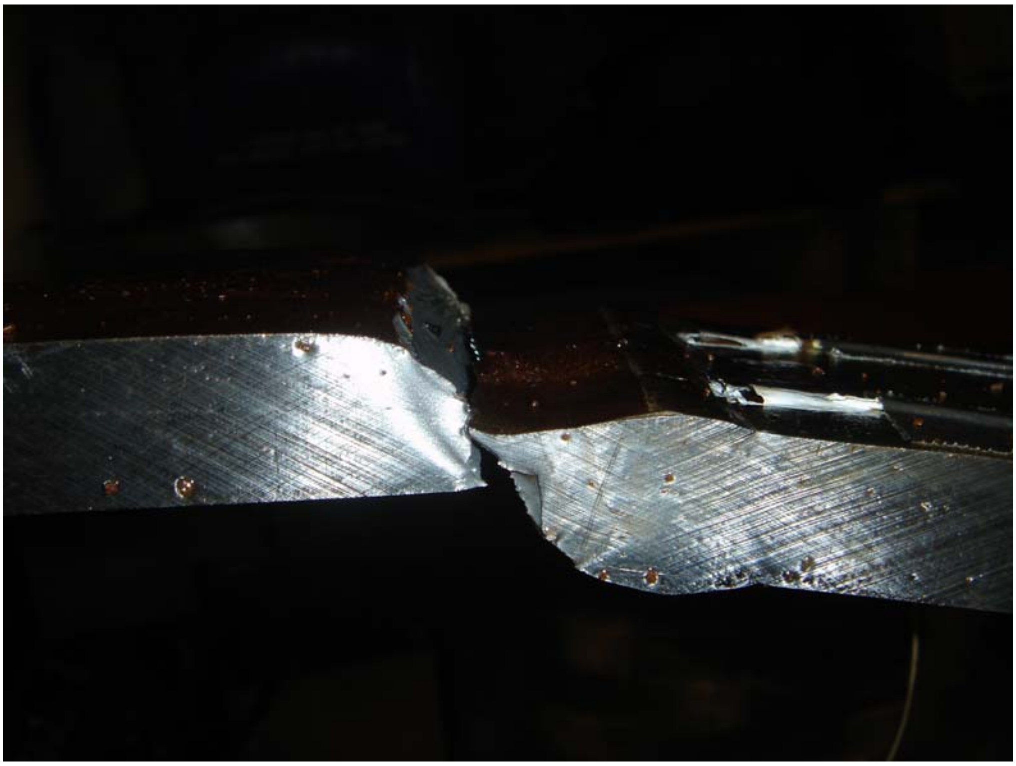

Figure 24 – Failure of Test Sample HLR2

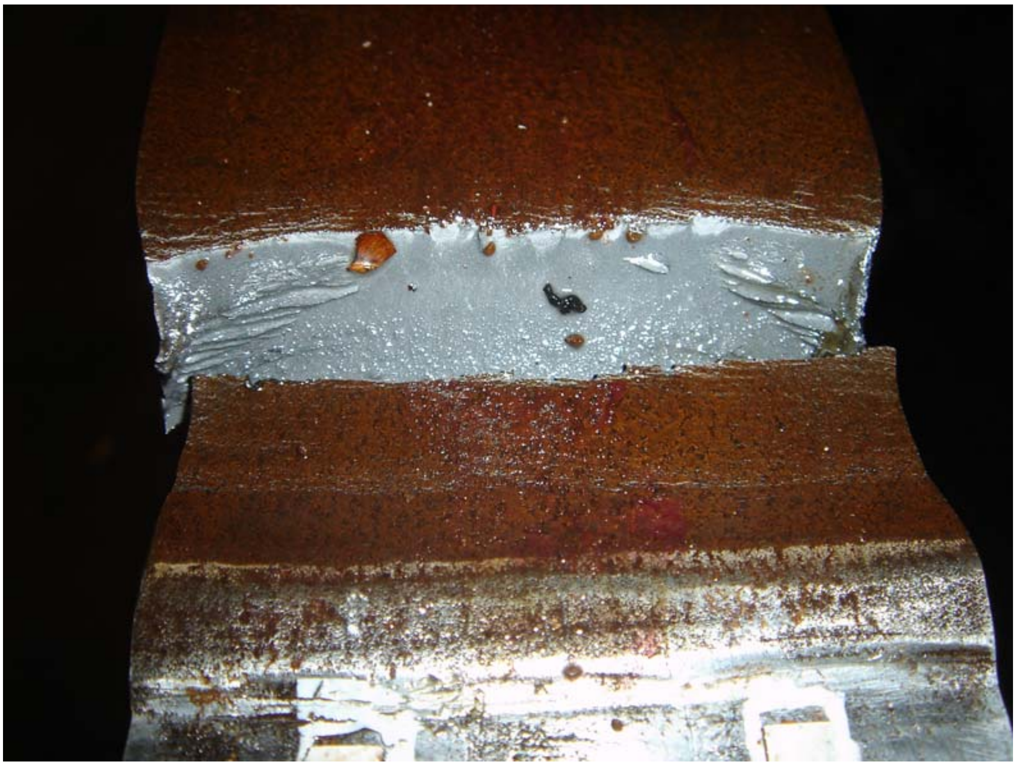

Figure 25 – Failure of Test Sample HLR2

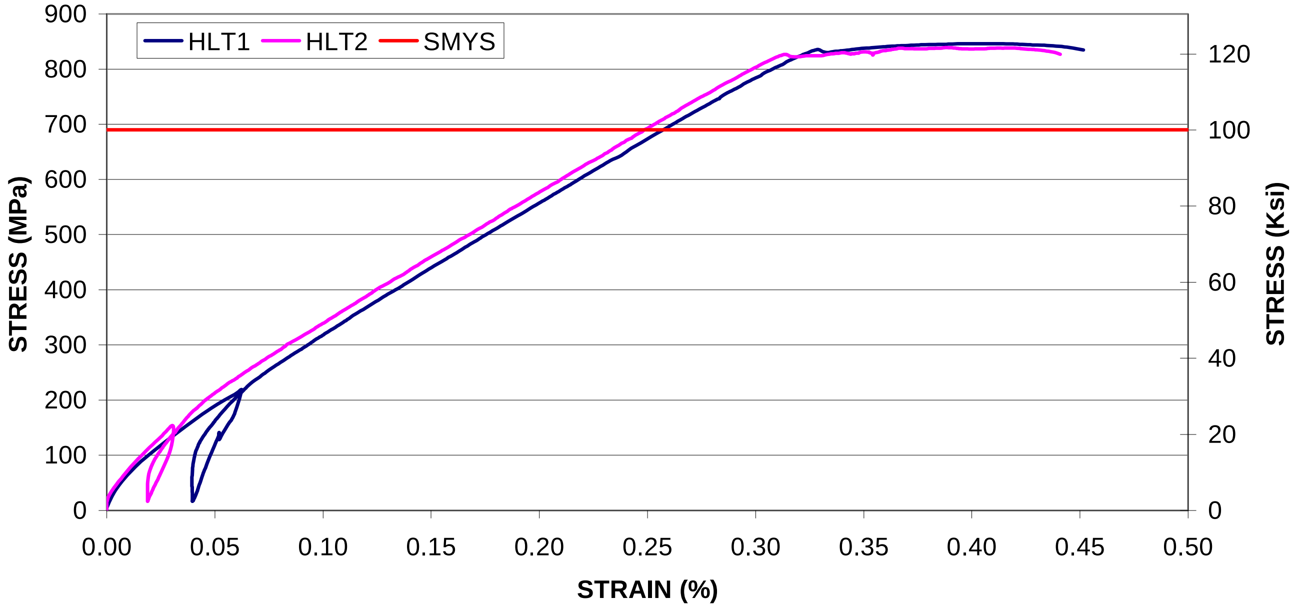

Figure 26 – Manufacturer A Ring Expansion Test Results

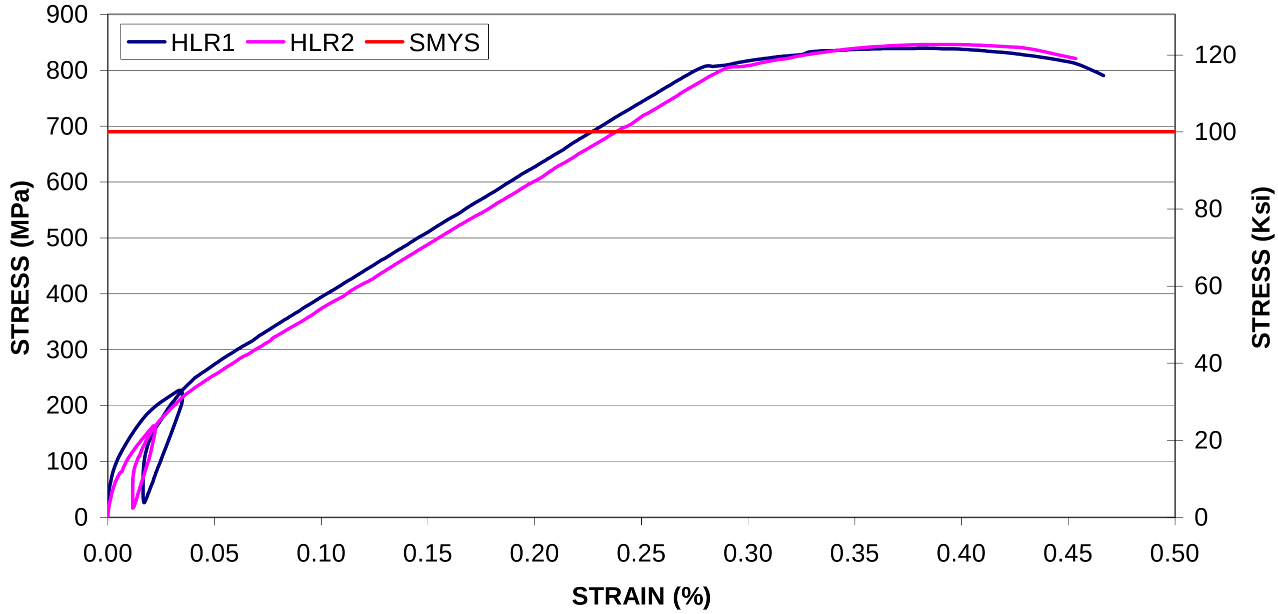

Figure 27 – Manufacturer B Ring Expansion Test Results

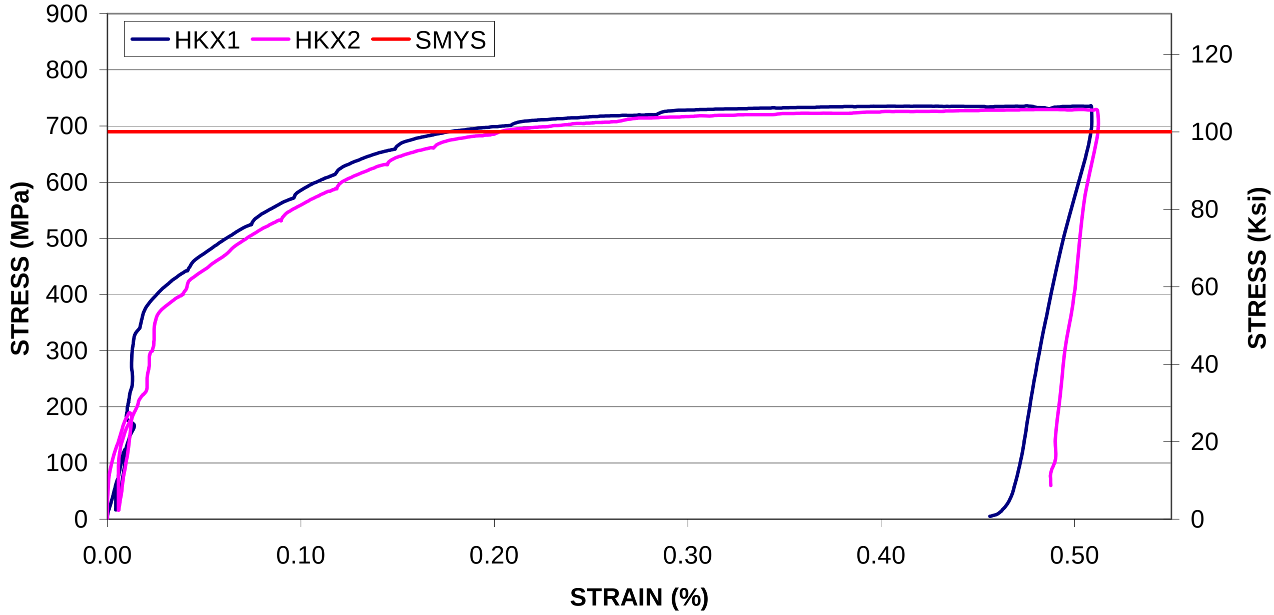

Figure 28 – Manufacturer C Ring Expansion Test Results

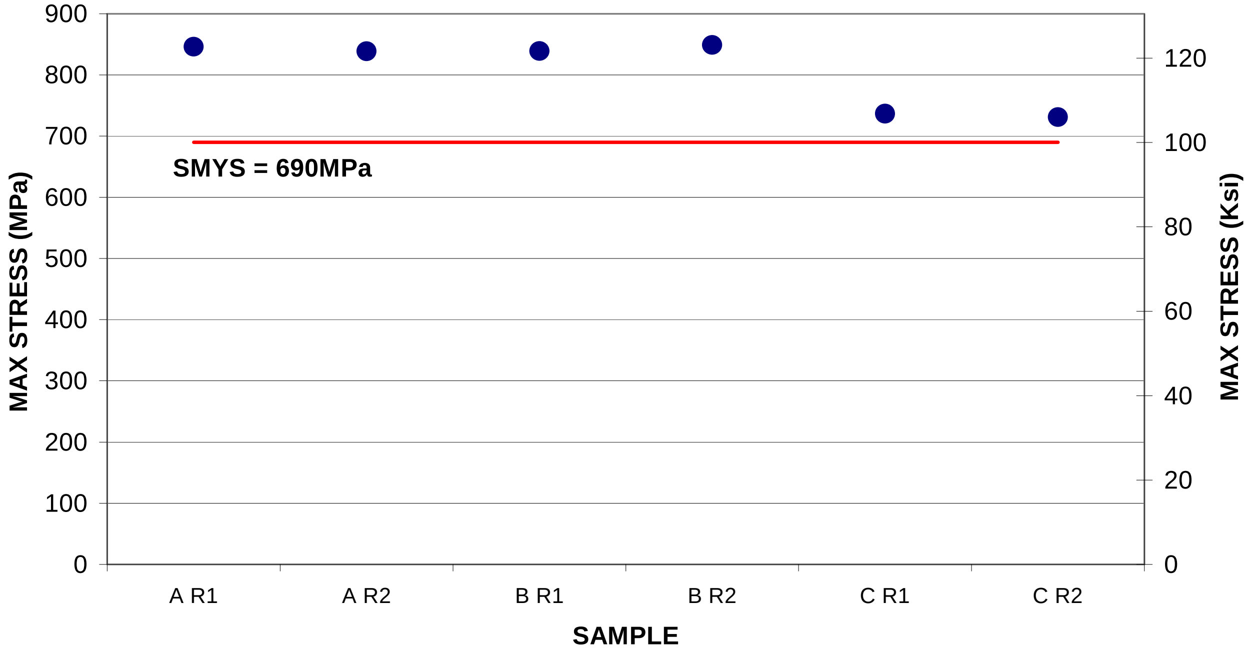

Figure 29 – Maximum Stresses Achieved in Ring Expansion Tests

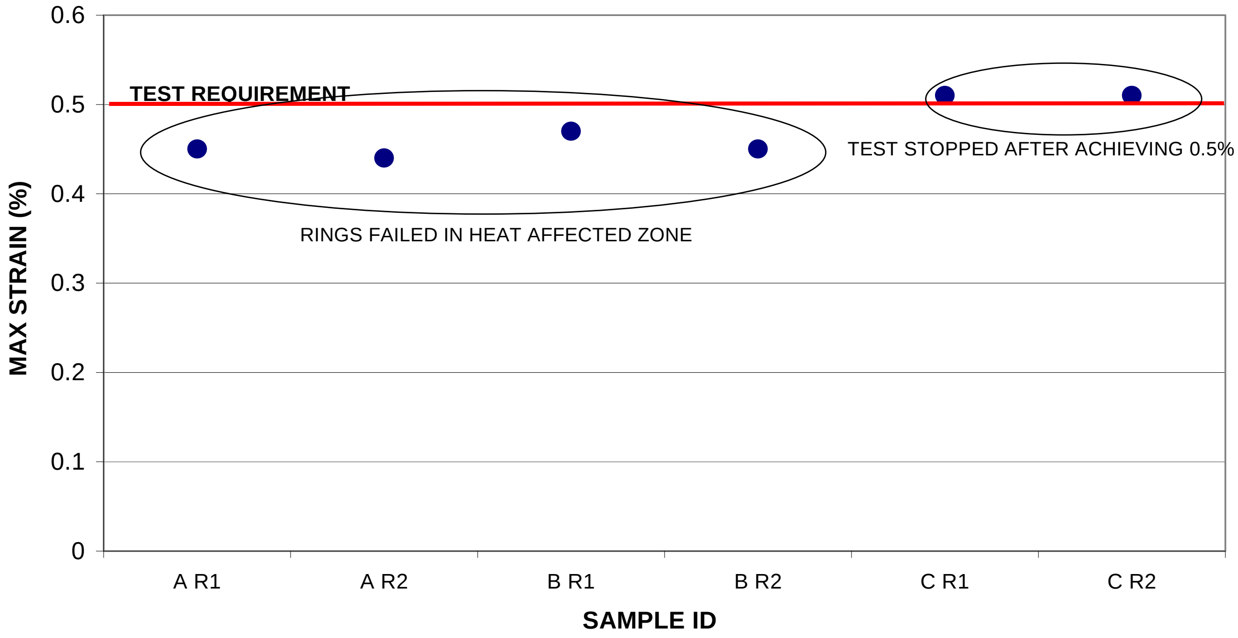

Figure 30 – Summary of Strains Achieved in Ring Expansion Tests

Figure 31 – Test 1 – Fully Fabricated Vessel

Figure 32 – Test 2 – Fully Fabricated Vessel

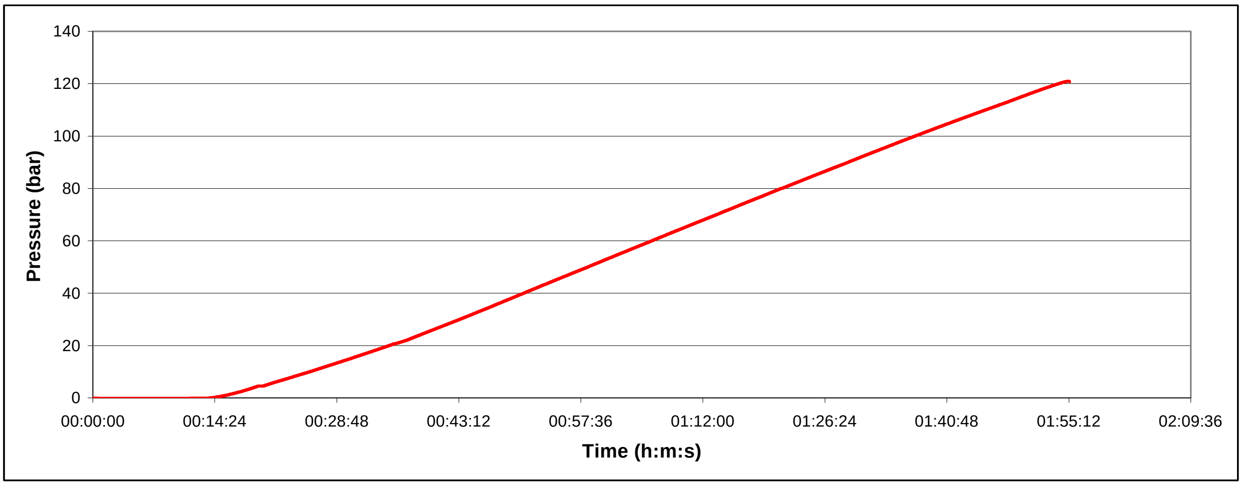

Figure 33 – Pressure versus Time Plot for Test 1

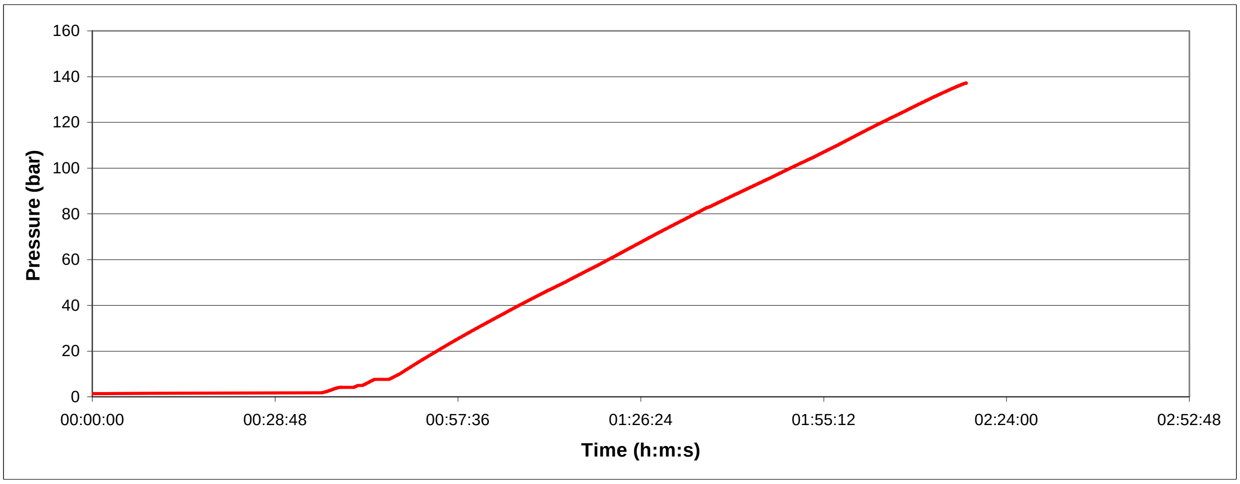

Figure 34 – Pressure versus Time Plot for Test 2

Figure 35 – Test 1 Vessel After Rupture

Figure 36 – Test 2 Vessel After Rupture

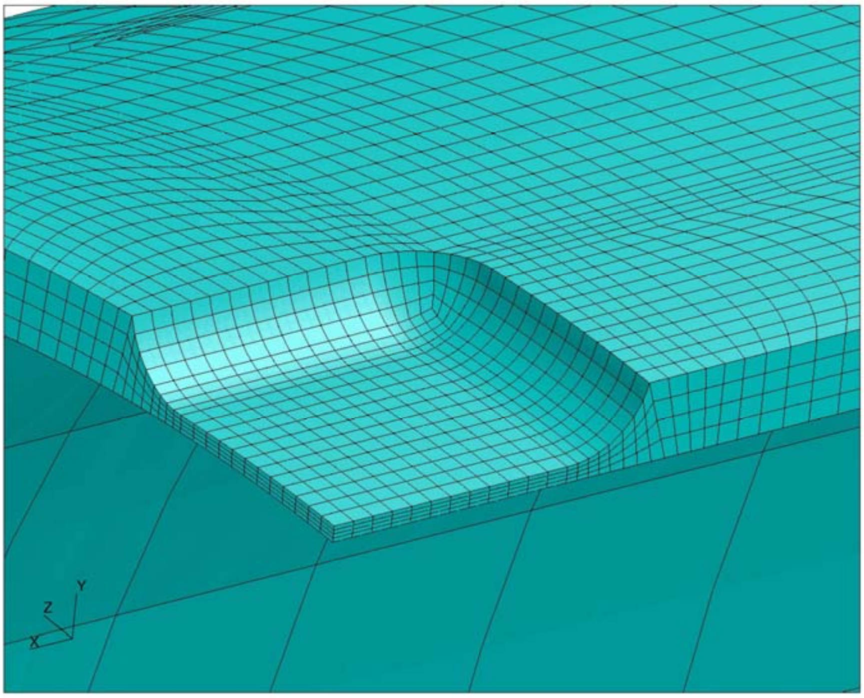

Figure 37 - FE Mesh of 80% Deep Patch Defect

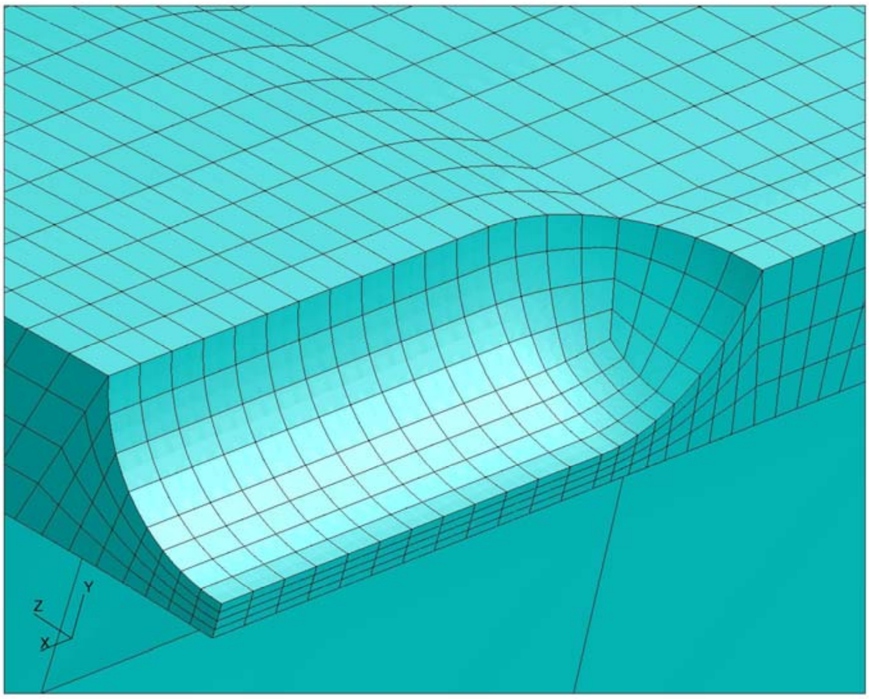

Figure 38 – FE Mesh of 80% Deep Defect Axial Groove Defect

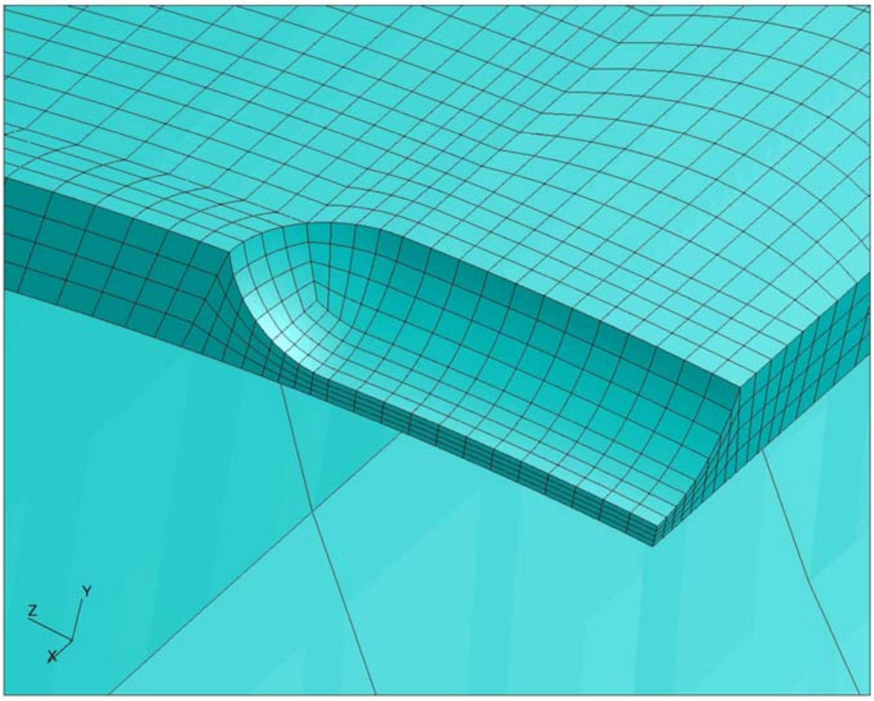

Figure 39 – FE Mesh of 80% Deep Circumferential Groove Defect

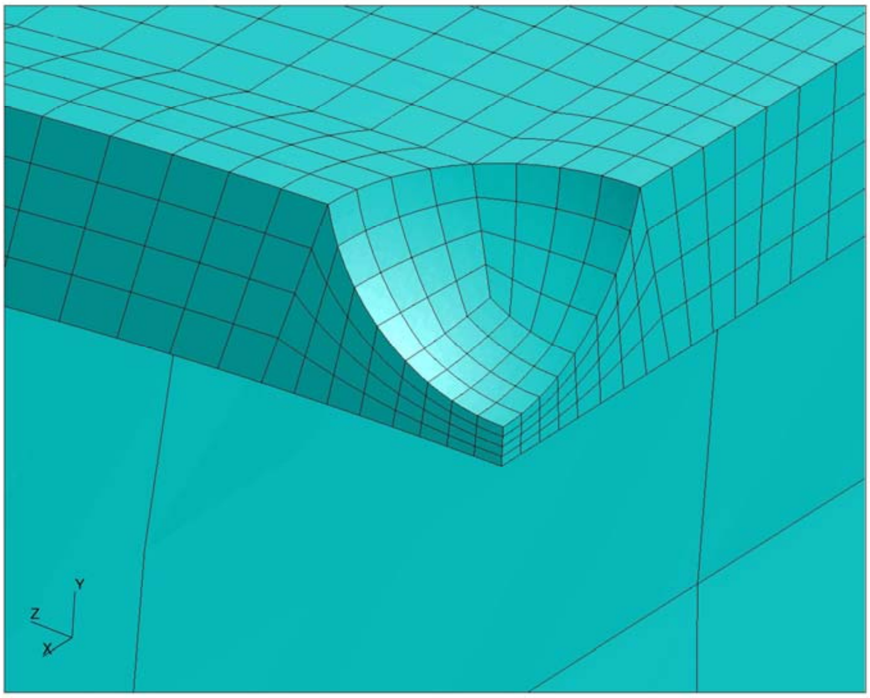

Figure 40 - FE Mesh of 80% Deep Pit Defect

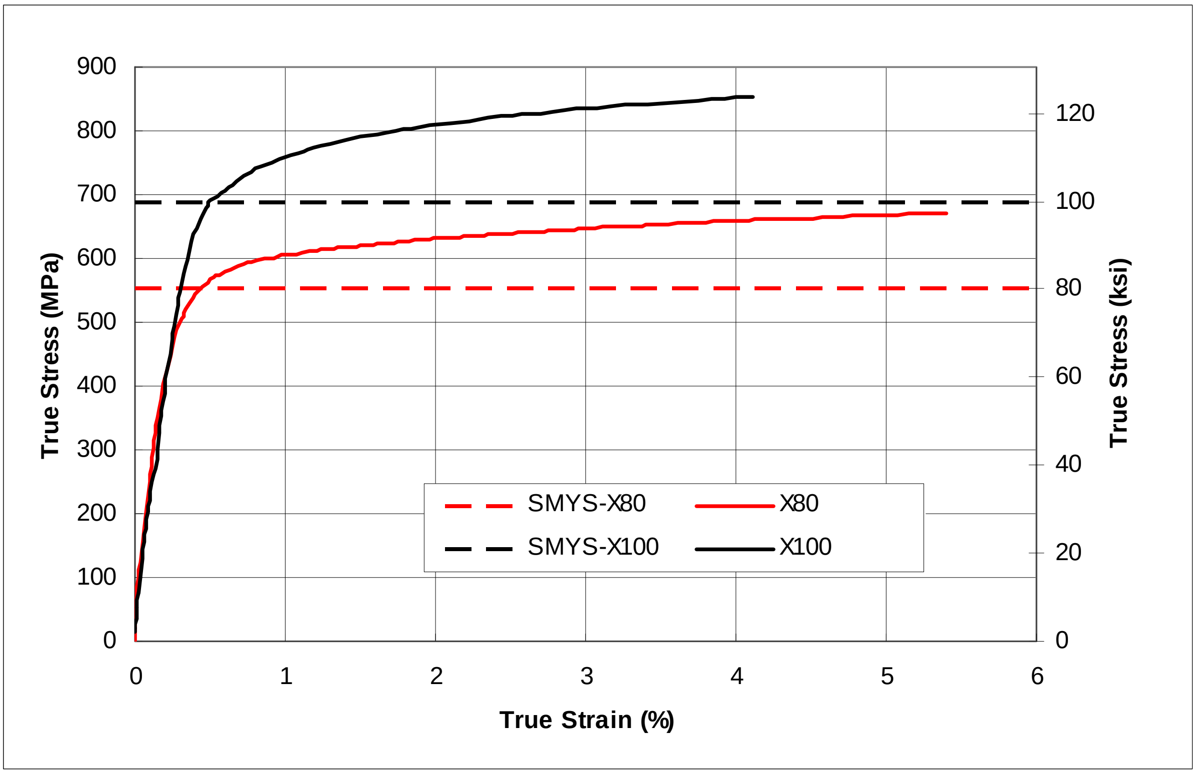

Figure 41 - Stress v Strain Curve Used in FE Analysis

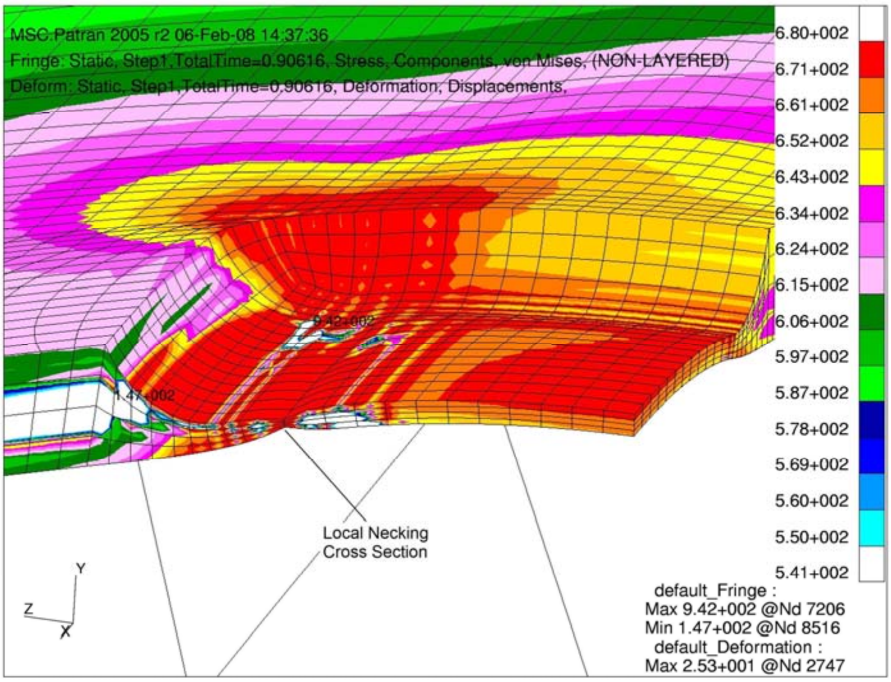

Figure 42 – Local Necking at an 80% Deep Patch Defect (48-inch Diameter Grade X80 Pipe, Pressure 2625 PSI/18.1MPa)

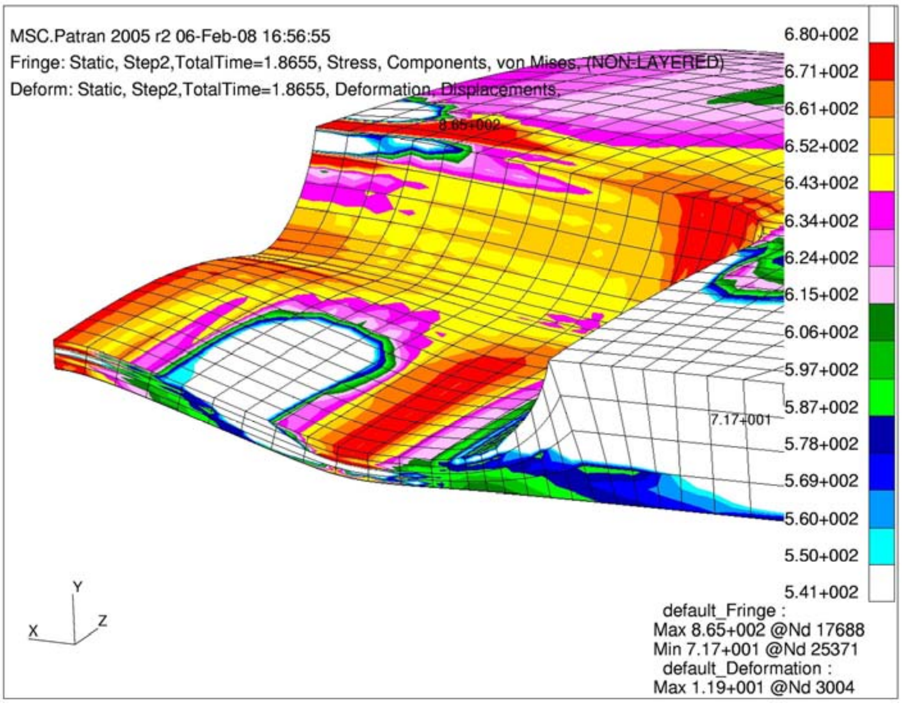

Figure 43 – Local Buckling at an 80% Deep Patch (48-inch Diameter Grade X80 Pipe, Axial Compressive Force of 38.7MN)

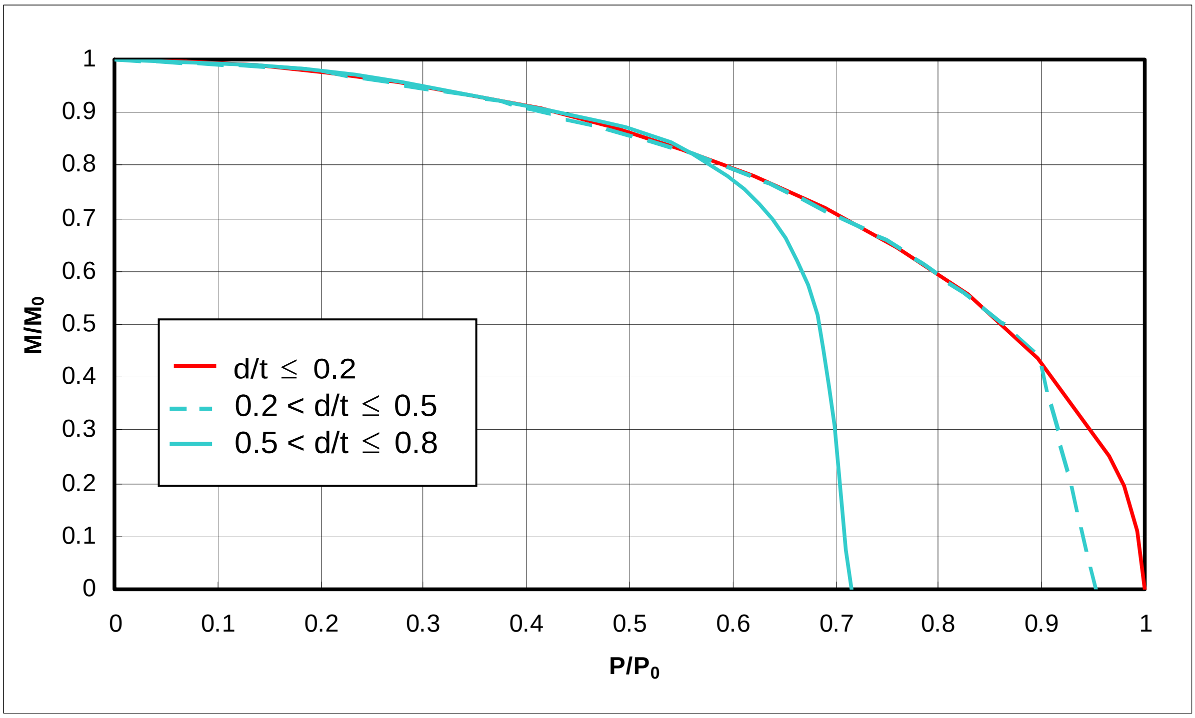

Figure 44 – Non-dimensional Pressure-Moment Failure Boundary Loci for Pipes with a Patch Defect and Strength Grades up to X100

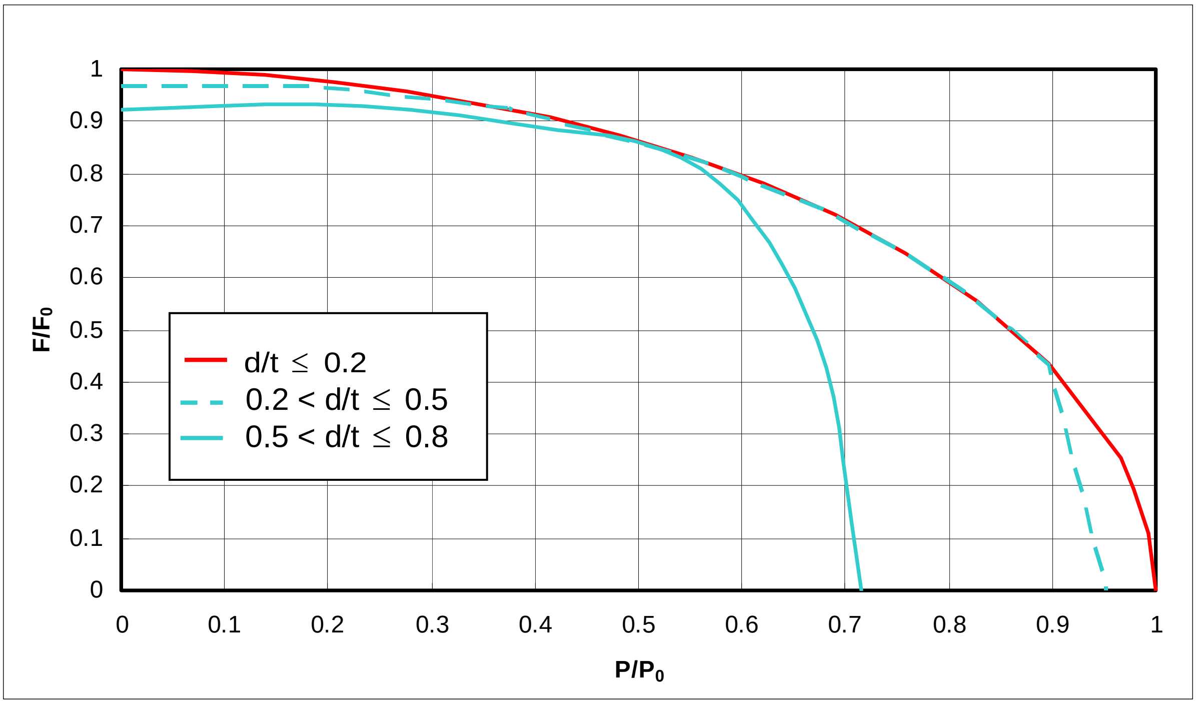

Figure 45 – Non-dimensional Pressure-Compressive Force Failure Boundary Loci for Pipes with a Patch Defect and Strength Grades up to X100

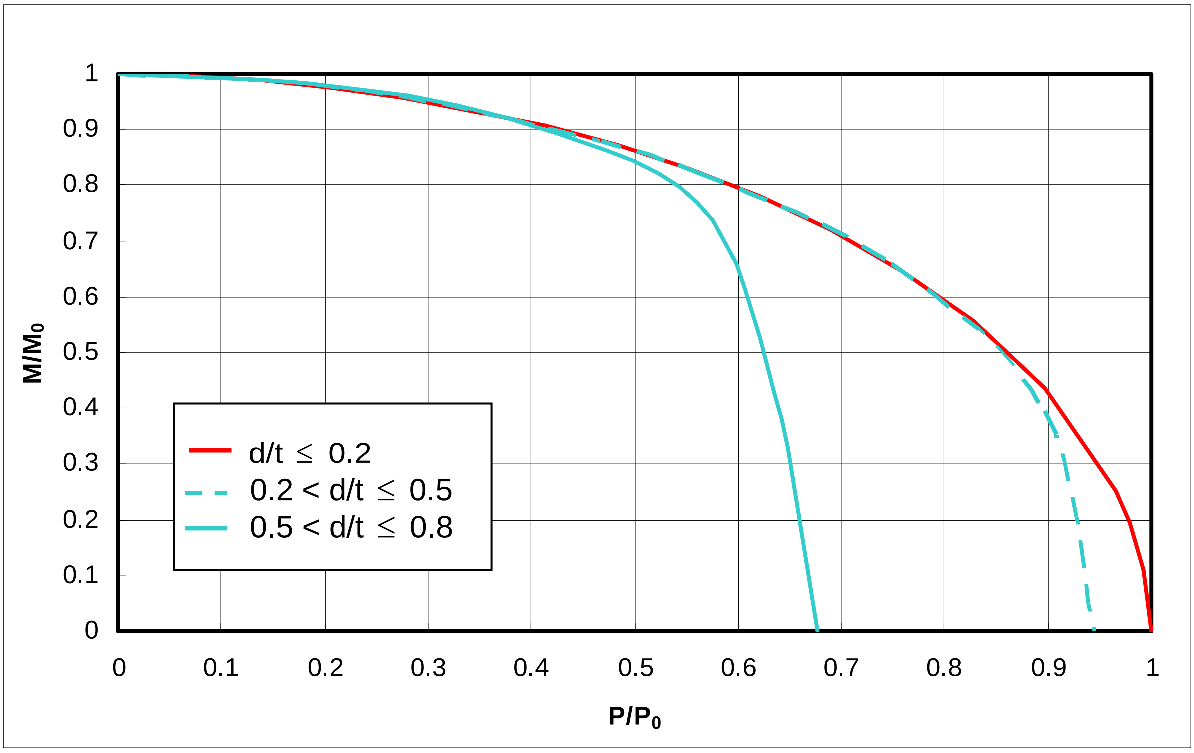

Figure 46 – Non-dimensional Pressure-Moment Failure Boundary Loci for Pipes with an Axial Groove Defect and Strength Grades up to X100

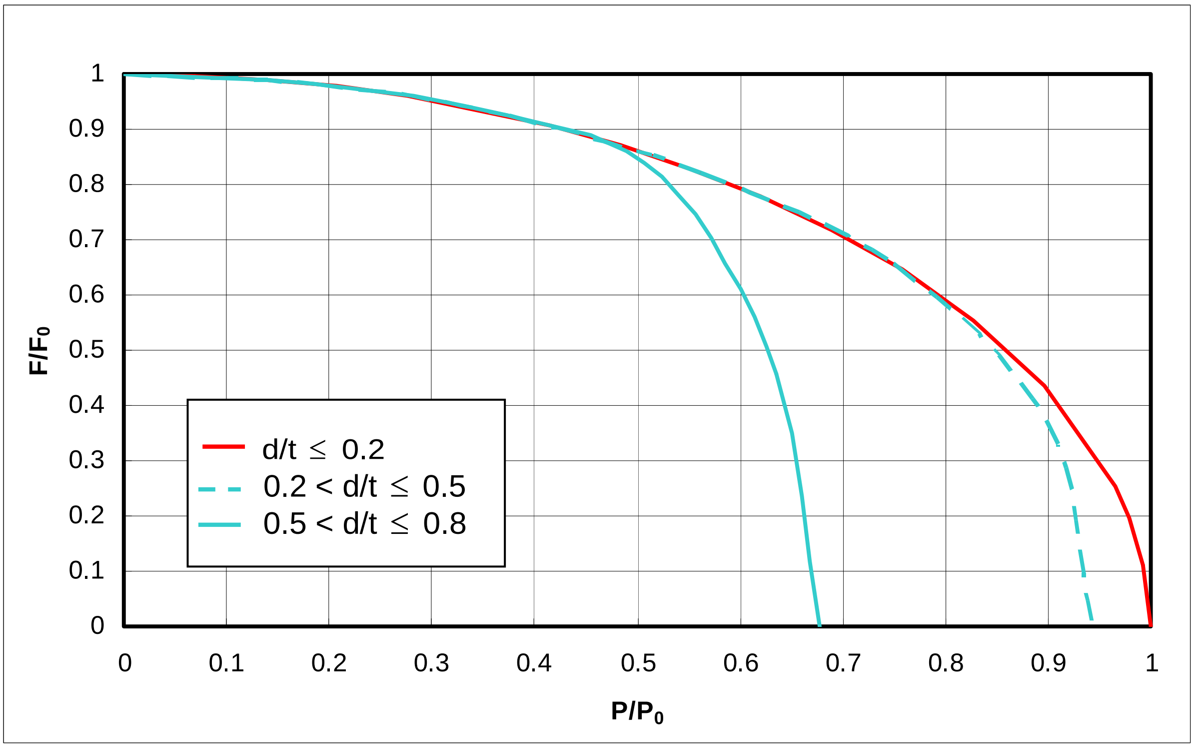

Figure 47 – Non-dimensional Pressure-Compressive Force Failure Boundary Loci for Pipes with an Axial Groove Defect and Strength Grades up to X100

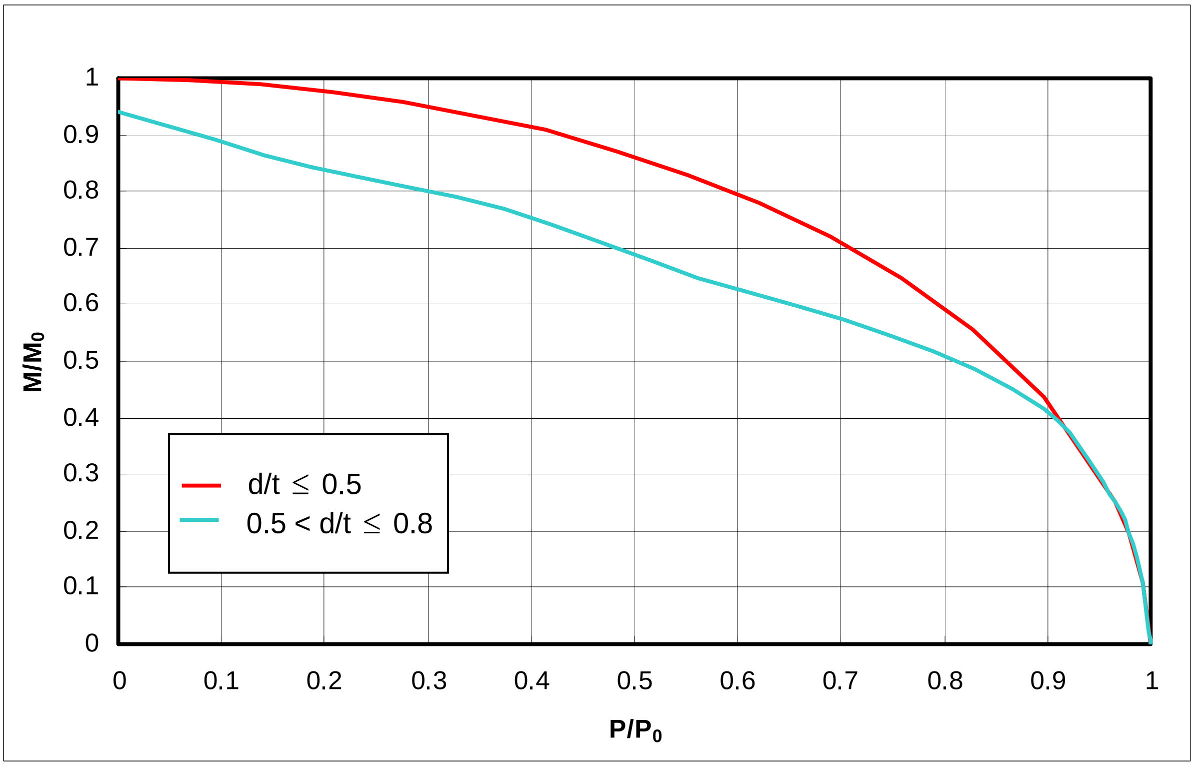

Figure 48 - Non-dimensional Pressure-Moment Failure Boundary Loci for Pipes with a Circumferential Groove Defect and Strength Grades up to X100

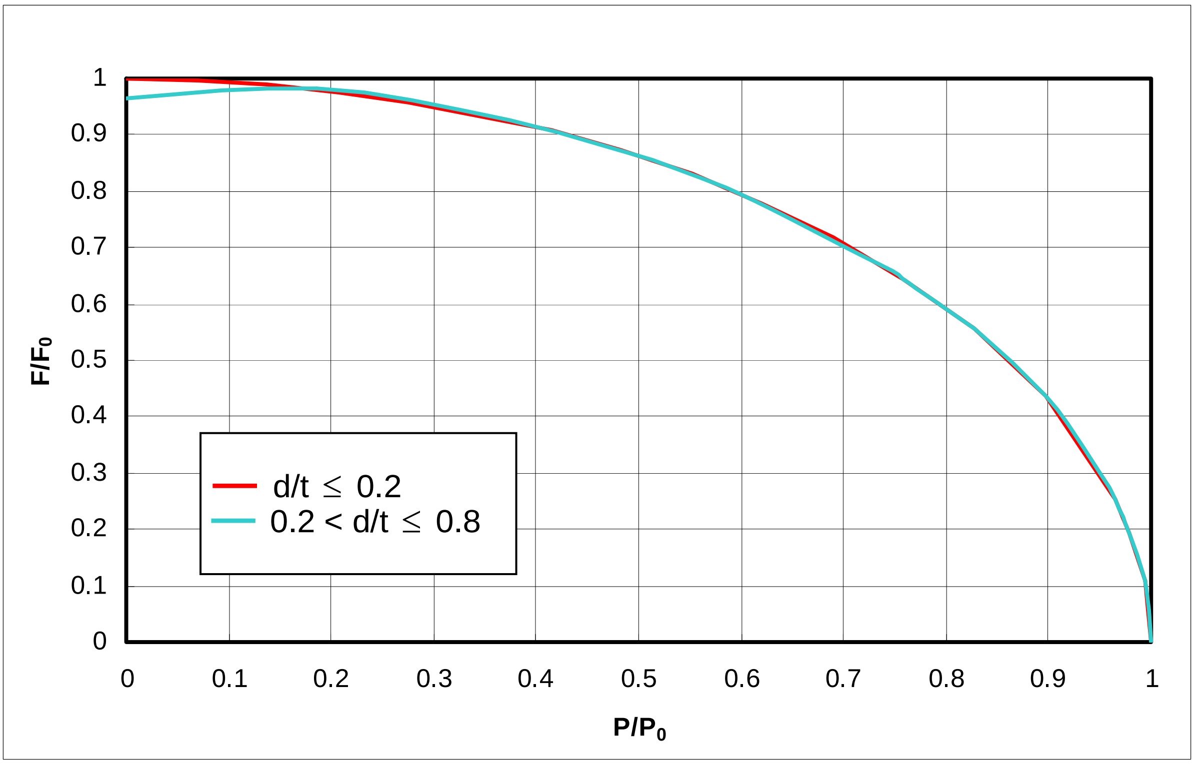

Figure 49 – Non-dimensional Pressure-Compressive Force Failure Boundary Loci for Pipes with a Circumferential Groove Defect and Strength Grades up to X100

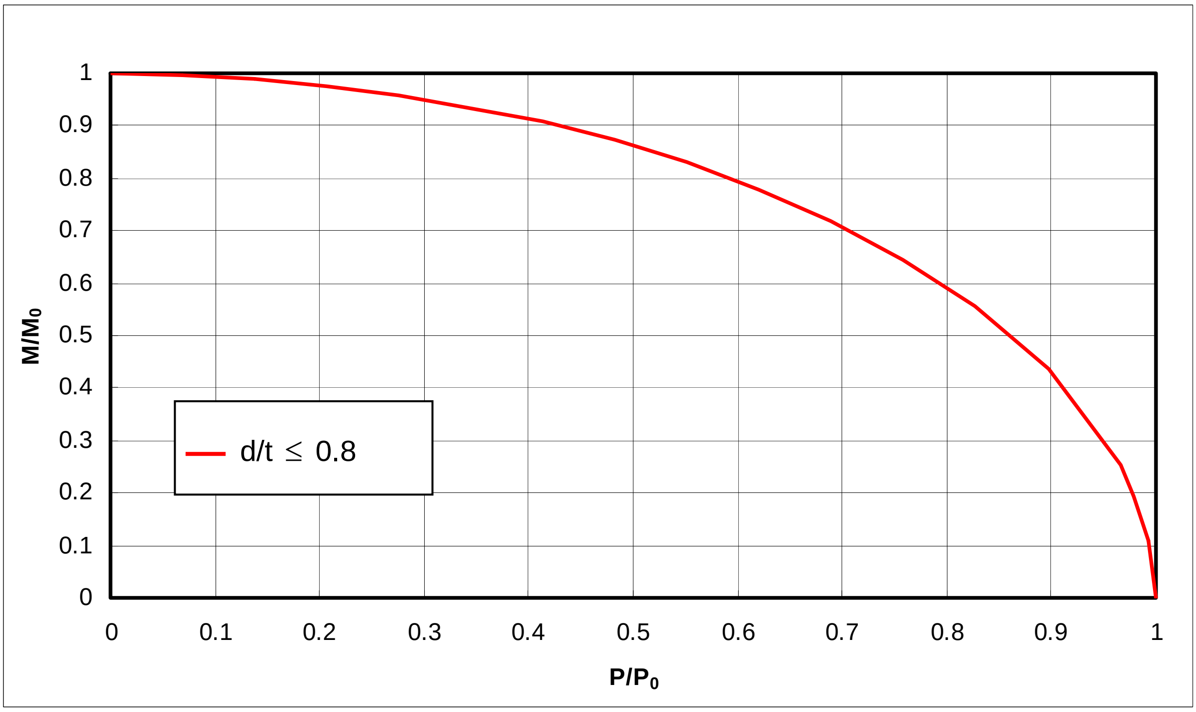

Figure 50 – Non-dimensional Pressure-Moment Failure Boundary Loci for Pipes with a Pit Defect and Strength Grades up to X100

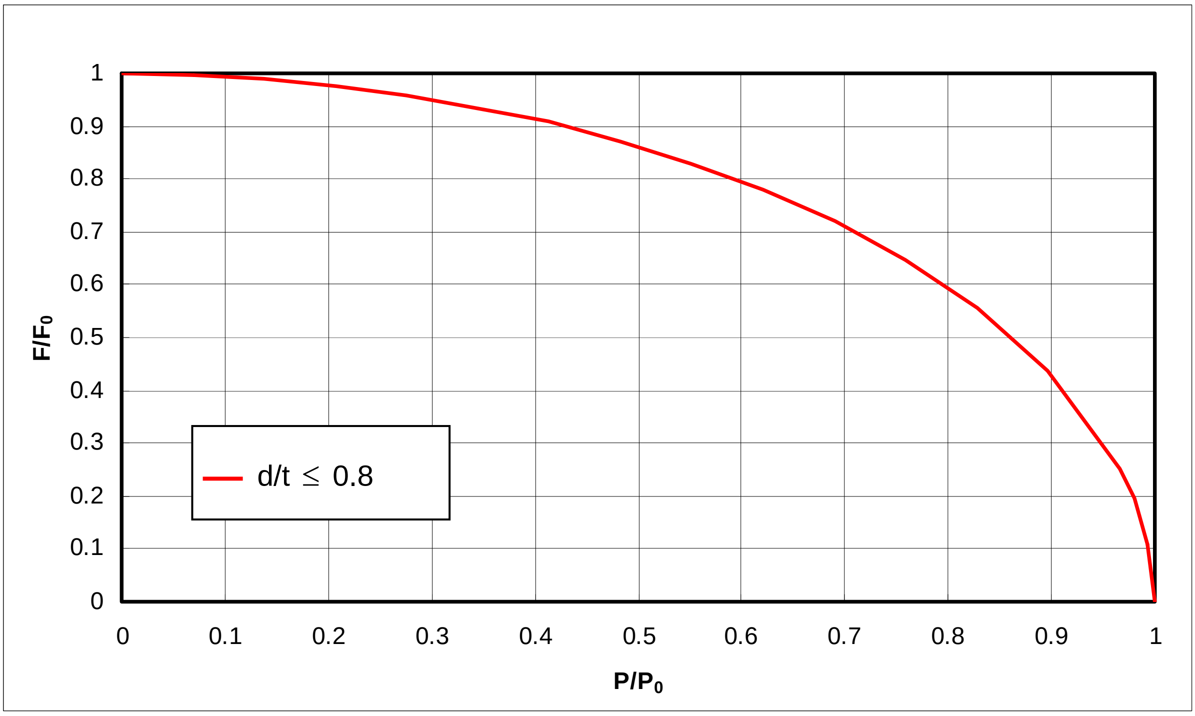

Figure 51 – Non-dimensional Pressure-Compressive Force Failure Boundary Loci for Pipes with a Pit Defect

Appendix A GKSS Miniature Flat Tensile Test Final Report

ADVANTICA Limited
Holywell Park
Ashby Road
Loughborough.
Leicestershire LE11 3GR
U.K.

Institute of Materials Research
Materials Mechanics
Max-Planck-Str. 1
D-21502 Geesthacht, Germany.
Tel.: +49-4152-872563
Fax: +49-4152-872670
E-Mail: bilal.dogan@gkss.de

16.11.2007

FINAL REPORT

ROOM TEMPERATURE SMALL SCALE TESTING OF PIPE WELDS USING MINIATURE FLAT TENSILE TEST TECHNIQUE and COMPARISON WITH STANDARD TENSILE (ST) TESTS

Project: Small Scale Testing of x100 Steel Pipe Welds using Miniature Flat Tensile and Standard Tensile (ST) Specimen Technique for ADVANTICA Limited

Order By: ADVANTICA Limited
Holywell Park
Ashby Road
Loughborough
Leicestershire LE11 3GR
UK

Project Content
miniature flat tensile Tests
Order Dated: 13.3.2007
Order No: 9900048819/Vendor No.: 15007
GKSS No.: LK11102WMF0252
Order Delivery: 1- Total of 120 specimen Test Data in Excel spread sheet format,
2- Engineering stress versus strain curves,
3- True stress versus strain curves.
Order Delivery Date: 07.05.2007

ST Tests
Order Dated: 01.08.2007
Order No: 9900050313/Vendor No.: 15007
GKSS No.: LK11102WMF0252
Order Delivery:
1- Total of 24 ST standard tensile specimens test data in Excel spread sheet format,
2- Engineering stress vs. strain curves,
3- True stress vs. strain curves.
4- Calibration factors for ST and miniature flat tensile tests.
Order Delivery Date: 24.9.2007 and Final Report on 16.11.2007
Contact Person at ADVANTICA: Mr. Andrew Brealey, Mr. Vinod Chauhan

Final Report Content

1. A combined final report on both miniature flat tensile and ST test (as requested by Vinod Chauhan) that include:
a. Comparison of micro-flat tensile and ST test results both graphical and tabular format
b. Calibration applicable to miniature flat tensile test results in comparison with ST test data.
c. Discussion of results and conclusions.

Project Work
1. Material:
X100 Pipeline steel, delivered by ADVANTICA to GKSS.
miniature flat tensile and ST tests to be done on Base Metal (BM) only.
Six Plates (Dimensions of about 15cmx 16cmx2cm) marked by ADVANTICA as in the following:
1- SUMO 12 3 o'clock,
2- SUMO 12 6 O'C,

3- 20003 3 O'C,
4- 20003 6 O'C,

5- HKX 90° 3 O'C,
6- HKX 180° 6 O'C,

2. Specimens:
From each of above given 6 Plates miniature flat tensile and ST specimens are machined out in two directions:
a- Longitudinal, Marked L (Laengst in German),
b- Circumferential or Transverse (T) or Marked Q for miniature flat tensile (Quer in German),

2.1 Number of Specimens:
2.1.1. miniature flat tensile Specimens

Total: 120 of specimens
These are: 6 Plates X 2 Directions X 10 Specimens each= 120.

ST Specimens:
Total of 24 round bar specimens.
These include: 6 Plates x 2 Directions x 2 Specimens each =24.

2.2. Specimens marked as: in the following:
1- SUMO 12 3 o'clock: a) miniature flat tensile: 10 Specimens: S3L1-S3L10,
10 Specimens: S3Q1-S3Q10,
b) ST: 2 Specimens: S3L-ST1 and S3L-ST2
2 Specimens: S3T-ST1 and S3T-ST2
2- SUMO 12 6 O'C: a) miniature flat tensile: 10 Specimens: S6L1-S6L10,
10 Specimens: S6Q1-S6Q10,
b) ST: 2 Specimens: S6L-ST1 and S6L-ST2
2 Specimens: S6T-ST1 and S6T-ST2

3- 20003 3 O'C: a) miniature flat tensile: 10 Specimens: 23L1-23L10
10 Specimens: 23Q1-23Q10,
b) ST: 2 Specimens: 23L-ST1 and 23L-ST2
2 Specimens: 23T-ST1 and 23T-ST2

4- 20003 6 O'C: a) miniature flat tensile: 10 Specimens: 26L1-26L10
10 Specimens: 26Q1-26Q10,

b) ST: 2 Specimens: 26L-ST1 and 26L-ST2
2 Specimens: 26T-ST1 and 26T-ST2

5- HKX 90° 3 O'C,: a) miniature flat tensile: 10 Specimens: H3L1-H3L10
10 Specimens: H3Q1-H3Q10,
b) ST: 2 Specimens: H3L-ST1 and H3L-ST2
2 Specimens: H3T-ST1 and H3T-ST2

6- HKX 180° 6 O'C: a) miniature flat tensile: 10 Specimens: H6L1-H6L10
10 Specimens: H6Q1-H6Q10,
b) ST: 2 Specimens: H6L-ST1 and H6L-ST2
2 Specimens: H6T-ST1 and H6T-ST2

2.3. Specimen dimensions:
2.3.1. miniature flat tensile Specimens:
The miniature flat tensile specimen dimensions are given in Figure 1a.

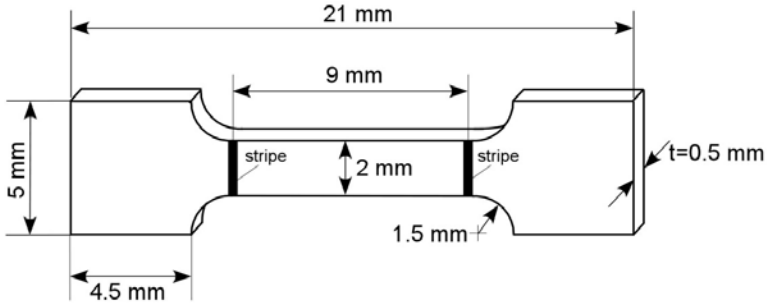

Fig.1a. Specimen dimensions and TiO_2 Stripe for displacement measurement using Laser [1].
2.3.2. ST Specimens:
The ST specimen dimensions are given in Figure 1b.

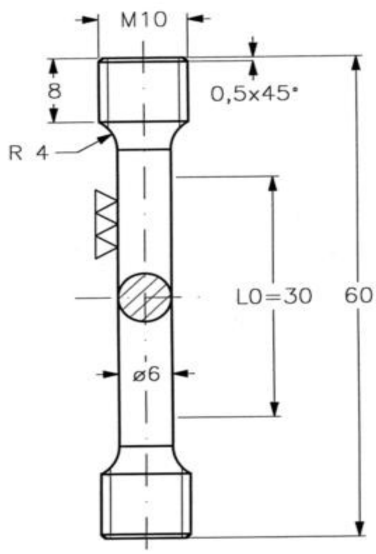

Fig.1.b. ST specimens-DIN50125-B 6x30, specimen diameter 6 mm and gauge length is 30 mm.

2.4 Machining of specimens:

2.4.1. miniature flat tensile Specimens: The specimens are Electric Discharge Machined (EDM) from pipe, as seen in Figure.2, (Figure from ADVANTICA) where the pipe segment plates were provided by ADVANTICA, as schematically shown in Figure 3a.
2.4.2. ST Specimens: ST specimens are machined out of the same plates from which miniature flat tensile specimens were produced. The specimens are produced mid way though the plate thickness as shown in Figure 3b.

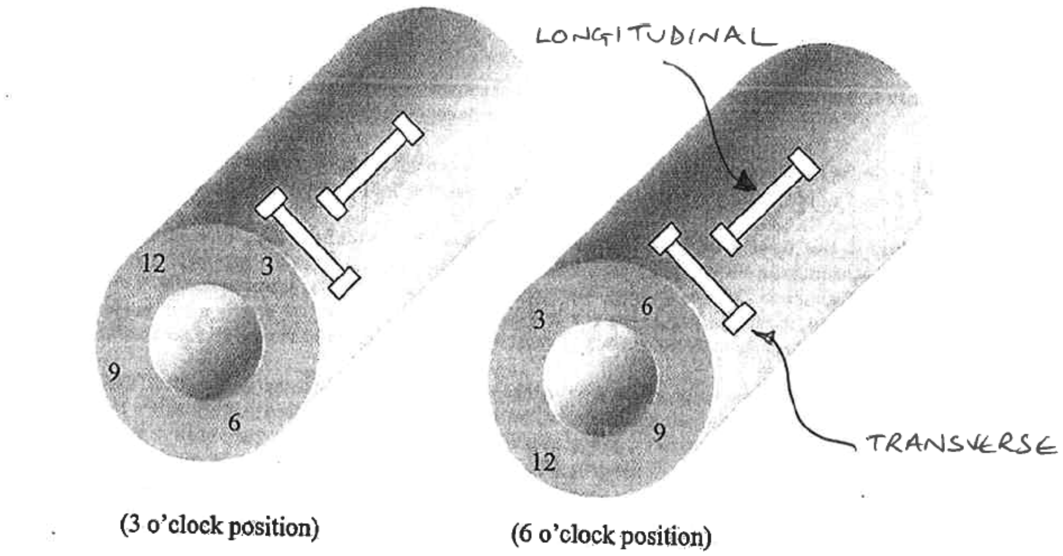

Fig 2 Location of specimen extraction from 3 and 6 o'clock positions (weld seam at 12 o'clock position).

2.5 Specimen Preparation:

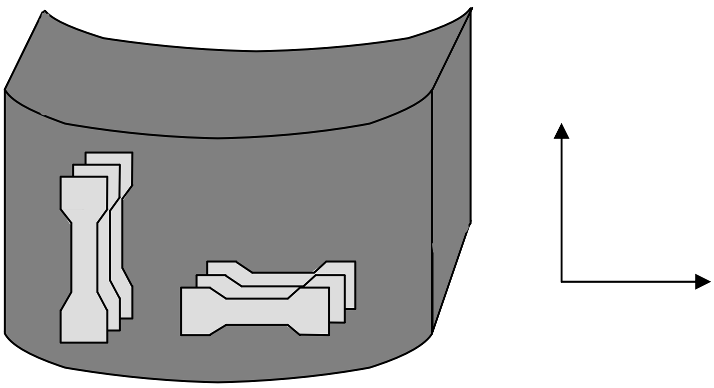

Fig.3a. Sectioning of the miniature flat tensile Specimens: Längst (Longitudinal) (Specimens:xxL1-xxL10), Quer (Circumferential) (Specimens: xxQ1-xxQ10). Specimen 1 is the first specimen near the outer pipe segment surface and Specimen 10 is the one nearest to the inner pipe segment surface.

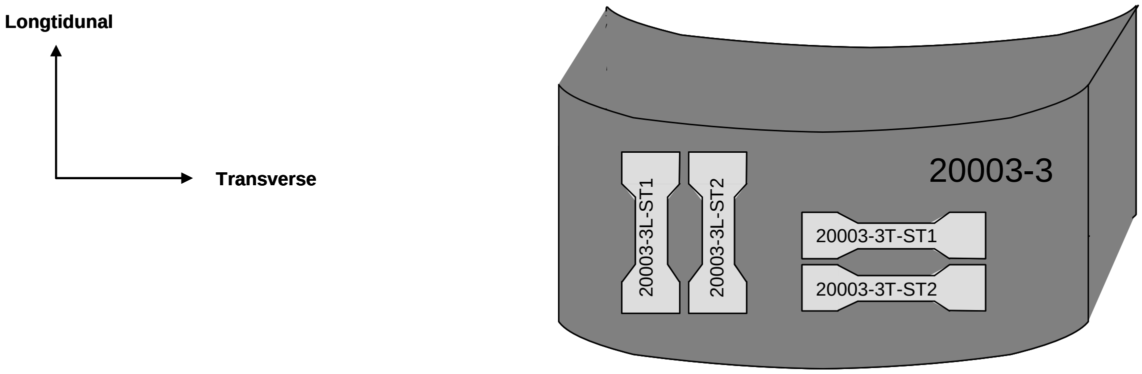

Fig.3b. Sectioning of the ST Specimens

2.5.1 The miniature flat tensile specimens are tested in as EDM machined condition. Titanium oxide Stripes (see Fig.1) are put on the flat surfaces by spraying on the masked specimen. These Stripes facilitate measuring the displacement using laser system. The strain is calculated from the measured displacement.
2.5.2 ST specimens are tested in as machined condition

3 Test Apparatus:

3.1 The miniature flat tensile tests are carried out in a 2.5 kN Zwick-Roell Electro-mechanical tensile testing machine equipped with laser displacement measurement system which is computer controlled. See Figure 4.
3.2 ST tests are done in an electro-mechanical 200kN Zwick machine. The load cell range was 30 kN.

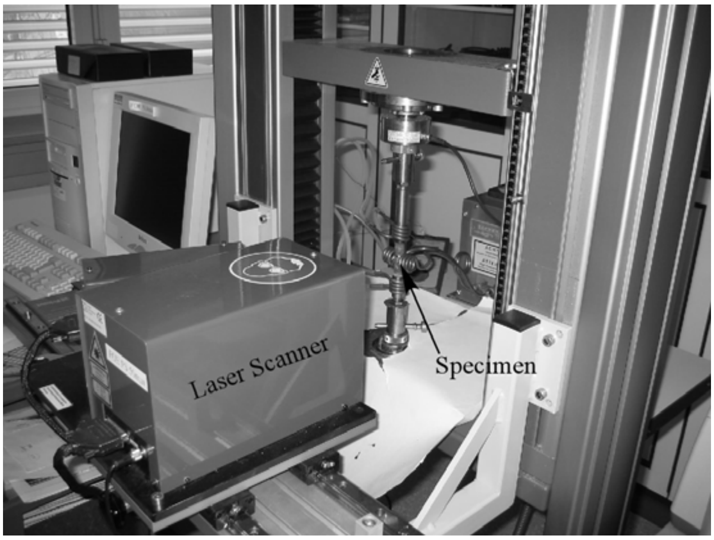

Fig.4. miniature flat tensile Test set-up with laser Scanner [1].

The specimen is shown within loading grip in Figure 5.

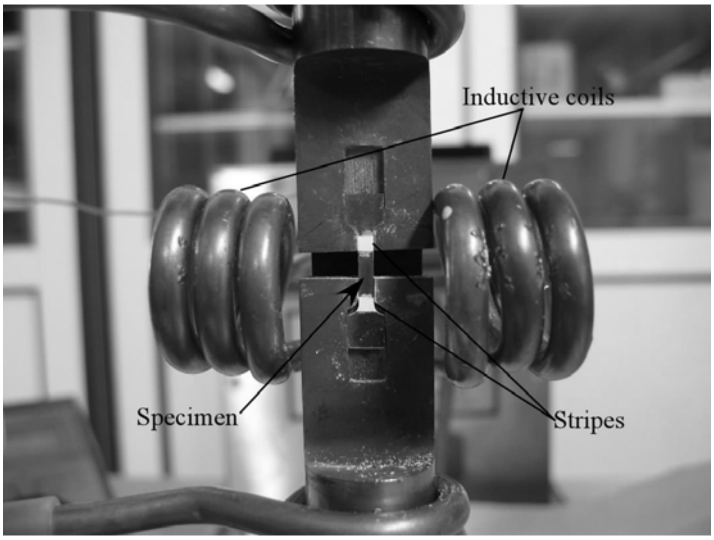

Fig. 5. miniature flat tensile Specimen in the loading grip [1].

4 miniature flat tensile Tests and Data Assessment:

4.1. miniature flat tensile Tests:

The tests are carried out at room temperature at a loading rate of 0.2mm/min. (See details of miniature flat tensile testing and Metallographic studies in Ref. 1).

The engineering stress-strain data are determined from load -displacement data using the specimen cross section and the gauge length necessary for calculations. Furthermore the true stress-true strain data are calculated from engineering stress –engineering strain data up to maximum value of engineering stress where necking starts.

4.2. ST Tests:

Room temperature standard tensile tests are done under cross head speed control of 0.5 mm/min where the load and displacement were continuously recorded. An MTS extensometer with 25 mm gauge length was used or displacement measurements.

5. Results: Attached Files.

5.1. miniature flat tensile Tests (Previous contract work already concluded)

The present test report contains results stated in the Order delivery content, namely:

1- Total of 120 specimen Test Data in Excel spread sheet format. Note the specimen code on the heading as in section 2.2.

2- Engineering stress versus strain curves: 12 Diagrams each containing 10 specimens as in Section 2.2 are presented. Note that the diagram axes are named as Engineering stress and Engineering strain. The attached data are reduced stress –strain data taken every 20 points.

3- True stress versus strain curves: 12 Diagrams each containing 10 specimens as in Section 2.2 are presented. The diagram axes are named true stress and true strain. The attached data are reduced stress –strain data taken every 10 points.

The true stress-true strain data is cut off at maximum stress as the decrease in specimen dimensions, in thickness and width in the necked section, is not possible to determine.

4- Yield and Tensile strength data: A table containing the yield and tensile strength data together with cumulative plots through wall thickness trend of tensile strength for all tested materials are presented.

Note that some of the specimens failed with little elongation. This may be due to failure in the micro structural constituent, cracking at structural discontinuity or failure of the stripe due to straining. Metallographic and fractographic examinations can help clarifying such behavior. Furthermore, the plots of through wall strength and strain which is also deduced from the stress-strain data, as the specimens are numbered in sequence 1-10 (see section 2.2 and Fig. 3a), provides insight into variation of properties of materials in through wall direction.

5.2. ST Tests

Total of 24 round bar specimens conforming DIN50125 were produced for testing at room temperature. The specimen codes are given in Section 2.2.
The test data is presented in excel format including yield ($R_{p0.2}$) and tensile (R_m) strengths, and % Elongation. The presented data also included engineering and true stress-strain values. The data together with diagrams were mailed to ADVANTICA on 24.September.2007. A revised data set is attached to the present report. The data processing followed the one used for miniature flat tensile tests described in Section 5.1.

The ST engineering and true stress versus strain diagrams (total of 24; 12 Engineering stress-strain, 12 True stress-strain) are presented containing the miniature flat tensile data. The aim is to compare the results from different tests using different specimen sizes and geometries.

Excel files containing material data, strength ($R_{p0.2}$ and R_m) and ductility (% Elongation) is prepared. The data is plotted for further assessment as presented in excel files.

Some discrepancy in data led to consideration of metallographic examination of fracture surfaces. A strong texture effect on fracture mode is observed 0n tested specimen fracture surfaces (Figures 6a-d).

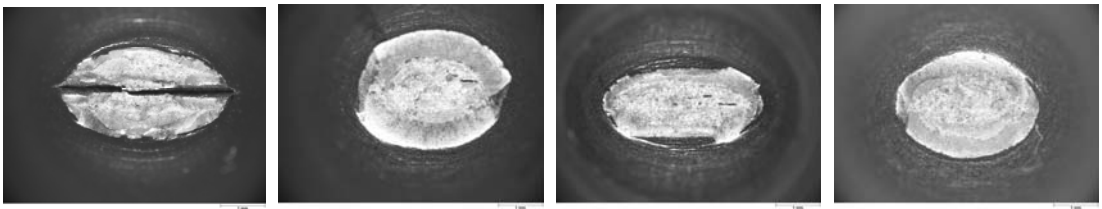

a) b) c) d)
Fig.6 Optical fracture surface pictures showing the effect of metal working texture on deformation behavior in round bar tensile test. a) 20003-3L-ST1, b) 20003-3T-ST1, c) HKX-3L-ST1, d) HKX-3T-ST1

Analytical approach is taken to compare the test results from ST and miniature flat tensile tests. The strength and ductility determined in ST tests are higher than those determined using miniature flat tensile specimens.

A table (Table 1) summarizing the calibration factors calculated in excel files (see point 4 above) is presented. The calibration factors are determined analytically by taking the ratio of average values of a property of ST simply divided by miniature flat tensile.

6. Summary:

6.1. miniature flat tensile Tests:

The Results presented in section 5 gives an overview of the material behavior determined testing small scale non-standard miniature flat tensile specimens. These data provide information on the behavior of the materials in different material directions (Longitudinal and Trans) affected by the texture. The plots of through wall strength and strain, with the specimens numbered in sequence 1-10, provides insight into variation of properties of materials in through wall direction. The presented data facilitates comparison of different materials provided by different manufacturers by following the material numbers assigned by ADVANTICA both in longitudinal and transverse directions, as well as their through wall property variation.
The miniature flat tensile tests are particularly useful when the test material is limited, as in weldments or from in-service components. However, the determined data is qualitative that serves for the purpose of comparison, as in the present work facilitating comparison of materials provided by different manufacturers, and not be taken as material property data. The material property data may be determined using standard tensile (ST) specimens machined out of the pipe segments following the standard test procedure such as British BS, ASTM Standard Test Methods for Tension Testing of Metallic Materials or German DIN Standard.
The present mechanical data need to be used with caution due to small amount of material contained in the test gauge where the deformation and fracture behavior may be affected by the micro structural constituents that may be comparable to the thickness of the test specimen. Such affect is attributed to the scatter in the data of S6L1-10, for example. Such information may be gained from the metallographic and fractographic examinations of the tested specimens which were not covered in the present Order. A follow up test programme included ST specimens for comparison of the present miniature flat tensile test results with those of the round bar ST test data.

6. ST Tests:

The ST test data contained less scatter than those of miniature flat tensile data. Some scatter, however, observed is related to a strong pipe-plate production texture and residual stresses.

The above discussion on texture effect is amplified in small specimen size miniature flat tensile tests. The scatter is higher even in a total of 10 specimen tested. When compared ST test data with those of miniature flat tensile data, all strength and ductility values are higher in ST data which is taken as materials property data, than those non-standard miniature flat tensile data. This leads to a conclusion that for design purposes ST test data is required. However if miniature flat tensile data to be used (i.e. for assessment purposes) the miniature flat tensile data needs to be calibrated by comparing to the ST data. The calibration of miniature flat tensile data may be done by comparing the strength data with those from ST tests using analytical approach. The calibration factor is determined from the difference between miniature flat tensile and ST data, in strength ($R_{p0.2}$ and R_m) and ductility (% Elongation). On the other hand, more sophisticated numerical approach may be taken which produces calibrated full stress-strain curves, which is more time consuming and costly. The reliability of the calibration improves with increased number of tests data.

The present test results led to calibration factors varying with pipe producer specific material condition and test specimen direction mostly affected by texture and residual stresses.

Therefore, use of present calibration factors need caution and not applicable to X100 steels in general. A wider applicability of a calibration factor depends on the material condition such as one with homogeneous microstructure and with relieved residual stresses.

References

Ref.[1]: U. Ceyhan, M. Horstmann and B. Dogan, “High Temperature Cross-Weld Characterization of Steel Weldments by Micro tensile Testing”, J. Materials at High Temperatures, Vol.23, No.3/4, 2006, pp.233-243).

Ref. [2]: ASTM E8-04. Standard Test Methods for Tension Testing of Metallic Materials. ASTM International / 01-Apr-2004.

Plates-Specimen Loc.&Dir.	C [illegible]$_{02Eng.}$	C R_{p02Eng}.	C [illegible]$_{mEng.}$	C R_{mEng}	C[illegible] [illegible]$_{fEng}$	C $R_{fEng.}$	C $R_{p02True}$	C [illegible]$_{mTrue}$	C R_{mTrue}
20003-3L	0,902	1,116	1,298	1,174	2,431	0,802	1,115	1,291	1,188
20003-3T	1,137	1,208	3,390	1,216	3,240	0,860	1,137	1,209	1,244
20003-6L	1,017	1,674	0,694	1,436	1,939	1,105	1,674	0,699	1,415
20003-6T	0,900	0,964	2,172	1,126	2,379	0,757	0,964	2,164	1,153
HKX-3L	0,923	1,054	1,565	1,177	1,616	0,799	1,054	1,549	1,202
HKX-3T	0,962	1,402	1,512	1,327	2,232	0,903	1,401	1,497	1,353
HKX-6L	0,945	1,046	1,590	1,191	2,085	0,859	1,046	1,575	1,213
HKX-6T	1,037	1,390	1,280	1,284	1,899	0,872	1,390	1,272	1,300
SUM012-3L	0,850	1,145	1,299	1,208	2,243	0,866	1,144	1,290	1,224
SUM012-3T	1,004	1,198	1,581	1,193	2,367	0,825	1,198	1,565	1,218
SUM012-6L	0,909	1,112	1,860	1,144	2,917	0,822	1,111	1,835	1,176
SUM012-6T	0,848	1,018	1,708	1,125	2,825	0,792	1,017	1,686	1,154

Table 1. Calibration factors for Standard Tensile (ST) and Miniature Flat Tensile (miniature flat tensile) tests on X100 Plates for ADVANTICA.

The present revised test report is prepared by B.Dogan of GKSS Research Centre on 12.11.2007.

Prof. Bilal Dogan
GKSS Research Centre
Institute for Materials Research, Materials Mechanics
Max-Planck-Str.1
D-21502 Geesthacht (Hamburg), Germany.
Tel.: +49-4152-872563
E-Mail: bilal.dogan@gkss.de

Appendix B X100 Vessel Burst Tests – Metrology Reports

PMC NO. 401347

PMC AMBERGATE

GENERAL INSPECTION REPORT

PROJECT CLIENT ADVANTICA 52" TESTS	DATE 12/4/07
LOCATION. PMC AMBERGATE	INSPECTOR (CAPITALS): R. ELLIOTT
INSPECTION TECHNIQUE VISUAL / PII EQUIPMENT	

HKX N° 1

LENGTH OF MACHINED SLOT – 2000 MM
DEPTH OF MACHINED SLOT – AS SHOWN AT POSITIONS A TO E
WIDTH OF MACHINED SLOT – AS SHOWN AT POSITIONS A TO E

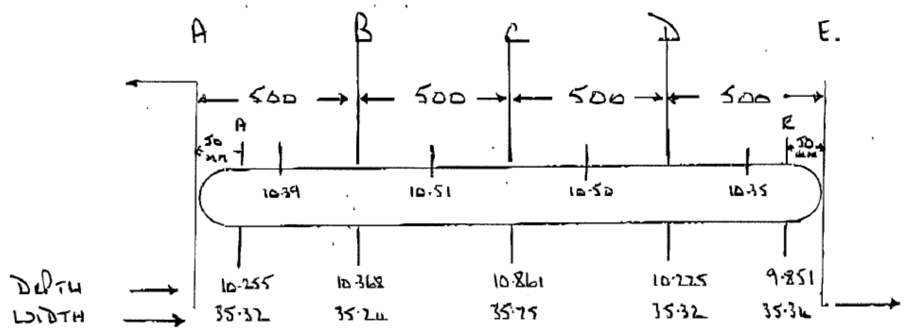

SIGNATURE R Elliott
APPROVAL & No. BGAS SWI 2513
DATE 12-4-07
CIRCULATION

Document No: NDT-004 | Issue 3 Dated 3.4.00

Figure B1 Test 1 Metrology Report

GL

PMC NO. 401347

PMC AMBERGATE

GENERAL INSPECTION REPORT

PROJECT CLIENT ADVANTICA 52" TESTS	DATE 12\4\07
LOCATION. PMC AMBERGATE	INSPECTOR (CAPITALS): R. ELLIOTT
INSPECTION TECHNIQUE VISUAL / PII EQUIPMENT	

HKX N° 1

LENGTH OF MACHINED SLOT - 2000 MM
DEPTH OF MACHINED SLOT - AS SHOWN AT POSITIONS A TO E
WIDTH OF MACHINED SLOT - AS SHOWN AT POSITIONS A TO E

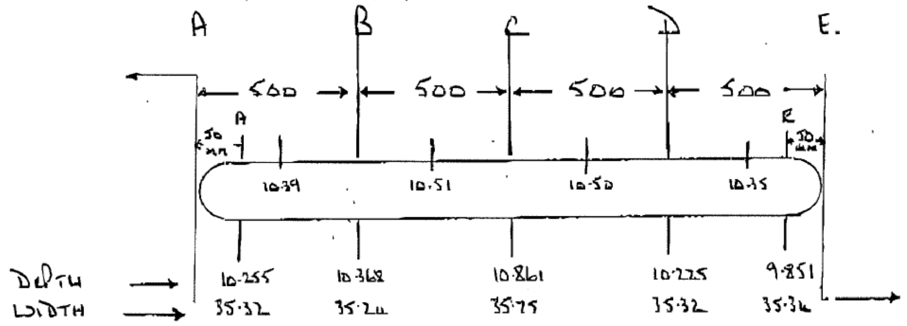

SIGNATURE
APPROVAL & No. BGAS SWI 2513
DATE 12-4-07

CIRCULATION

Document No: NDT-004 | Issue 3 Dated 3.4.00

Figure B2 Test 2 Metrology Report

Appendix C Derivation of Global Yielding Criteria

C.1 Internal Pressure

For pipe under internal pressure, *P*, loading with the effect of the capped end force, the hoop stress, σ_{hp}, and axial stress, σ_{xp}, are assumed to be uniformly distributed on the pipe cross section and

$$\sigma_{hp} = \frac{PR_i}{t} = P(\alpha - 1) \quad \text{and} \quad \sigma_{xp} = \frac{PR_i^2}{R_o^2 - R_i^2} = P\frac{(\alpha-1)^2}{2\alpha - 1}, \qquad \text{(C1,C2)}$$

where $\alpha = \frac{R_0}{t}$, (C3)

R_o, R_i and t are the pipe outer radius, inner radius and wall thickness, respectively.

The von Mises equivalent stress in the pipe is given by the following expression:

$$\sigma_{vm} = \sqrt{\sigma_{xp}^2 + \sigma_{hp}^2 - \sigma_{xp}\sigma_{hp}} = \sqrt{\left[P\frac{(\alpha-1)^2}{2\alpha-1}\right]^2 + [P(\alpha-1)]^2 - P^2\frac{(\alpha-1)^3}{2\alpha-1}}$$

$$= P\frac{\alpha-1}{2\alpha-1}\sqrt{(\alpha-1)^2 + (2\alpha-1)^2 - (\alpha-1)(2\alpha-1)} = P\frac{\alpha-1}{2\alpha-1}\sqrt{3\alpha^2 - 3\alpha + 1} \qquad \text{(C4)}$$

Plastic yielding occurs in the pipe when $\sigma_{vm} = \sigma_{SMYS}$, where σ_{SMYS} is the yield stress of the pipe material. Therefore, the critical pressure, P_0, for pipe at yield is given by Equation (5).

$$P_0 = \frac{(2\alpha-1)}{(\alpha-1)\sqrt{3\alpha^2 - 3\alpha + 1}}\sigma_{SMYS} \qquad \text{(C5)}$$

C.2 Pure Bending

It is assumed that the pipe cross section remains plane for under pure bending loading. It is also assumed that the pipe material is elastic, perfectly plastic. material.

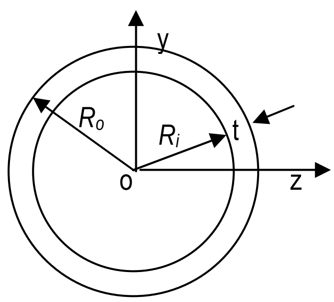

The strain can be expressed as:

$$\varepsilon = \kappa y \qquad \text{(C6)}$$

and the stress by

$$\sigma = E\varepsilon = E\kappa y \quad \text{for } \sigma < \sigma_{SMYS} \qquad \text{C7)}$$

and $\sigma = \sigma_{SMYS}$, (C8)

where *E* and σ_{SMYS} are the Young's modulus and the specified minimum yield strength respectively.

When the whole cross-section is in the elastic range with $\sigma < \sigma_{SMYS}$, the relationship between the stress and the bending moment is

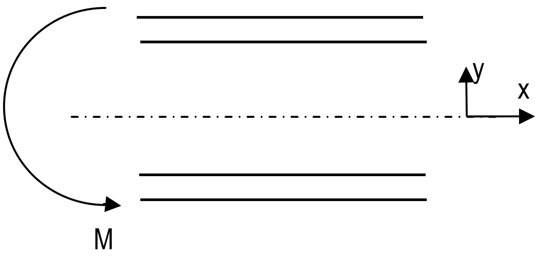

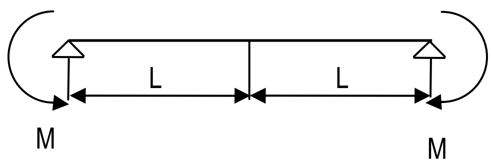

$$\sigma_{xb} = \frac{M}{I} y \,, \qquad \text{(C9)}$$

where $$I = \frac{\pi}{4}\left(R_o^4 - R_i^4\right) . \qquad \text{(C10)}$$

First yield occurs with $\sigma = \pm\sigma_{SMYS}$ at $y = \pm R_o$. The corresponding bending moment is the elastic limit moment, M_0, with

$$M_0 = \frac{\pi\left(R_o^4 - R_i^4\right)\sigma_{SMYS}}{4R_o} \qquad \text{(C11)}$$

C.3 Axial Compression

When the pipe is subjected a compressive force, *F*, loading at its end, the axial stress, σ_{xf}, is assumed to be uniformly distributed on the pipe cross section and

$$\sigma_{xf} = -\frac{F}{\pi\left(R_0^2 - R_i^2\right)} \qquad \text{(C12)}$$

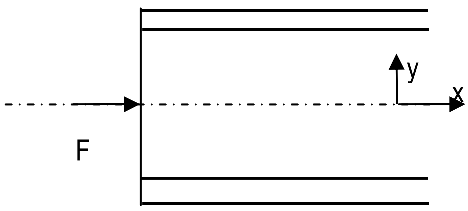

Yielding occurs when $\sigma_{xf} = -\sigma_{SMYS}$ and the limit force, F_0, is

$$F_0 = \pi\left(R_0^2 - R_i^2\right)\sigma_{SMYS} \qquad \text{(C13)}$$

C.4 Combined Internal Pressure and Bending

Under pressure loading, the hoop stress, σ_{hp}, and axial stress, σ_{xp}, are defined by equation (1) and (2) respectively. Under bending loading, the axial stress, σ_{xb}, is defined by equations (9) and (10).

The von Mises stress under pressure and bending loading is

$$\sigma_{vm} = \sqrt{\left(\sigma_{xp} + \sigma_{xb}\right)^2 + \sigma_{hp}^2 - \left(\sigma_{xp} + \sigma_{xb}\right)\sigma_{hp}} \qquad \text{(C14)}$$

Yielding occurs when $\sigma_{vm} = \sigma_{SMYS}$, which gives

$$\left(\sigma_{xp}+\sigma_{xb}\right)^2-\left(\sigma_{xp}+\sigma_{xb}\right)\sigma_{hp}+\sigma_{hp}^2-\sigma_{SMYS}{}^2=0$$

or $$\sigma_{xp}+\sigma_{xb}=\frac{1}{2}\left(\sigma_{hp}\pm\sqrt{4\sigma_{SMYS}{}^2-3\sigma_{hp}^2}\right) \qquad \text{(C15)}$$

$$\sigma_{xb}=\frac{1}{2}\left[P(\alpha-1)\pm\sqrt{4\sigma_{SMYS}{}^2-3P^2(\alpha-1)^2}\right]-P\frac{(\alpha-1)^2}{2\alpha-1}$$

$$=P\frac{\alpha-1}{2\alpha-1}\left[\frac{1}{2}(2\alpha-1)-(\alpha-1)\right]\pm\frac{1}{2}\sqrt{4\sigma_{SMYS}{}^2-3P^2(\alpha-1)^2}$$

$$=\frac{1}{2}P\frac{\alpha-1}{2\alpha-1}\pm\frac{1}{2}\sqrt{4\sigma_{SMYS}{}^2-3P^2(\alpha-1)^2} \qquad \text{(C16)}$$

For $\sigma_{xb}>0$, i.e., $y>0$ and $M>0$ or $y<0$ and $M<0$

$$\sigma_{xb}=\frac{1}{2}P\frac{\alpha-1}{2\alpha-1}+\frac{1}{2}\sqrt{4\sigma_{SMYS}{}^2-3P^2(\alpha-1)^2} \qquad \text{(C17)}$$

For $\sigma_{xb}<0$, i.e., $y>0$ and $M<0$ or $y<0$ and $M>0$

$$\sigma_{xb}=\frac{1}{2}P\frac{\alpha-1}{2\alpha-1}-\frac{1}{2}\sqrt{4\sigma_{SMYS}{}^2-3P^2(\alpha-1)^2} \qquad \text{(C18)}$$

For PRCI corrosion assessment with stress at 180°, or $y<0$, then

$$\sigma_{xb}=\frac{1}{2}P\frac{\alpha-1}{2\alpha-1}+\frac{1}{2}\sqrt{4\sigma_{SMYS}{}^2-3P^2(\alpha-1)^2} \qquad \text{when } M<0 \qquad \text{(C19)}$$

and $$\sigma_{xb}=\frac{1}{2}P\frac{\alpha-1}{2\alpha-1}-\frac{1}{2}\sqrt{4\sigma_{SMYS}{}^2-3P^2(\alpha-1)^2} \qquad \text{when } M>0 \qquad \text{(C20)}$$

The moment when yield occurs at $y=-R_o$ is

$$M_e=-\frac{\pi\left(R_o^4-R_i^4\right)}{4R_o}\left[\frac{1}{2}P\frac{\alpha-1}{2\alpha-1}+\frac{1}{2}\sqrt{4\sigma_{SMYS}{}^2-3P^2(\alpha-1)^2}\right] \qquad \text{when } M<0 \qquad \text{(C21)}$$

$$M_e=-\frac{\pi\left(R_o^4-R_i^4\right)}{4R_o}\left[\frac{1}{2}P\frac{\alpha-1}{2\alpha-1}-\frac{1}{2}\sqrt{4\sigma_{SMYS}{}^2-3P^2(\alpha-1)^2}\right] \qquad \text{when } M>0 \qquad \text{(C22)}$$

Equations (21) and (22) show that the critical value of the absolute moment is smaller when the pipe is loaded by a positive bending moment loading, i.e., $M>0$. Therefore, the relationship between the critical moment, M_{crit}, and critical pressure, P_{crit}, for pipe global yielding is given by:

$$M_{crit}=-\frac{\pi\left(R_o^4-R_i^4\right)}{4R_o}\left[\frac{1}{2}P_{crit}\frac{\alpha-1}{2\alpha-1}-\frac{1}{2}\sqrt{4\sigma_{SMYS}{}^2-3P_{crit}^2(\alpha-1)^2}\right],$$

or $$\frac{M_{crit}}{M_0}=-\frac{1}{\sigma_{SMYS}}\left[\frac{1}{2}P_0\frac{\alpha-1}{2\alpha-1}\left(\frac{P_{crit}}{P_0}\right)-\frac{1}{2}\sqrt{4\sigma_{SMYS}{}^2-3P_0^2(\alpha-1)^2\left(\frac{P_{crit}}{P_0}\right)^2}\right]$$

(C23)

Substituting equation (3) into the above equation gives:

$$\frac{M_{crit}}{M_0} = \frac{1}{2}\sqrt{4 - 3\frac{(2\alpha - 1)^2}{3\alpha^2 - 3\alpha + 1}\left(\frac{P_{crit}}{P_0}\right)^2} - \frac{1}{2\sqrt{3\alpha^2 - 3\alpha + 1}}\left(\frac{P_{crit}}{P_0}\right) \quad \text{(C24)}$$

For a large $\alpha \ (= R_0 / t)$, the relationship between the critical moment and the critical pressure can be approximated by:

$$\frac{M_{crit}}{M_0} \approx \sqrt{1 - \left(\frac{P_{crit}}{P_0}\right)^2} \quad \text{(C25)}$$

C.5 Combined Internal Pressure and Axial Compression

Under pressure loading, the hoop stress, σ_{hp}, and axial stress, σ_{xp}, are defined by equation (1) and (2) respectively. Under compressive force loading, the axial stress, σ_{xf}, is defined by equation (12).

The von Mises stress under pressure and bending loading is

$$\sigma_{vm} = \sqrt{(\sigma_{xp} + \sigma_{xf})^2 + \sigma_{hp}^2 - (\sigma_{xp} + \sigma_{xf})\sigma_{hp}} \quad \text{(C26)}$$

The yield occurs when $\sigma_{vm} = \sigma_y$, which gives

$$(\sigma_{xp} + \sigma_{xf})^2 - (\sigma_{xp} + \sigma_{xf})\sigma_{hp} + \sigma_{hp}^2 - \sigma_{SMYS}{}^2 = 0$$

or

$$\sigma_{xp} + \sigma_{xf} = \frac{1}{2}\left(\sigma_{hp} \pm \sqrt{4\sigma_{SMYS}{}^2 - 3\sigma_{hp}^2}\right) \quad \text{(C27)}$$

$$\begin{aligned} \sigma_{xf} &= \frac{1}{2}\left(\sigma_{hp} \pm \sqrt{4\sigma_{SMYS}{}^2 - 3\sigma_{hp}^2}\right) - \sigma_{xp} \\ &= \frac{1}{2}P\frac{\alpha - 1}{2\alpha - 1} \pm \frac{1}{2}\sqrt{4\sigma_{SMYS}{}^2 - 3P^2(\alpha - 1)^2} \\ &= \frac{1}{2}P\frac{\alpha - 1}{2\alpha - 1} - \frac{1}{2}\sqrt{4\sigma_{SMYS}{}^2 - 3P^2(\alpha - 1)^2} \end{aligned} \quad \text{(C28)}$$

since $\sigma_{xf} < 0$.

Therefore, the critical compressive force, F_{crit}, is

$$F_{crit} = \pi(R_0^2 - R_i^2)\left[\frac{1}{2}\sqrt{4\sigma_{SMYS}{}^2 - 3P^2(\alpha - 1)^2} - \frac{1}{2}P\frac{\alpha - 1}{2\alpha - 1}\right], \quad \text{(C29)}$$

and the relationship between the critical compressive force, F_{crit}, and the critical pressure, P_{crit}, for the global pipe yielding is

$$\begin{aligned} \frac{F_{crit}}{F_0} &= \frac{1}{\sigma_{SMYS}}\left[\frac{1}{2}\sqrt{4\sigma_{SMYS}{}^2 - 3P_0^2(\alpha - 1)^2\left(\frac{P_{crit}}{P_0}\right)^2} - \frac{1}{2}P_0\frac{\alpha - 1}{2\alpha - 1}\left(\frac{P_{crit}}{P_0}\right)\right] \\ &= \frac{1}{2}\sqrt{4 - 3\frac{(2\alpha - 1)^2}{3\alpha^2 - 3\alpha + 1}\left(\frac{P_{crit}}{P_0}\right)^2} - \frac{1}{2\sqrt{3\alpha^2 - 3\alpha + 1}}\left(\frac{P_{crit}}{P_0}\right). \end{aligned} \quad \text{(C30)}$$

For a large $\alpha \left(=R_0/t\right)$, the relationship between the critical compressive force and the critical pressure can be approximated by:

$$\frac{F_{crit}}{F_0} \approx \sqrt{1-\left(\frac{P_{crit}}{P_0}\right)^2} \quad \text{(C31)}$$